

Developed at the request of:



Research conducted by:



Climate: Observations, projections and impacts

Russia



We have reached a critical year in our response to climate change. The decisions that we made in Cancún put the UNFCCC process back on track, saw us agree to limit temperature rise to 2 °C and set us in the right direction for reaching a climate change deal to achieve this. However, we still have considerable work to do and I believe that key economies and major emitters have a leadership role in ensuring a successful outcome in Durban and beyond.

To help us articulate a meaningful response to climate change, I believe that it is important to have a robust scientific assessment of the likely impacts on individual countries across the globe. This report demonstrates that the risks of a changing climate are wide-ranging and that no country will be left untouched by climate change.

I thank the UK's Met Office Hadley Centre for their hard work in putting together such a comprehensive piece of work. I also thank the scientists and officials from the countries included in this project for their interest and valuable advice in putting it together. I hope this report will inform this key debate on one of the greatest threats to humanity.

The Rt Hon. Chris Huhne MP, Secretary of State for Energy and Climate Change



There is already strong scientific evidence that the climate has changed and will continue to change in future in response to human activities. Across the world, this is already being felt as changes to the local weather that people experience every day.

Our ability to provide useful information to help everyone understand how their environment has changed, and plan for future, is improving all the time. But there is still a long way to go. These reports – led by the Met Office Hadley Centre in collaboration with many institutes and scientists around the world – aim to provide useful, up to date and impartial information, based on the best climate science now available. This new scientific material will also contribute to the next assessment from the Intergovernmental Panel on Climate Change.

However, we must also remember that while we can provide a lot of useful information, a great many uncertainties remain. That's why I have put in place a long-term strategy at the Met Office to work ever more closely with scientists across the world. Together, we'll look for ways to combine more and better observations of the real world with improved computer models of the weather and climate; which, over time, will lead to even more detailed and confident advice being issued.

Julia Slingo, Met Office Chief Scientist

Introduction

Understanding the potential impacts of climate change is essential for informing both adaptation strategies and actions to avoid dangerous levels of climate change. A range of valuable national studies have been carried out and published, and the Intergovernmental Panel on Climate Change (IPCC) has collated and reported impacts at the global and regional scales. But assessing the impacts is scientifically challenging and has, until now, been fragmented. To date, only a limited amount of information about past climate change and its future impacts has been available at national level, while approaches to the science itself have varied between countries.

In April 2011, the Met Office Hadley Centre was asked by the United Kingdom's Secretary of State for Energy and Climate Change to compile scientifically robust and impartial information on the physical impacts of climate change for more than 20 countries. This was done using a consistent set of scenarios and as a pilot to a more comprehensive study of climate impacts. A report on the observations, projections and impacts of climate change has been prepared for each country. These provide up to date science on how the climate has already changed and the potential consequences of future changes. These reports complement those published by the IPCC as well as the more detailed climate change and impact studies published nationally.

Each report contains:

- A description of key features of national weather and climate, including an analysis of new data on extreme events.
- An assessment of the extent to which increases in greenhouse gases and aerosols in the atmosphere have altered the probability of particular seasonal temperatures compared to pre-industrial times, using a technique called 'fraction of attributable risk.'
- A prediction of future climate conditions, based on the climate model projections used in the Fourth Assessment Report from the IPCC.
- The potential impacts of climate change, based on results from the UK's Avoiding Dangerous Climate Change programme (AVOID) and supporting literature.
For details visit: <http://www.avoid.uk.net>

The assessment of impacts at the national level, both for the AVOID programme results and the cited supporting literature, were mostly based on global studies. This was to ensure consistency, whilst recognising that this might not always provide enough focus on impacts of most relevance to a particular country. Although time available for the project was short, generally all the material available to the researchers in the project was used, unless there were good scientific reasons for not doing so. For example, some impacts areas were omitted, such as many of those associated with human health. In this case, these impacts are strongly dependant on local factors and do not easily lend themselves to the globally consistent framework used. No attempt was made to include the effect of future adaptation actions in the assessment of potential impacts. Typically, some, but not all, of the impacts are avoided by limiting global average warming to no more than 2 °C.

The Met Office Hadley Centre gratefully acknowledges the input that organisations and individuals from these countries have contributed to this study. Many nations contributed references to the literature analysis component of the project and helped to review earlier versions of these reports.

We welcome feedback and expect these reports to evolve over time. For the latest version of this report, details of how to reference it, and to provide feedback to the project team, please see the website at www.metoffice.gov.uk/climate-change/policy-relevant/obs-projections-impacts

In the longer term, we would welcome the opportunity to explore with other countries and organisations options for taking forward assessments of national level climate change impacts through international cooperation.

Summary

Climate observations

- There has been widespread warming over Russia since 1960 with increases in the frequency of warm days and nights and decreases in the frequency of cool days and nights.
- There is evidence for a general increase in seasonal temperatures averaged over the country as a result of human influence on climate, making the occurrence of warm seasonal temperatures more frequent and cold seasonal temperatures less frequent.
- Between 1960 and 2003, over western Russia there has been a widespread increase in annual total precipitation.

Climate change projections

- For the A1B emissions scenario projected changes in temperature are higher over northern parts of the country, with increases of above 5.5°C in the Arctic regions. In central parts of the country, increases range between around 4.5-5.5°C, and in southern and western regions, increases lie in the range of 3.5-4°C. There is moderate agreement between the CMIP3 models over most of Russia.
- The CMIP3 models project that precipitation will increase over almost the entire country. Increases of above 20% are projected in the north of the country, with most other regions projected to experience increases of between 10% and 20%. In the Caucasus region, projected precipitation change ranges from an increase of 5% to a decrease of 5%. Agreement between the CMIP3 model is high over most of the country, but more moderate in parts of the southwest.

Climate change impacts projections

Crop yields

- Whilst a definitive conclusion on the impact of climate change on crop yields in Russia cannot be drawn, the majority of global- and regional-scale studies included in this report project a decrease in the yield of wheat, Russia's major crop, as a consequence of climate change.

- Studies from the AVOID programme suggest a mixed outcome, with some areas of cultivated land becoming more suitable for agriculture, and other areas becoming less suitable, as a result of climate change.

Food security

- Russia is currently a country with extremely low levels of undernourishment. The majority of global- and regional-scale studies included here project that although negatively affected, the country is unlikely to face severe food security issues over the next 40 years as a consequence of climate change.
- National-scale assessments are consistent in showing that climate change could have a negative impact on food security in Russia.

Water stress and drought

- Global-scale studies included here show that the west of Russia is the most vulnerable region of the country to water stress. For the rest of the country and particularly the east, vulnerability is presently low.
- The majority of global-scale studies included here project an increase in water stress across the country as a whole with climate change, although there is regional variation.
- However, recent simulations from the AVOID programme show consensus across models for little change in the population exposed to increased or decreased water stress with climate change.

Pluvial flooding and rainfall

- Recent studies suggest that winter precipitation could increase for Russia under climate change, and there is consistency across different climate models in this change.
- Increases in precipitation from extreme storm events are also possible with climate change, although it is not possible to directly translate these into detailed pluvial flood projections.

Fluvial flooding

- Recent studies have suggested that flood magnitudes for Central and Eastern Siberia and the Russian Far East may increase with climate change, but decrease in European Russia and West Siberia, due to smaller maximum rates of snowmelt runoff.
- Results from simulations by the AVOID programme, show, a high level of agreement among climate models, that flood risk across Russia as a whole could decrease with climate change throughout the 21st century.
- Although most studies present a useful indicator of exposure to flood risk with climate change, none of them account for the effect that hydropower reservoirs, present in most large rivers, can have on the height of the annual flood peak, which can be substantial. Also, few studies have investigated the occurrence of ice dams and the potential resultant flooding with climate change.

Coastal regions

- There is very little work on the impact of climate change on Russia's coastal regions, however one study estimates that the population exposure to sea level rise (SLR) could increase from 189,000 in present to 226,000 under un-mitigated A1B emissions in 2070. Relative to A1B an aggressive mitigation policy could avoid an exposure of around 28,000 people by 2070.

Table of contents

Chapter 1 – Climate Observations	7
Rationale	8
Climate overview	10
Analysis of long-term features in the mean temperature	11
Temperature extremes	13
Recent extreme temperature events	14
Extreme Siberian winter, December 2000-February 2001	14
Cold spell, January 2006.....	15
Heat wave, July-August 2010	15
Analysis of long-term features in moderate temperature extremes	15
Attribution of changes in likelihood of occurrence of seasonal mean temperatures	21
Winter 2000/01.....	21
Winter 2005/06.....	21
Summer 2010.....	22
Precipitation extremes	24
Recent extreme precipitation events	26
Flooding, June 2002.....	26
Drought, August 2008	26
Analysis of precipitation extremes from 1960	26
Summary	31
Methodology annex	32
Recent, notable extremes.....	32
Observational record	33
Analysis of seasonal mean temperature	33
Analysis of temperature and precipitation extremes using indices	34
Presentation of extremes of temperature and precipitation	43
Attribution.....	46
References	49
Acknowledgements	53
Chapter 2 – Climate Change Projections	55
Introduction	56
Climate projections	58
Summary of temperature change in Russia	59
Summary of precipitation change in Russia	59
Chapter 3 – Climate Change Impact Projections	61
Introduction	62
Aims and approach.....	62
Impact sectors considered and methods	62
Supporting literature	63
AVOID programme results.....	63
Uncertainty in climate change impact assessment.....	64
Summary of findings for each sector	69
Crop yields	72
Headline.....	72
Supporting literature	72
Introduction	72
Assessments that include a global or regional perspective	73
National-scale or sub-national scale assessments	77
AVOID programme results.....	79

Methodology.....	79
Results	80
Food security	82
Headline.....	82
Supporting literature	82
Introduction	82
Assessments that include a global or regional perspective	83
National-scale or sub-national scale assessments	93
Water stress and drought	97
Headline.....	97
Supporting literature	97
Introduction	97
Assessments that include a global or regional perspective	98
National-scale or sub-national scale assessments	107
AVOID Programme Results	109
Methodology.....	109
Pluvial flooding and rainfall	111
Headline.....	111
Supporting literature	111
Introduction	111
Assessments that include a global or regional perspective	111
National-scale or sub-national scale assessments	112
Fluvial flooding	114
Headline.....	114
Supporting literature	114
Introduction	114
Assessments that include a global or regional perspective	115
National-scale or sub-national scale assessments	117
AVOID programme results.....	117
Methodology.....	117
Results	118
Tropical cyclones.....	120
Coastal regions	121
Headline.....	121
Assessments that include a global or regional perspective	121
National-scale or sub-national scale assessments	127
References.....	128

Chapter 1 – Climate Observations

Rationale

Present day weather and climate play a fundamental role in the day to day running of society. Seasonal phenomena may be advantageous and depended upon for sectors such as farming or tourism. Other events, especially extreme ones, can sometimes have

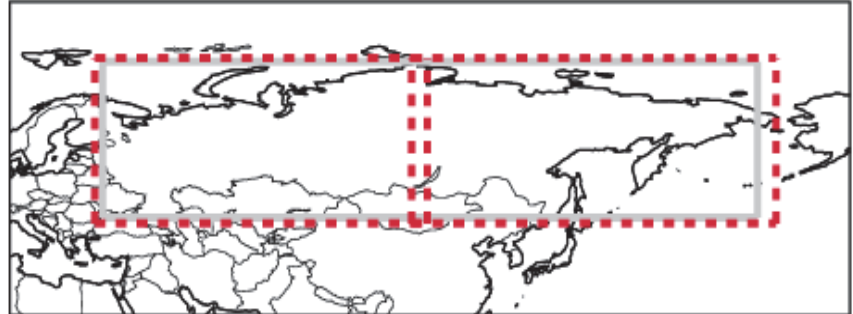


Figure 1. Location of boxes for the regional average time series (red dashed box) in Figures 2 and 3 and the attribution region (grey box) in Figures 4, 5 and 6.

serious negative impacts posing risks to life and infrastructure, and significant cost to the economy. Understanding the frequency and magnitude of these phenomena, when they pose risks or when they can be advantageous and for which sectors of society, can significantly improve societal resilience. In a changing climate it is highly valuable to understand possible future changes in both potentially hazardous events and those reoccurring seasonal events that are depended upon by sectors such as agriculture and tourism. However, in order to put potential future changes in context, the present day must first be well understood both in terms of common seasonal phenomena and extremes.

The purpose of this chapter is to summarise the weather and climate from 1960 to present day. This begins with a general climate overview including an up to date analysis of changes in surface mean temperature. These changes may be the result of a number of factors including climate change, natural variability and changes in land use. There is then a focus on extremes of temperature and precipitation selected from 2000 onwards, reported in the World Meteorological Organization (WMO) Annual Statement on the Status of the Global Climate and/or the Bulletin of the American Meteorological Society (BAMS) State of the Climate reports. This is followed by a discussion of changes in moderate extremes from 1960 onwards using an updated version of the HadEX extremes database (Alexander et al., 2006) which categorises extremes of temperature and precipitation. These are core climate variables which have received significant effort from the climate research community in terms of data acquisition and processing and for which it is possible to produce long high quality records for monitoring. For seasonal temperature extremes, an attribution analysis then puts the seasons with highlighted extreme events into context of the recent climate versus a hypothetical climate in the absence of anthropogenic emissions (Christidis et al.,

2011). It is important to note that we carry out our attribution analyses on seasonal mean temperatures over the entire country. Therefore these analyses do not attempt to attribute the changed likelihood of individual extreme events. The relationship between extreme events and the large scale mean temperature is likely to be complex, potentially being influenced by *inter alia* circulation changes, a greater expression of natural internal variability at smaller scales, and local processes and feedbacks. Attribution of individual extreme events is an area of developing science. The work presented here is the foundation of future plans to systematically address the region's present and projected future weather and climate and the associated impacts.

The methodology section that follows provides details of the data shown here and of the scientific analyses underlying the discussions of changes in the mean temperature and in temperature and precipitation extremes. It also explains the methods used to attribute the likelihood of occurrence of seasonal mean temperatures.

Climate overview

The most well known feature of the Russian climate is its very cold winter, brought about by the country's high latitudes (40-75°N), vast land mass and lack of any topographic obstructions to protect it from arctic winds sweeping across its long, north-facing and often frozen coastline. The country is bounded by high mountains along its southern and eastern flank but the west is exposed to occasional winter incursions of milder Atlantic air, so that winters become progressively more severe eastwards. Average daily maximum temperatures along, approximately, the 55°N line of latitude in January are -6°C in Moscow (longitude 38°E), -11°C at Chelyabinsk (61°E), -12°C at Novosibirsk (84°E) and -14°C at Irkutsk (105°E), with even lower values further north. During the winter, an intense area of high pressure develops over particularly the Asian part of Russia, with intensely cold air spiralling out from it to affect countries well beyond Russia's boundaries.

However, the extreme continental nature of the Russian climate means that the difference between mid-winter and mid-summer monthly mean temperature is large and typically at least 30°C, so that summers are warm even, for a short time, within the Arctic Circle. For instance coastal Archangel'sk at 64.5°N has typical July daily maxima of 21°C. In southern Russia, and in some years elsewhere, summer is hot – e.g. Astrakhan, at 46°N near the Caspian Sea, has typical July daily maxima of 31-32°C. Annual mean temperatures are, nonetheless, quite low, for instance (in a north-south line from 65°N to 46°N) 1°C at Archangelsk, 5°C at Moscow and 10°C at Astrakhan. The transition from winter to summer and from summer back to winter is very quick so that effectively there are only 2 seasons over most of Russia.

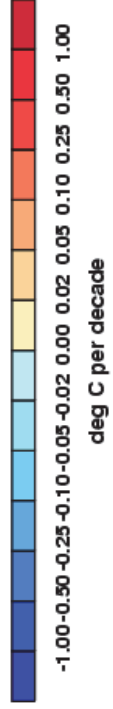
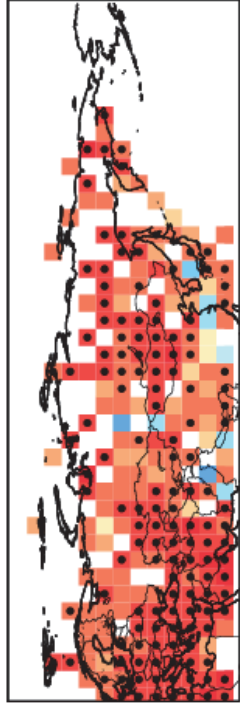
Annual precipitation is mostly not particularly high and is spread throughout the year with a summer convective peak. Examples of annual average precipitation are 690mm at Moscow but only 400-500 mm further east at Chelybinsk, Novosibirsk and Irkutsk. Annual average precipitation typically becomes very low towards the most southerly parts of Russia, for instance only 213 mm at Astrakhan. A small portion of Russia along its eastern (Pacific) seaboard, characterised by Vladivostock, has rather more rainfall in summer, brought about by the Asian summer monsoon in which low pressure develops over the heated land mass of Asia and causes moist winds to blow onshore. Most winter precipitation in Russia falls as snow but this, though frequent, is rarely very heavy and strong winds often sweep the ground bare of snow.

In the north and east of Siberia (Asiatic Russia) a phenomenon known as permafrost occurs in which the subsoil remains frozen all year, causing special issues to the construction industry, even though the topsoil thaws in summer. Other weather hazards in Russia include floods and extremes of heat and cold.

Analysis of long-term features in the mean temperature

CRUTEM3 data (Brohan et al., 2006) have been used to provide an analysis of mean temperatures from 1960 to 2010 over Russia using the median of pairwise slopes method to fit the trend (Sen, 1968; Lanzante, 1996). The methods are fully described in the methodology section. In agreement with increasing global average temperatures (Sánchez-Lugo et al., 2011), over the period 1960 to 2010 there is a geographically widespread warming signal over Russia as shown in Figure 2, consistent with previous research (UNFCCC, 2010). Grid boxes in which the 5th to 95th percentiles of the slopes are of the same sign can be more confidently regarded as showing a signal different to zero trend. There is higher confidence in this warming signal for a number of grid boxes in summer (June to August), mostly towards the south. For winter (December to February) confidence in the grid box signals is lower for the majority of grid boxes. There are few data over the northern and eastern regions. Here, cooling is shown in winter but there is lower confidence in this signal. Regionally averaged trends (over grid boxes included in the red dashed box in Figure 1) calculated by the median of pairwise slopes show warming signals but with lower confidence. For winter this is 0.35 °C per decade (5th to 95th percentile of slopes: -0.08 to 0.71 °C per decade) and for summer this is 0.11 °C per decade (5th to 95th percentile of slopes: -0.01 to 0.23 °C per decade).

JJA



DJF

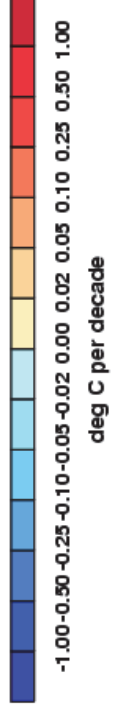
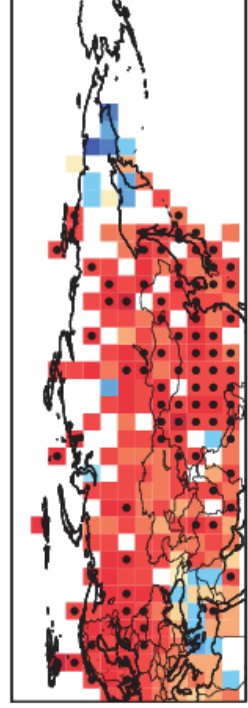


Figure 2. Decadal trends in seasonally averaged temperatures for Russia and the surrounding regions over the period 1960 to 2010. Monthly mean anomalies from CRUTEM3 (Brohan et al., 2006) are averaged over each 3 month season (June-July-August – JJA and December-January-February – DJF). Trends are fitted using the median of pairwise slopes method (Sen, 1968; Lanzante, 1996). There is high confidence in the trends shown if the 5th to 95th percentiles of the pairwise slopes do not encompass zero because here the trend is considered to be significantly different from a zero trend (no change). This is shown by a black dot in the centre of the respective grid-box.

Temperature extremes

Both hot and cold temperature extremes can place many demands on society. While seasonal changes in temperature are normal and indeed important for a number of societal sectors (e.g. tourism, farming etc.), extreme heat or cold can have serious negative impacts. Importantly, what is 'normal' for one region may be extreme for another region that is less well adapted to such temperatures.

Table 1 shows extreme events since 2000 that are reported in WMO Statements on Status of the Global Climate and/or BAMS State of the Climate reports. Two periods of extreme cold, the winters of 2001 and 2006, and one of extreme heat, summer 2010, are highlighted below as examples of recent extreme temperature events that have affected Russia.

Year	Month	Event	Details	Source
2000	May	Cold	Western regions experienced temperatures 4-5 °C colder than normal.	WMO (2001)
2001	Dec '00- Feb '01	Cold	Siberia/Mongolia/E Russia had a severe winter, with temperatures dropping to -60 °C in January.	WMO (2002)
2002	Jan-Feb	Warm	In S. Siberia temperatures were up to 10 °C higher than normal in January. Across SE Siberia warm records were broken in February.	BAMS (Bulygina et al., 2003)
2002	Dec	Cold	Central and southern European Russia experienced the coldest mean monthly temperature in 70 years.	BAMS (Bulygina et al., 2003)
2003	Jan	Cold	In NW Russia temperatures dropped to -45 °C.	WMO (2004)
2003	Jun	Cold	European Russia experienced one of coldest Junes in 100 years. Lowest ever June temperatures recorded at some stations, with June temperatures typically 3-4 °C lower than normal.	BAMS (Bulygina, 2004)
2005	Feb	Cold	Republic of Tuva had the most severe frosts in 20 years. Temperatures dropped to -48 °C.	BAMS (Bulygina et al., 2006)
2005	Mar	Cold	European Russia experienced record cold monthly means in some places.	BAMS (Bulygina et al., 2006)
2005	May	Heat	Ural Federal District had the warmest May in 105 years.	BAMS (Bulygina et al., 2006)

(Table 1 continued)

Year	Month	Event	Details	Source
2005	Jul	Heat wave	Western and southern-central regions of Siberia recorded temperatures reaching 39 °C.	BAMS (Bulygina et al., 2006)
2006	Jan	Cold	Western Russian Federation experienced the coldest Moscow temperatures for 30 years. Western Siberia had record-breaking low monthly mean temperatures. Lowest temperatures across Russia reached -58.5 °C.	WMO (2007), BAMS (Bulygina et al., 2007)
2006	Aug	Heat wave	Southern Federal District recorded temperatures reaching 37–43 °C.	BAMS (Bulygina et al., 2007)
2007	May	Heat wave	The highest temperatures recorded in Moscow since 1891. Temperatures reached 38-39 °C in the Volgograd Region and north of the Astrakhan Region.	WMO (2008), BAMS (Bulygina et al., 2008)
2008	Aug	Heat wave	Southern European Russia recorded maximum temperatures exceeding 30 °C for 24-25 days. Highest temperatures reached 36-40 °C.	BAMS (Bulygina et al., 2009)
2009	Feb	Cold	Russian Federation recorded temperatures 3-6 °C colder than normal.	WMO (2009)
2009	Jul	Heat wave	European Russia recorded air temperatures of 40-42 °C in Volgograd and Astrakhan regions.	BAMS (Bulygina et al., 2010)
2010	Jun-Aug	Heat wave	Hottest summer on record. Most extreme in western Russia. Moscow had record high temperature of 38.2 °C.	WMO (2011)

Table 1. Extreme temperature events reported in WMO Statements on Status of the Global Climate and/or BAMS State of the Climate reports since 2000.

Recent extreme temperature events

Extreme Siberian winter, December 2000-February 2001

Siberia, the far east of Russia, and Mongolia experienced a particularly severe winter season. The anomalously cold conditions began in November and, for Siberia, this was the coldest November-January period for 30 years (Waple et al., 2002). In January, Some areas in central and southern Siberia experienced minimum temperatures of -60 °C (WMO, 2002). High energy demand and fuel prices led to power cuts, and cold-related illnesses, such as frostbite and hypothermia, were more common than usual (Waple et al., 2002). The cold conditions were not confined to Siberia and temperatures were reported to be more than

3 °C colder than normal across much of Russia; in Moscow, hypothermia resulted in more than 100 deaths (WMO, 2002).

Cold spell, January 2006

During the early part of 2006, much of Russia experienced very cold temperatures and severe frosts. Monthly mean low temperature records were broken in parts of western Siberia. Nationwide, the lowest temperature recorded was -58.5 °C on 30th January in the Evenki Autonomous Area (Bulygina et al., 2007). January 2006 also saw Moscow experience its coldest temperatures in 30 years (WMO, 2007).

Heat wave, July-August 2010

From early July through to the first half of August western Russia experienced an intense heat wave, having already been subject to significantly above average temperature in the previous 2 months. In Moscow, temperatures were 7.6 °C above average for July, making it the hottest July on record by 2 °C. On 29th July, Moscow recorded its hottest ever temperature of 38.2 °C. There were also 33 consecutive days above 30 °C in the city (WMO, 2011). Around 14,000 deaths resulted from the summer heat, with half of them in and around Moscow alone (Maier et al., 2011).

The heat was accompanied by destructive forest fires, leaving thousands of people homeless. The wildfires combined with the severe drought conditions, particularly in the Volga region, led to widespread crop failures, where over 20% of Russian crops were destroyed. Economic losses amounted to US\$15 billion (WMO, 2011; Maier et al., 2011).

Analysis of long-term features in moderate temperature extremes

ECA&D data (Klein Tank et al., 2002) have been used to update the HadEX extremes analysis for Russia from 1960 to 2010 using daily maximum and minimum temperatures. Here we discuss changes in the frequency of cool days and nights and warm days and nights which are moderate extremes. Cool days/nights are defined as being below the 10th percentile of daily maximum/minimum temperature and warm days/nights are defined as being above the 90th percentile of the daily maximum/minimum temperature. The methods are fully described in the methodology section.

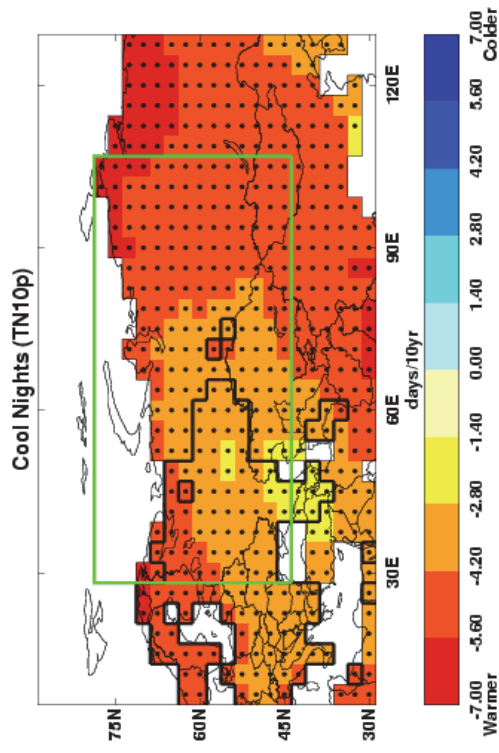
Between 1960 and 2009, there have been widespread increases in the frequency of warm days/nights and decreases in the frequency of cool days/nights, in agreement with warming

mean temperature (Figure 3) and previous research (UNFCCC, 2010). There is high confidence that this signal is different to zero for a high proportion of grid boxes, especially for the nights. The data presented here are annual totals, averaged across all seasons, and so direct interpretation in terms of summer heat waves and winter cold snaps is not possible.

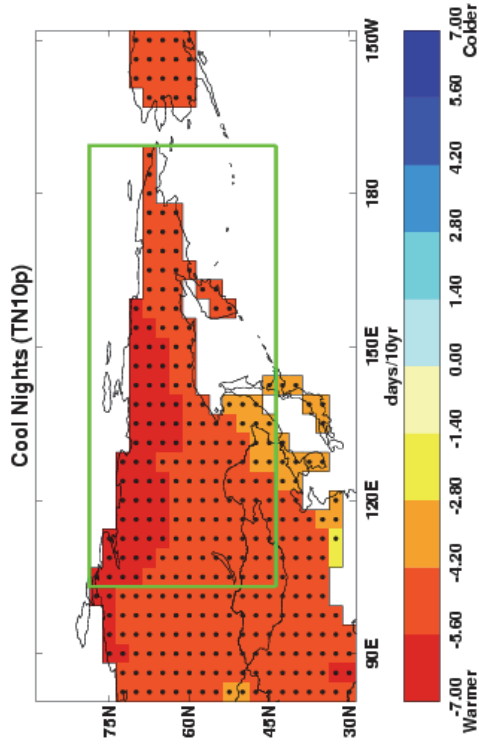
Night-time temperatures (daily minima) show spatially consistent decreasing cool night frequency and increasing warm night frequency (Figure 3 a,b,c,d). Higher confidence in these signals is widespread although limited to central and eastern regions for decreasing cool nights. Regional averages, both for eastern and western Russia, concur with higher confidence in these signals.

Daytime temperatures (daily maxima) show spatially consistent decreasing cool day frequency and increasing warm day frequency (Figure 3 e,f,g,h). Higher confidence in these signals is widespread although not ubiquitous. Regional averages, both for eastern and western Russia, concur with higher confidence in these signals.

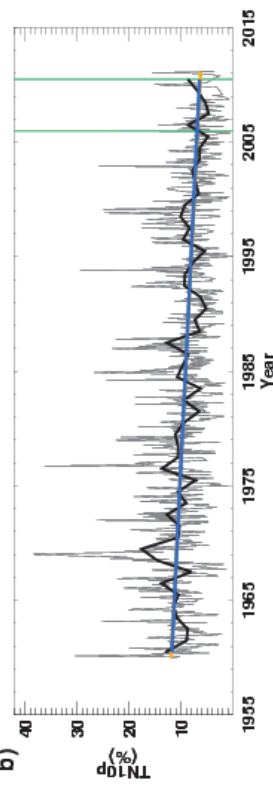
a)



a)

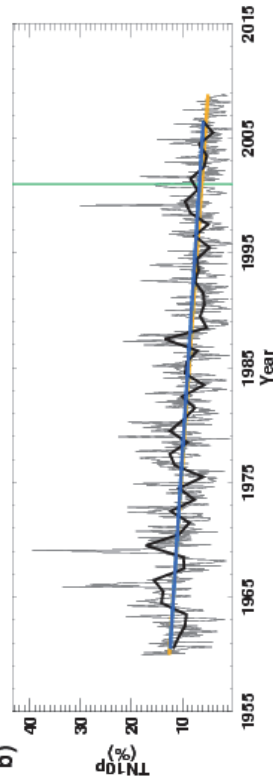


b)



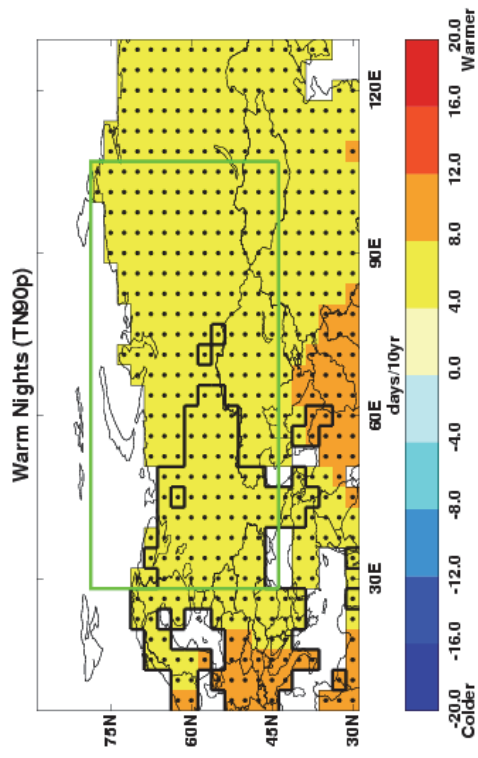
Monthly: -1.11% per decade (-1.36 to -0.86)
 Total change of -5.56% from 1960 to 2011 (-6.80% to -4.30%)
 Annual: -1.07% per decade (-1.50 to -0.65)
 Total change of -5.36% from 1960 to 2010 (-7.51% to -3.24%)

b)

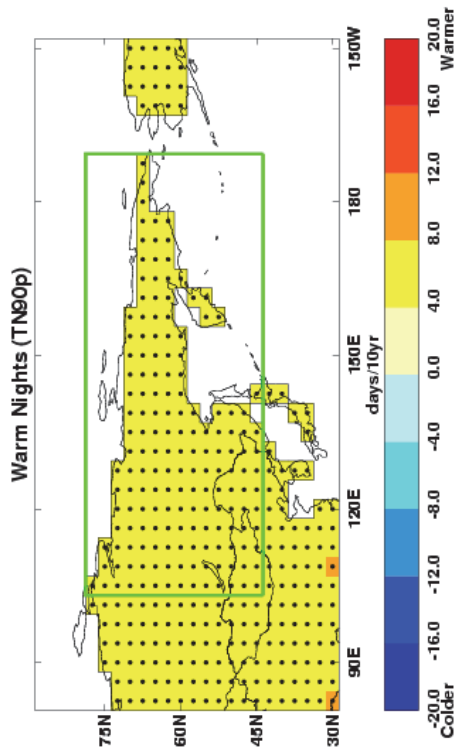


Monthly: -1.55% per decade (-1.80 to -1.31)
 Total change of -6.22% from 1960 to 2008 (-7.21% to -5.24%)
 Annual: -1.42% per decade (-1.95 to -0.94)
 Total change of -5.68% from 1960 to 2006 (-7.81% to -3.75%)

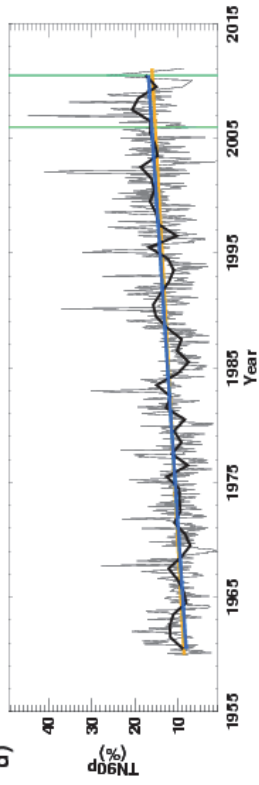
c)



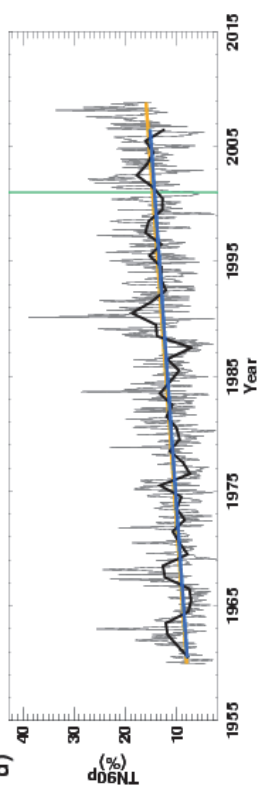
c)



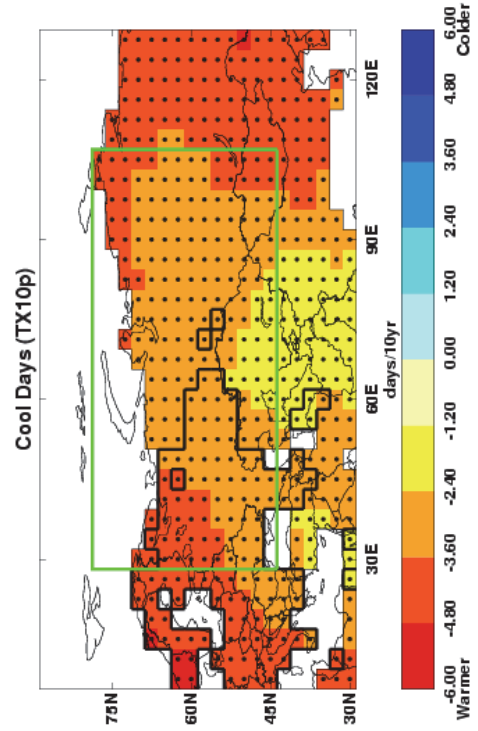
d)



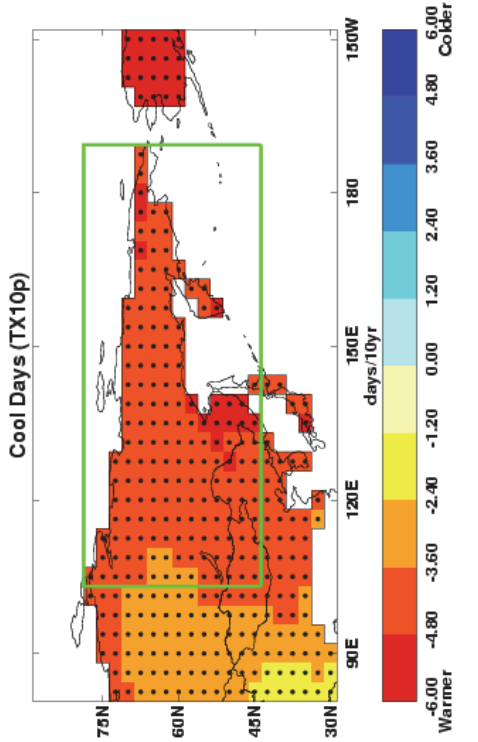
d)



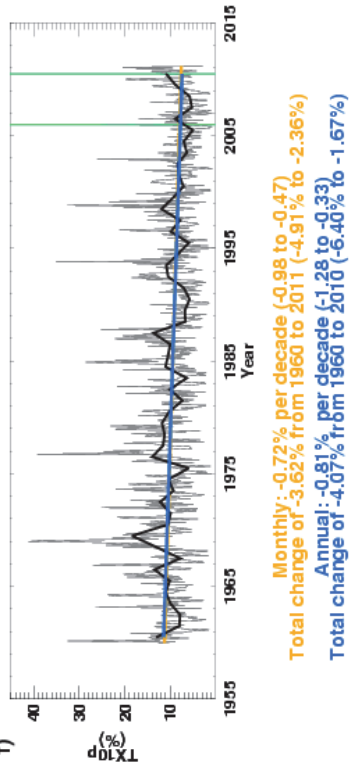
e)



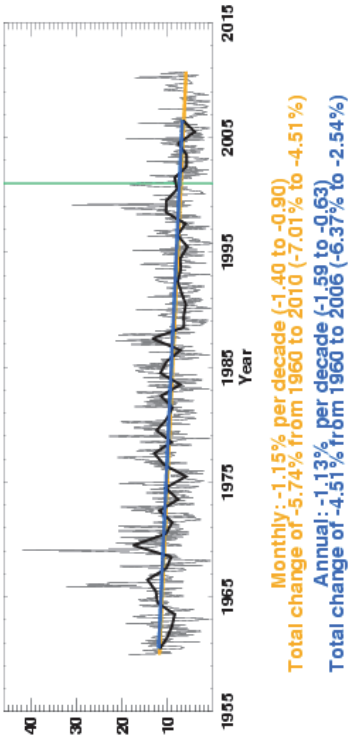
e)



f)



f)



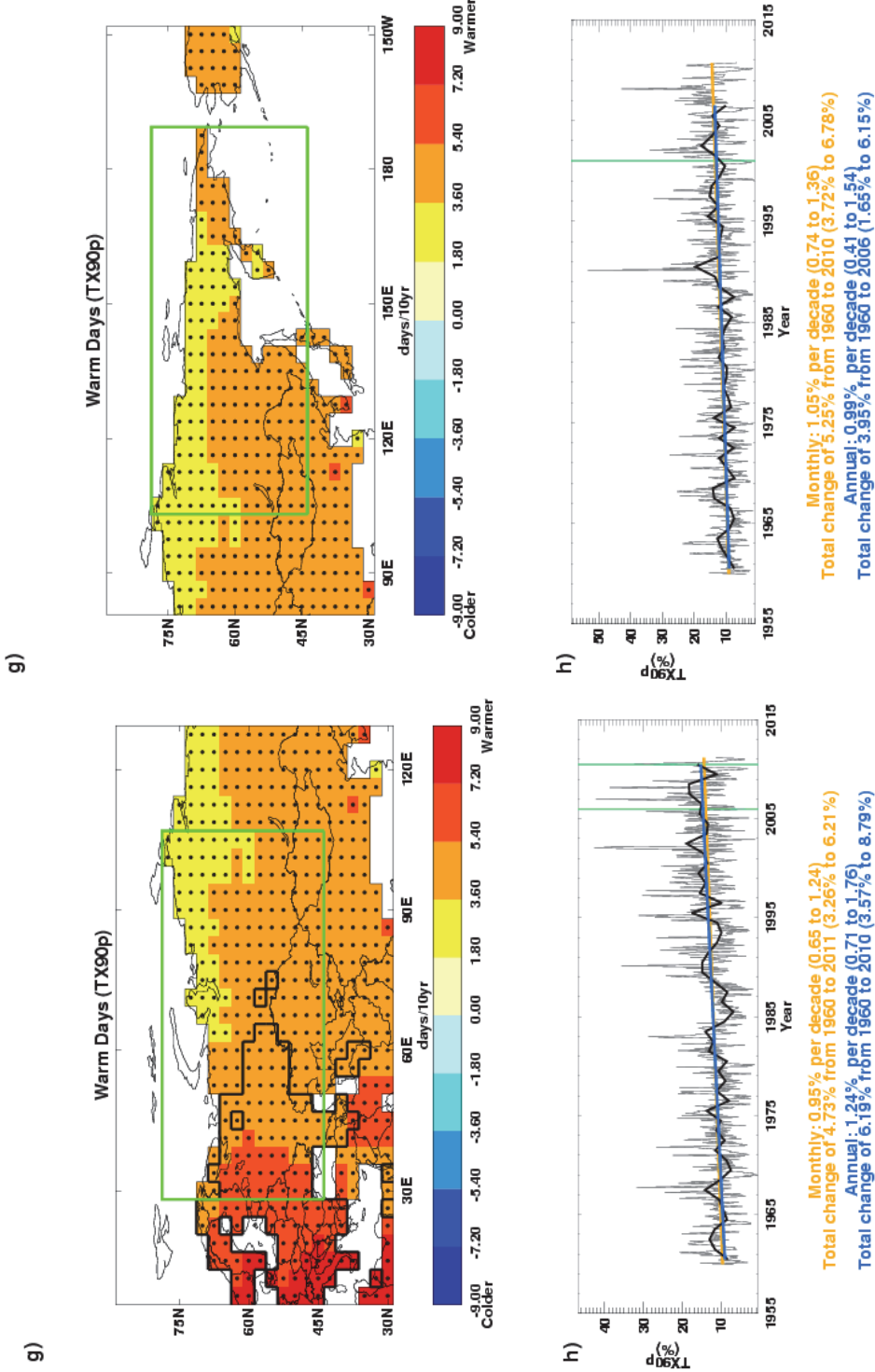


Figure 3. Change in cool nights (a,b), warm nights (c,d), cool days (e,f) and warm days (g,h) for Russia (split into eastern and western halves for clarity) over the period 1960 to 2010 relative to 1961–1990 from the ECA&D dataset (Klein Tank et al., 2002). a,c,e,g) Grid-box decadal trends. Grid-boxes outlined in solid black contain at least 3 stations and so are likely to be more representative of the wider grid box. Trends are fitted using the median of pairwise slopes method (Sen, 1968; Lanzante, 1996). Higher confidence in a long-term trend is shown by a black dot if the 5th to 95th percentile slopes are of the same sign. Differences in spatial coverage occur because each index has its own decorrelation length scale (see methodology section). b,d,f,h) Area averaged annual time series for West: 28.125° to 106.875° E 43.75° to 78.75° N, East: 103.125° to 189.375° E and 43.75° to 78.75° N as shown by the green boxes on the map and red boxes in Figure 1. Thin and thick black lines show the monthly and annual variations respectively. Monthly (orange) and annual (blue) trends are fitted as described above. The decadal trend and its 5th to 95th percentile confidence intervals are stated along with the change over the period for which there are data available. All the trends have higher confidence that they are different from zero as their 5th to 95th percentile slopes are of the same sign. The green vertical lines show the dates of the heat wave in 2010 and the cold spell in 2006 for western Russia, and the cold snap in 2000/01 for eastern Russia.

Attribution of changes in likelihood of occurrence of seasonal mean temperatures

Today's climate covers a range of likely extremes. Recent research has shown that the temperature distribution of seasonal means would likely be different in the absence of anthropogenic emissions (Christidis et al., 2011). Here we discuss the seasonal means, within which the highlighted extreme temperature events occur, in the context of recent climate and the influence of anthropogenic emissions on that climate. The methods are fully described in the methodology section.

Winter 2000/01

The distributions of the December-January-February (DJF) mean regional temperature in recent years in the presence and absence of anthropogenic forcings are shown in Figure 4. Analyses with both models suggest that human influences on the climate have shifted the distribution to higher temperatures. Considering the average over the entire region, the 2000/01 winter is cold, as it lies in the cold tail of the temperature distributions for the climate influenced by anthropogenic forcings (distributions plotted in red). In the absence of human influences on the climate (green distributions) the season would be less extreme, as it lies in the central sector of the temperature distribution. The winter of 2000/01 is also considerably warmer than the one in 1968/69, the coldest in the CRUTEM3 dataset. The attribution results shown here refer to temperature anomalies over the entire region and over an entire season, and do not rule out the occurrence of a cold extreme event that has a shorter duration and affects a smaller region.

Winter 2005/06

The observed anomaly in winter 2005/06 is also shown in Figure 4. Considering the average over the entire region, the 2005/06 winter is cold, as it lies in the cold tail of the temperature distributions for the climate influenced by anthropogenic forcings (distributions plotted in red). In the absence of human influences on the climate (green distributions) the season would be less extreme, as it lies in the central sector of the temperature distribution. The winter of 2005/06 is also considerably warmer than the winter of 1968/69, the coldest in the CRUTEM3 dataset.

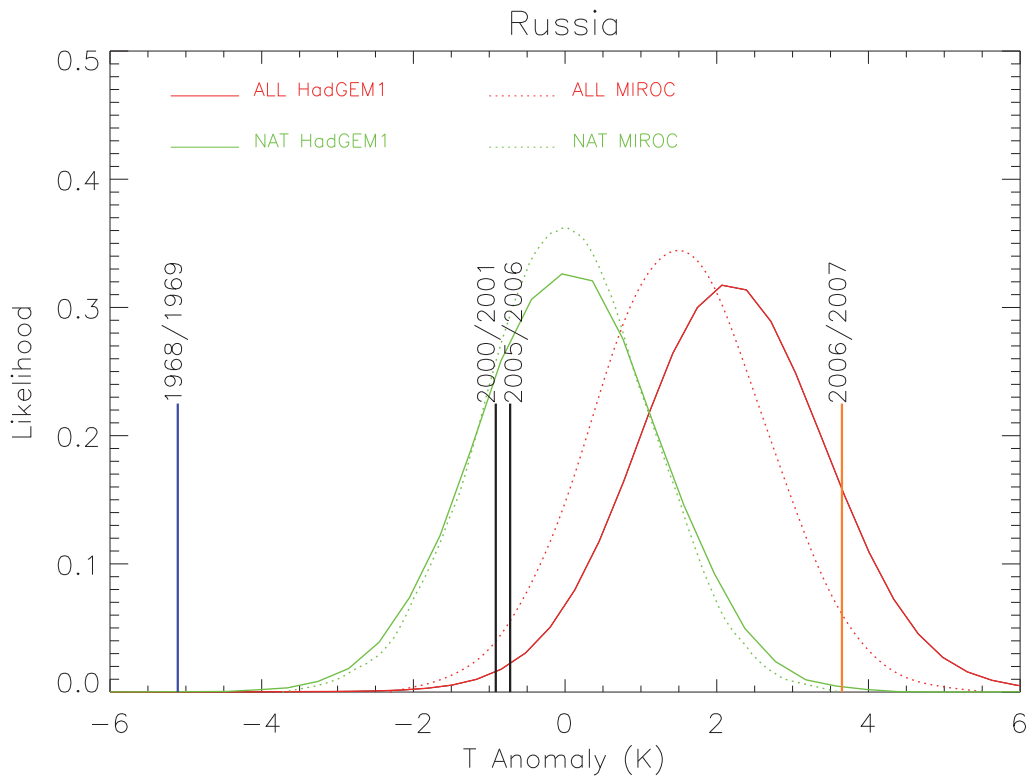


Figure 4. Distributions of the December-January-February mean temperature anomalies (relative to 1961-1990) averaged over the Russian region (30-185E, 45-78N – as shown in Figure 1) including (red lines) and excluding (green lines) the influence of anthropogenic forcings. The distributions describe the seasonal mean temperatures expected in recent years (2000-2009) and are based on analyses with the HadGEM1 (solid lines) and MIROC (dotted lines) models. The vertical black lines mark the observed anomalies in 2000/01 and 2005/06. The vertical orange and blue lines correspond to the maximum and minimum anomaly in the CRUTEM3 dataset since 1900 respectively.

Summer 2010

The distributions of the summer mean regional temperature in recent years in the presence and absence of anthropogenic forcings are shown in Figure 5. Analyses with both models suggest that human influences on the climate have shifted the distribution to higher temperatures. Considering the average over the entire region, the 2010 summer is hot, as it lies in the warm tail of the temperature distributions for the climate influenced by anthropogenic forcings (red distributions) and is also the hottest in the CRUTEM3 dataset. In the absence of human influences on the climate (green distributions), the season would be even more extreme. It should be noted that the attribution results shown here refer to temperature anomalies over the entire region and over an entire season, whereas the actual extreme event had a shorter duration and affected a smaller region.

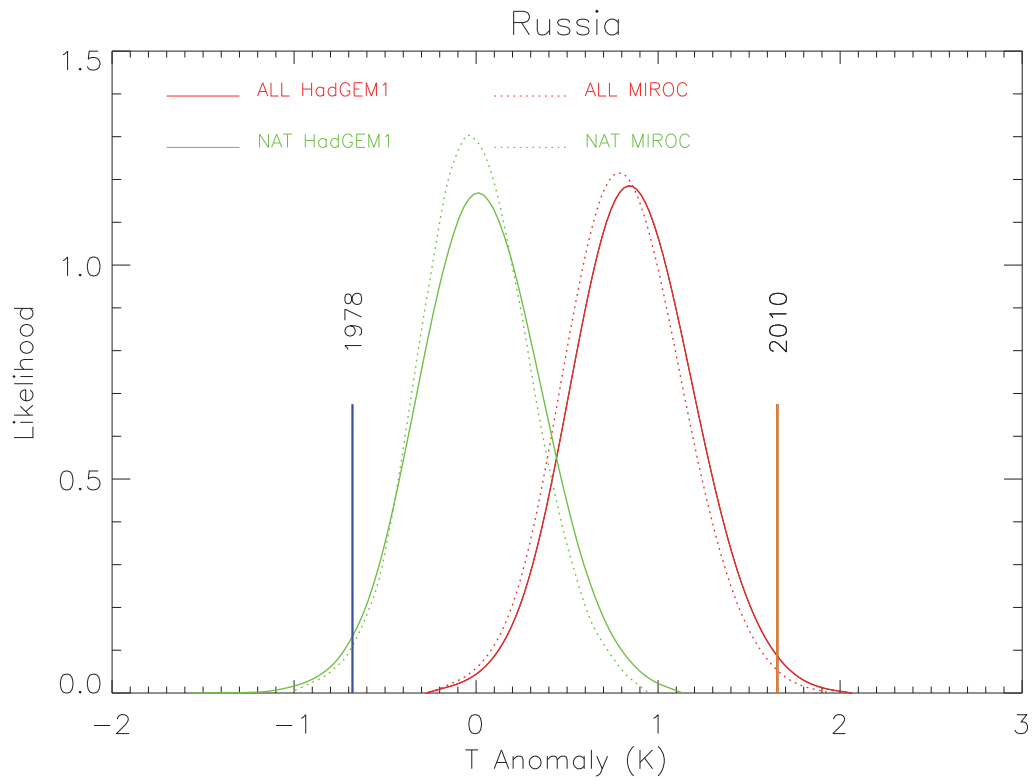


Figure 5. Distributions of the June-July-August mean temperature anomalies (relative to 1961-1990) averaged over the Russian region (30-185E, 45-78N) including (red lines) and excluding (green lines) the influence of anthropogenic forcings. The distributions describe the seasonal mean temperatures expected in recent years (2000-2009) and are based on analyses with the HadGEM1 (solid lines) and MIROC (dotted lines) models. The vertical orange and blue lines correspond to the maximum and minimum anomaly in the CRUTEM3 dataset since 1900 respectively.

Precipitation extremes

Precipitation extremes, either excess or deficit, can be hazardous to human health, societal infrastructure, and livestock and agriculture. While seasonal fluctuations in precipitation are normal and indeed important for a number of societal sectors (e.g. tourism, farming etc.), flooding or drought can have serious negative impacts. These are complex phenomena and often the result of accumulated excesses or deficits or other compounding factors such as spring snow-melt, high tides/storm surges or changes in land use. The analysis section below deals purely with precipitation amounts.

Table 2 shows selected extreme events since 2000 that are reported in WMO Statements on Status of the Global Climate and/or BAMS State of the Climate reports. The flooding in June 2002 and the drought in August 2008 are highlighted below as examples of recent extreme precipitation events that have affected Russia.

Year	Month	Event	Details	Source
2001	May	Flooding	In Siberia a warm May leads to rapid snow melt following very cold winter resulting in severe flooding. 300,000 homes damaged/destroyed in Yakutia.	WMO (2002)
2002	Jan	Flooding	Western North Caucasus experiences devastating floods	WMO (2003)
2002	Apr-Aug	Drought	Severe drought across central European Russia.	WMO (2003)
2002	Jun	Flooding	North Caucasian region experience flooding causing more than 100 fatalities.	BAMS (Bulygina et al., 2003)
2004	Apr	Flooding	Flooding in western Siberia. Northern Caucasus experiences severe damage to infrastructure and crops.	WMO (2005)
2005	Apr-May	Flooding	Southern parts of Russian Federation suffer from widespread floods and landslides, affecting 4000 people.	WMO (2006)
2005	Jun	Flooding	2-day 100-mm rainfall event leads to record June flood level for the Arkhara River, Amur.	BAMS (Bulygina et al., 2006)
2006	Apr	Flooding	Severe flooding in southwestern Siberia, caused 500 houses to be impounded, and many evacuated.	BAMS (Bulygina et al., 2007)
2006	Jun-Aug	Drought	Drought in the Rostov region, steppe zone of the Kabardino-Balkaria Republic, southern and Volga areas of the Volgograd region, republics of Mordovia, Chuvashia, and Udmurtia.	BAMS (Bulygina et al., 2007)
2007	May-Jul	Drought	Drought conditions prevailed in the Republic of North Ossetia-Alaniya in May, and Republic of North Ossetia-Alaniya in June/July.	BAMS (Bulygina et al., 2008)
2008	Aug	Drought	Southern European Russia suffered from a 31 day drought event.	BAMS (Bulygina et al., 2009)
2009	Jun	Flooding	Record high early season precipitation amounts in southern Sakhalin and the Ternei area of the Maritime Territory. Flooding in Dagestan, Northern Caucasia.	BAMS (Bulygina et al., 2010)
2010	Jun-Aug	Drought	Worst drought since 1972, exacerbated by intense summer heat wave.	WMO (2011)

Table 2. Extreme precipitation events reported in WMO Statements on Status of the Global Climate and/or BAMS State of the Climate reports since 2000.

Recent extreme precipitation events

Flooding, June 2002

The north Caucasian region experienced heavy rains from 20th to 23rd June which led to severe flooding. Almost all rivers of the Kuban and Terek basin flooded causing mud flows in mountain regions. The regions economy suffered damage due to this disaster which caused the deaths of over 100 people (Bulygina et al., 2003).

Drought, August 2008

Over most of Russia August was warm, with hot winds in the Altai Territory in early August. In southern European Russia the very hot and dry conditions continued through the second half of August. Some regions experienced maximum air temperatures above 30 °C for up to 25 days. The period was very dry, with less than 5 mm of precipitation for 31 days, resulting in prolonged drought conditions (Bulygina et al., 2009).

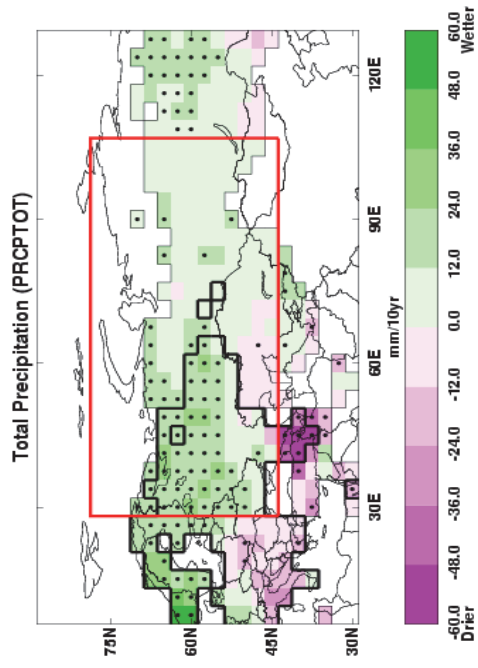
Analysis of precipitation extremes from 1960

ECA&D data (Klein Tank et al., 2002) have been used to update the HadEX extremes analysis for Russia from 1960 to 2010 for daily precipitation totals. Here we discuss changes in the annual total precipitation, and in the frequency of prolonged (greater than 6 days) wet and dry spells. The methods are fully described in the methodology section.

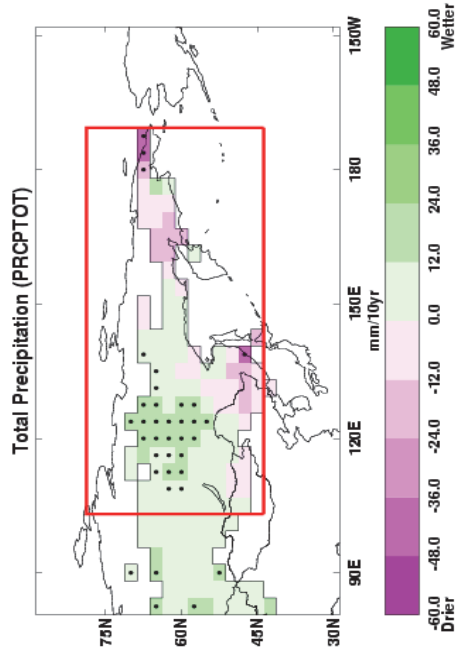
Between 1960 and 2003, over western Russia there has been a widespread increase in annual total precipitation. Confidence is higher in this change for some grid boxes than others, and also when regionally averaged (Figure 6). This is consistent with previous research that found increasing precipitation between 1978 and 2005 (UNFCCC, 2010) although with some seasonal differences. The signal shown here is more mixed for dry spell length and especially wet spell length where data-coverage is sparser. There are spatially consistent regions of both increasing and decreasing dry spell lengths but with low confidence that these trends are different from zero throughout. Over eastern Russia there have been spatially consistent increases and decreases in annual total precipitation although confidence is lower for the vast majority of grid boxes and when regionally averaged (Figure 6b). There is very poor coverage for wet spell length, but there is a more coherent signal, albeit weak, for dry spell length. Increasing dry spell length concurs with decreasing annual precipitation over the easternmost regions. Conversely, decreasing dry spell length concurs

with increasing annual precipitation further west – there is higher confidence in these signals for a number of grid boxes.

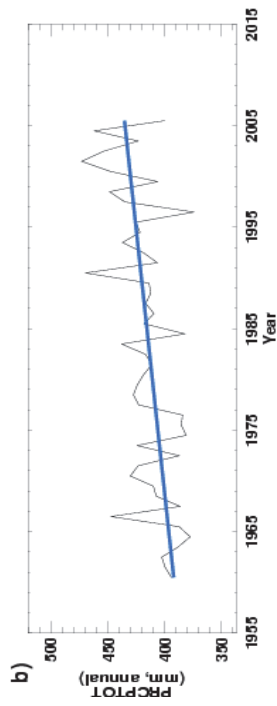
a)



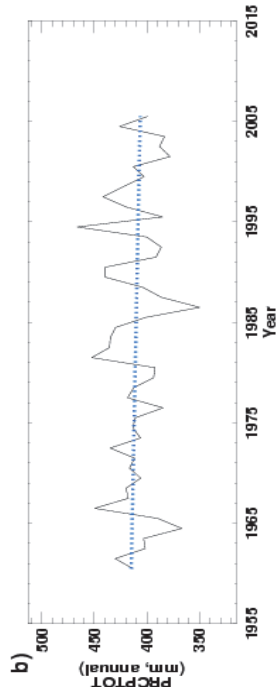
a)



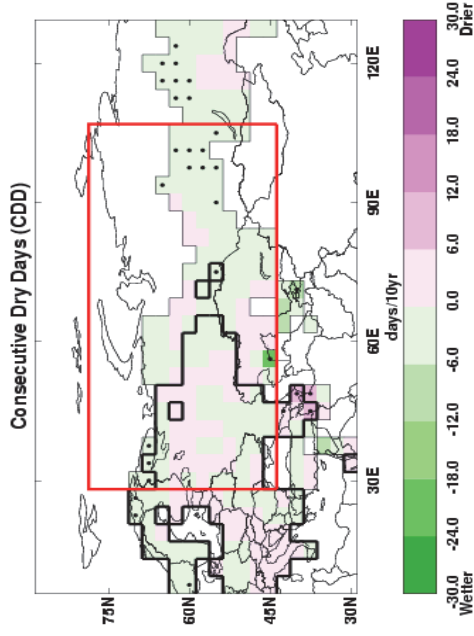
b)



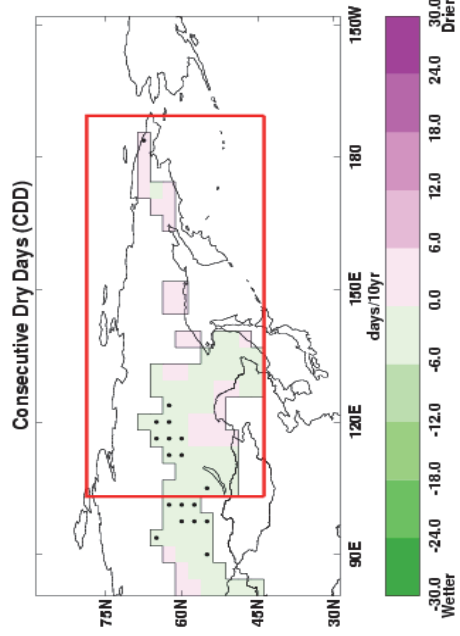
b)



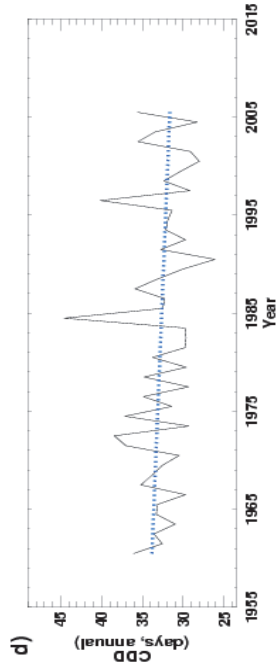
c)



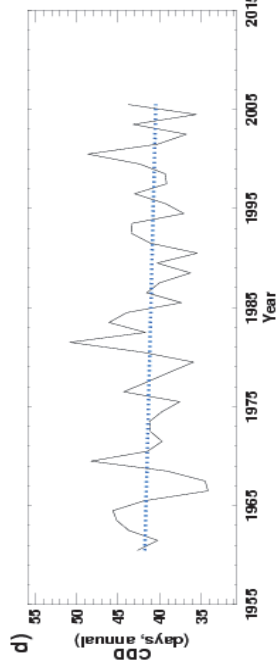
c)



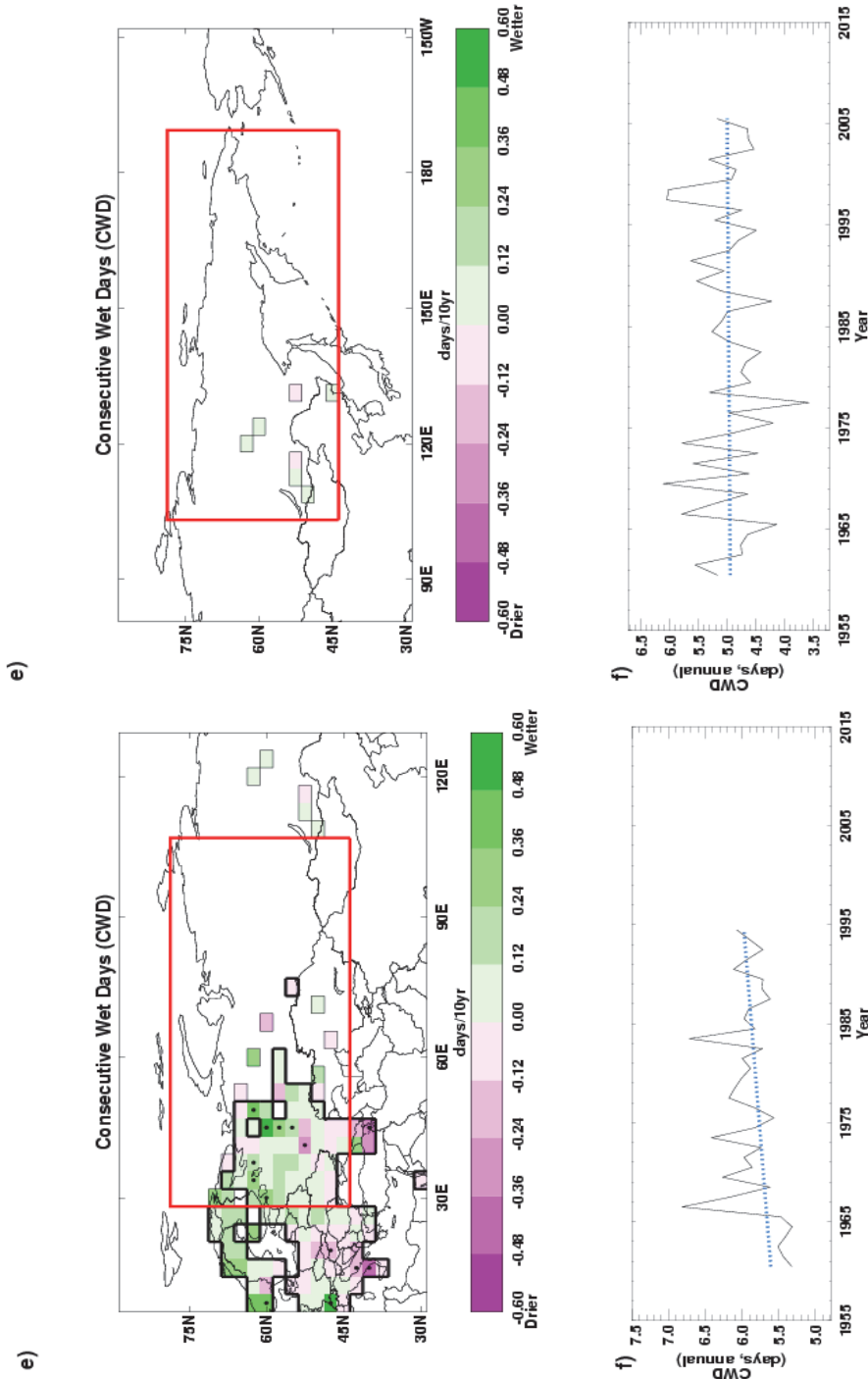
d)



Annual: -0.49days per decade (-1.23 to 0.15)
Total change of -1.95days from 1960 to 2005 (-4.92days to 0.62days)



Annual: -0.29days per decade (-0.98 to 0.65)
Total change of -1.17days from 1960 to 2005 (-3.90days to 2.59days)



Annual: 0.11 days per decade (-0.03 to 0.21)
 Total change of 0.32 days from 1960 to 1994 (-0.08 days to 0.64 days)

Annual: 0.01 days per decade (-0.12 to 0.14)
 Total change of 0.05 days from 1960 to 2005 (-0.48 days to 0.54 days)

Figure 6. The change in the annual total rainfall (a,b), the annual number of continuous dry days (c,d) and the annual number of continuous wet days (e,f) over the period 1960-2010. The maps and time series have been created in exactly the same way as Figure 3. Only annual regional averages are shown in b,d,f. Higher confidence in the trend, as defined above using the 5th and 9th percentiles, is shown as a solid line in b,d,f, lower confidence is shown with a dotted line.

Summary

The main features seen in observed climate over Russia from this analysis are:

- There has been widespread warming over Russia since 1960.
- Since 1960 there have been widespread increases in the frequency of warm days and nights and decreases in the frequency of cool days and nights.
- Model results indicate a general increase in seasonal temperatures averaged over the country as a result of human influence on climate, making the occurrence of warm seasonal temperatures more frequent and cold seasonal temperatures less frequent.
- Between 1960 and 2003, over western Russia there has been a widespread increase in annual total precipitation.

Methodology annex

Recent, notable extremes

In order to identify what is meant by 'recent' events the authors have used the period since 1994, when WMO Status of the Global Climate statements were available to the authors. However, where possible, the most notable events during the last 10 years have been chosen as these are most widely reported in the media, remain closest to the forefront of the memory of the country affected, and provide an example likely to be most relevant to today's society. By 'notable' the authors mean any event which has had significant impact either in terms of cost to the economy, loss of life, or displacement and long term impact on the population. In most cases the events of largest impact on the population have been chosen, however this is not always the case.

Tables of recent, notable extreme events have been provided for each country. These have been compiled using data from the World Meteorological Organisation (WMO) Annual Statements on the Status of the Global Climate. This is a yearly report which includes contributions from all the member countries, and therefore represents a global overview of events that have had importance on a national scale. The report does not claim to capture all events of significance, and consistency across the years of records available is variable. However, this database provides a concise yet broad account of extreme events per country. This data is then supplemented with accounts from the monthly National Oceanic and Atmospheric Administration (NOAA) State of the Climate reports which outline global extreme events of meteorological significance.

We give detailed examples of heat, precipitation and storm extremes for each country where these have had significant impact. Where a country is primarily affected by precipitation or heat extremes this is where our focus has remained. An account of the impact on human life, property and the economy has been given, based largely on media reporting of events, and official reports from aid agencies, governments and meteorological organisations. Some data has also been acquired from the Centre for Research on Epidemiological Disasters (CRED) database on global extreme events. Although media reports are unlikely to be completely accurate, they do give an indication as to the perceived impact of an extreme event, and so are useful in highlighting the events which remain in the national psyche.

Our search for data has not been exhaustive given the number of countries and events included. Although there are a wide variety of sources available, for many events, an official

account is not available. Therefore figures given are illustrative of the magnitude of impact only (references are included for further information on sources). It is also apparent that the reporting of extreme events varies widely by region, and we have, where possible, engaged with local scientists to better understand the impact of such events.

The aim of the narrative for each country is to provide a picture of the social and economic vulnerability to the current climate. Examples given may illustrate the impact that any given extreme event may have and the recovery of a country from such an event. This will be important when considering the current trends in climate extremes, and also when examining projected trends in climate over the next century.

Observational record

In this section we outline the data sources which were incorporated into the analysis, the quality control procedure used, and the choices made in the data presentation. As this report is global in scope, including 23 countries, it is important to maintain consistency of methodological approach across the board. For this reason, although detailed datasets of extreme temperatures, precipitation and storm events exist for various countries, it was not possible to obtain and incorporate such a varied mix of data within the timeframe of this project. Attempts were made to obtain regional daily temperature and precipitation data from known contacts within various countries with which to update existing global extremes databases. No analysis of changes in storminess is included as there is no robust historical analysis of global land surface winds or storminess currently available.

Analysis of seasonal mean temperature

Mean temperatures analysed are obtained from the CRUTEM3 global land-based surface-temperature data-product (Brohan et al. 2006), jointly created by the Met Office Hadley Centre and Climatic Research Unit at the University of East Anglia. CRUTEM3 comprises of more than 4000 weather station records from around the world. These have been averaged together to create 5° by 5° gridded fields with no interpolation over grid boxes that do not contain stations. Seasonal averages were calculated for each grid box for the 1960 to 2010 period and linear trends fitted using the median of pairwise slopes (Sen 1968; Lanzante 1996). This method finds the slopes for all possible pairs of points in the data, and takes their median. This is a robust estimator of the slope which is not sensitive to outlying points. High confidence is assigned to any trend value for which the 5th to 95th percentiles of the pairwise slopes are of the same sign as the trend value and thus inconsistent with a zero trend.

Analysis of temperature and precipitation extremes using indices

In order to study extremes of climate a number of indices have been created to highlight different aspects of severe weather. The set of indices used are those from the World Climate Research Programme (WCRP) Climate Variability and Predictability (CLIVAR) Expert Team on Climate Change Detection and Indices (ETCCDI). These 27 indices use daily rainfall and maximum and minimum temperature data to find the annual (and for a subset of the indices, monthly) values for, e.g., the ‘warm’ days where daily maximum temperature exceeds the 90th percentile maximum temperature as defined over a 1961 to 1990 base period. For a full list of the indices we refer to the website of the ETCCDI (<http://cccma.seos.uvic.ca/ETCCDI/index.shtml>).

Index	Description	Shortname	Notes
Cool night frequency	Daily minimum temperatures lower than the 10 th percentile daily minimum temperature using the base reference period 1961-1990	TN10p	---
Warm night frequency	Daily minimum temperatures higher than the 90 th percentile daily minimum temperature using the base reference period 1961-1990	TN90p	---
Cool day frequency	Daily maximum temperatures lower than the 10 th percentile daily maximum temperature using the base reference period 1961-1990	TX10p	---
Warm day frequency	Daily maximum temperatures higher than the 90 th percentile daily maximum temperature using the base reference period 1961-1990	TX90p	---
Dry spell duration	Maximum duration of continuous days within a year with rainfall <1mm	CDD	Lower data coverage due to the requirement for a ‘dry spell’ to be at least 6 days long resulting in intermittent temporal coverage
Wet spell duration	Maximum duration of continuous days with rainfall >1mm for a given year	CWD	Lower data coverage due to the requirement for a ‘wet spell’ to be at least 6 days long resulting in intermittent temporal coverage
Total annual precipitation	Total rainfall per year	PRCPTOT	---

Table 3. Description of ETCCDI indices used in this document.

A previous global study of the change in these indices, containing data from 1951-2003 can be found in Alexander et al. 2006, (HadEX; see <http://www.metoffice.gov.uk/hadobs/hadex/>).

In this work we aimed to update this analysis to the present day where possible, using the most recently available data. A subset of the indices is used here because they are most easily related to extreme climate events (Table 3).

Use of HadEX for analysis of extremes

The HadEX dataset comprises all 27 ETCCDI indices calculated from station data and then smoothed and gridded onto a $2.5^\circ \times 3.75^\circ$ grid, chosen to match the output from the Hadley Centre suite of climate models. To update the dataset to the present day, indices are calculated from the individual station data using the RClimDex/FClimDex software; developed and maintained on behalf of the ETCCDI by the Climate Research Branch of the Meteorological Service of Canada. Given the timeframe of this project it was not possible to obtain sufficient station data to create updated HadEX indices to present day for a number of countries: Brazil; Egypt; Indonesia; Japan (precipitation only); South Africa; Saudi Arabia; Peru; Turkey; and Kenya. Indices from the original HadEX data-product are used here to show changes in extremes of temperature and precipitation from 1960 to 2003. In some cases the data end prior to 2003. Table 4 summarises the data used for each country. Below, we give a short summary of the methods used to create the HadEX dataset (for a full description see Alexander et al. 2006).

To account for the uneven spatial coverage when creating the HadEX dataset, the indices for each station were gridded, and a land-sea mask from the HadCM3 model applied. The interpolation method used in the gridding process uses a decorrelation length scale (DLS) to determine which stations can influence the value of a given grid box. This DLS is calculated from the e-folding distance of the individual station correlations. The DLS is calculated separately for five latitude bands, and then linearly interpolated between the bands. There is a noticeable difference in spatial coverage between the indices due to these differences in decorrelation length scales. This means that there will be some grid-box data where in fact there are no stations underlying it. Here we apply black borders to grid-boxes where at least 3 stations are present to denote greater confidence in representation of the wider grid-box area there. The land-sea mask enables the dataset to be used directly for model comparison with output from HadCM3. It does mean, however, that some coastal regions and islands over which one may expect to find a grid-box are in fact empty because they have been treated as sea

Data sources used for updates to the HadEX analysis of extremes

We use a number of different data sources to provide sufficient coverage to update as many countries as possible to present day. These are summarised in Table 4. In building the new datasets we have tried to use exactly the same methodology as was used to create the original HadEX to retain consistency with a product that was created through substantial international effort and widely used, but there are some differences, which are described in the next section.

Wherever new data have been used, the geographical distributions of the trends were compared to those obtained from HadEX, using the same grid size, time span and fitting method. If the pattern of the trends in the temperature or precipitation indices did not match that from HadEX, we used the HadEX data despite its generally shorter time span. Differences in the patterns of the trends in the indices can arise because the individual stations used to create the gridded results are different from those in HadEX, and the quality control procedures used are also very likely to be different. Countries where we decided to use HadEX data despite the existence of more recent data are Egypt and Turkey.

GHCND:

The Global Historical Climate Network Daily data has near-global coverage. However, to ensure consistency with the HadEX database, the GHCND stations were compared to those stations in HadEX. We selected those stations which are within 1500m of the stations used in the HadEX database and have a high correlation with the HadEX stations. We only took the precipitation data if its $r > 0.9$ and the temperature data if one of its r -values > 0.9 . In addition, we required at least 5 years of data beyond 2000. These daily data were then converted to the indices using the *fclimdex* software

ECA&D and SACA&D:

The European Climate Assessment and Dataset and the Southeast Asian Climate Assessment and Dataset data are pre-calculated indices comprising the core 27 indices from the ETCCDI as well as some extra ones. We kindly acknowledge the help of Albert Klein Tank, the KNMI¹ and the BMKG² for their assistance in obtaining these data.

¹ Koninklijk Nederlands Meteorologisch Instituut – The Royal Netherlands Meteorological Institute

² Badan Meteorologi, Klimatologi dan Geofisika – The Indonesian Meteorological, Climatological and Geophysical Agency

Mexico:

The station data from Mexico has been kindly supplied by the SMN³ and Jorge Vazquez. These daily data were then converted to the required indices using the *Fclimdex* software. There are a total of 5298 Mexican stations in the database. In order to select those which have sufficiently long data records and are likely to be the most reliable ones we performed a cross correlation between all stations. We selected those which had at least 20 years of data post 1960 and have a correlation with at least one other station with an *r*-value >0.95. This resulted in 237 stations being selected for further processing and analysis.

Indian Gridded:

The India Meteorological Department provided daily gridded data (precipitation 1951-2007, temperature 1969-2009) on a 1° x 1° grid. These are the only gridded daily data in our analysis. In order to process these in as similar a way as possible the values for each grid were assumed to be analogous to a station located at the centre of the grid. We keep these data separate from the rest of the study, which is particularly important when calculating the decorrelation length scale, which is on the whole larger for these gridded data.

³ Servicio Meteorológico Nacional de México – The Mexican National Meteorological Service

Country	Region box (red dashed boxes in Fig. 1 and on each map at beginning of chapter)	Data source (T = temperature, P = precipitation)	Period of data coverage (T = temperature, P = precipitation)	Indices included (see Table 3 for details)	Temporal resolution available	Notes
Argentina	73.125 to 54.375 ° W, 21.25 to 56.25 ° S	Matilde Rusticucci (T,P)	1960-2010 (T,P)	TN10p, TN90p, TX10p, TX90p, PRCPTOT, CDD, CWD	annual	
Australia	114.375 to 155.625 ° E, 11.25 to 43.75 ° S	GHCND (T,P)	1960-2010 (T,P)	TN10p, TN90p, TX10p, TX90p, PRCPTOT, CDD, CWD	monthly, seasonal and annual	Land-sea mask has been adapted to include Tasmania and the area around Brisbane
Bangladesh	88.125 to 91.875 ° E, 21.25 to 26.25 ° N	Indian Gridded data (T,P)	1960-2007 (P), 1970-2009 (T)	TN10p, TN90p, TX10p, TX90p, PRCPTOT, CDD, CWD	monthly, seasonal and annual	Interpolated from Indian Gridded data
Brazil	73.125 to 31.875 ° W, 6.25 ° N to 33.75 ° S	HadEX (T,P)	1960-2000 (P) 2002 (T)	TN10p, TN90p, TX10p, TX90p, PRCPTOT, CDD, CWD	annual	Spatial coverage is poor
China	73.125 to 133.125 ° E, 21.25 to 53.75 ° N	GHCND (T,P)	1960-1997 (P) 1960-2003 (T _{min}) 1960-2010 (T _{max})	TN10p, TN90p, TX10p, TX90p, PRCPTOT, CDD, CWD	monthly, seasonal and annual	Precipitation has very poor coverage beyond 1997 except in 2003-04, and no data at all in 2000-02, 2005-11
Egypt	24.375 to 35.625 ° E, 21.25 to 31.25 ° N	HadEX (T,P)	No data	TN10p, TN90p, TX10p, TX90p, PRCPTOT,	annual	There are no data for Egypt so all grid-box values have been interpolated from stations in Jordan, Israel, Libya and Sudan

France	5.625 ° W to 9.375 ° E, 41.25 to 51.25 ° N	ECA&D (T,P)	1960-2010 (T,P)	TN10p, TN90p, TX10p, TX90p, PRCPTOT, CDD, CWD	monthly, seasonal and annual	
Germany	5.625 to 16.875 ° E, 46.25 to 56.25 ° N	ECA&D (T,P)	1960-2010 (T,P)	TN10p, TN90p, TX10p, TX90p, PRCPTOT, CDD, CWD	monthly, seasonal and annual	
India	69.375 to 99.375 ° E, 6.25 to 36.25 ° N	Indian Gridded data (T,P)	1960-2003 (P), 1970-2009 (T)	TN10p, TN90p, TX10p, TX90p, PRCPTOT, CDD, CWD	monthly, seasonal and annual	
Indonesia	95.625 to 140.625 ° E, 6.25 ° N to 11.25 ° S	HadEX (T,P)	1968-2003 (T,P)	TN10p, TN90p, TX10p, TX90p, PRCPTOT,	annual	Spatial coverage is poor
Italy	5.625 to 16.875 ° E, 36.25 to 46.25 ° N	ECA&D (T,P)	1960-2010 (T,P)	TN10p, TN90p, TX10p, TX90p, PRCPTOT, CDD, CWD	monthly, seasonal and annual	Land-sea mask has been adapted to improve coverage of Italy
Japan	129.375 to 144.375 ° E, 31.25 to 46.25 ° N	HadEX (P) GHCND (T)	1960-2003 (P) 1960-2000 (T _{min}) 1960-2010 (T _{max})	TN10p, TN90p, TX10p, TX90p, PRCPTOT,	monthly, seasonal and annual (T), annual (P)	
Kenya	31.875 to 43.125 ° E, 6.25 ° N to 6.25 ° S	HadEX (T,P)	1960-1999 (P)	TN10p, TN90p, TX10p, TX90p, PRCPTOT	annual	There are no temperature data for Kenya and so grid-box values have been interpolated from neighbouring Uganda and the United Republic of Tanzania. Regional averages include grid-boxes from outside Kenya that enable continuation to 2003
Mexico	118.125 to 88.125 ° W, 13.75 to 33.75 ° N	Raw station data from the Servicio Meteorológico Nacional (SMN) (T,P)	1960-2009 (T,P)	TN10p, TN90p, TX10p, TX90p, PRCPTOT, CDD, CWD	monthly, seasonal and annual	237/5298 stations selected. Non uniform spatial coverage. Drop in T and P coverage in 2009.

Peru	84.735 to 65.625 ° W, 1.25 ° N to 18.75 ° S	HadEX (T,P)	1960-2002 (T,P)	TN10p, TN90p, TX10p, TX90p, PRCPTOT, CDD, CWD	annual	Intermittent coverage in TX90p, CDD and CWD
Russia	West Russia 28.125 to 106.875 ° E, 43.75 to 78.75 ° N, East Russia 103.125 to 189.375 ° E, 43.75 to 78.75 ° N	ECA&D (T,P)	1960-2010 (T,P)	TN10p, TN90p, TX10p, TX90p, PRCPTOT, CDD, CWD	monthly, seasonal and annual	Country split for presentation purposes only.
Saudi Arabia	31.875 to 54.375 ° E, 16.25 to 33.75 ° N	HadEX (T,P)	1960-2000 (T,P)	TN10p, TN90p, TX10p, TX90p, PRCPTOT	annual	Spatial coverage is poor
South Africa	13.125 to 35.625 ° W, 21.25 to 36.25 ° S	HadEX (T,P)	1960-2000 (T,P)	TN10p, TN90p, TX10p, TX90p, PRCPTOT, CDD, CWD	annual	---
Republic of Korea	125.625 to 129.375 ° E, 33.75 to 38.75 ° N	HadEX (T,P)	1960-2003 (T,P)	TN10p, TN90p, TX10p, TX90p, PRCPTOT, CDD	annual	There are too few data points for CWD to calculate trends or regional timeseries
Spain	9.375 ° W to 1.875 ° E, 36.25 to 43.75 ° N	ECA&D (T,P)	1960-2010 (T,P)	TN10p, TN90p, TX10p, TX90p, PRCPTOT, CDD, CWD	monthly, seasonal and annual	
Turkey	24.375 to 46.875 ° E, 36.25 to 43.75 ° N	HadEX (T,P)	1960-2003 (T,P)	TN10p, TN90p, TX10p, TX90p, PRCPTOT, CDD, CWD	annual	Intermittent coverage in CWD and CDD with no regional average beyond 2000
United Kingdom	9.375 ° W to 1.875 ° E, 51.25 to 58.75 ° N	ECA&D (T,P)	1960-2010 (T,P)	TN10p, TN90p, TX10p, TX90p, PRCPTOT, CDD, CWD	monthly, seasonal and annual	
United States of America	125.625 to 65.625 ° W, 23.75 to 48.75 ° N	GHCND (T,P)	1960-2010 (T,P)	TN10p, TN90p, TX10p, TX90p, PRCPTOT, CDD, CWD	monthly, seasonal and annual	

Table 4. Summary of data used for each country.

Quality control and gridding procedure used for updates to the HadEX analysis of extremes

In order to perform some basic quality control checks on the index data, we used a two-step process on the indices. Firstly, internal checks were carried out, to remove cases where the 5 day rainfall value is less than the 1 day rainfall value, the minimum T_{min} is greater than the minimum T_{max} and the maximum T_{min} is greater than the maximum T_{max}.

Although these are physically impossible, they could arise from transcription errors when creating the daily dataset, for example, a misplaced minus sign, an extra digit appearing in the record or a column transposition during digitisation. During these tests we also require that there are at least 20 years of data in the period of record for the index for that station, and that some data is found in each decade between 1961 and 1990, to allow a reasonable estimation of the climatology over that period.

Weather conditions are often similar over many tens of kilometres and the indices calculated in this work are even more coherent. The correlation coefficient between each station-pair combination in all the data obtained is calculated for each index (and month where appropriate), and plotted as a function of the separation. An exponential decay curve is fitted to the data, and the distance at which this curve has fallen by a factor $1/e$ is taken as the decorrelation length scale (DLS). A DLS is calculated for each dataset separately. For the GHCND, a separate DLS is calculated for each hemisphere. We do not force the fitted decay curve to show perfect correlation at zero distance, which is different to the method employed when creating HadEX. For some of the indices in some countries, no clear decay pattern was observed in some data sets or the decay was so slow that no value for the DLS could be determined. In these cases a default value of 200km was used.

We then perform external checks on the index data by comparing the value for each station with that of its neighbours. As the station values are correlated, it is therefore likely that if one station measures a high value for an index for a given month, its neighbours will also be measuring high. We exploit this coherence to find further bad values or stations as follows. Although raw precipitation data shows a high degree of localisation, using indices which have monthly or annual resolution improves the coherence across wider areas and so this neighbour checking technique is a valid method of finding anomalous stations.

We calculate a climatology for each station (and month if appropriate) using the mean value for each index over the period 1961-1990. The values for each station are then anomalised using this climatology by subtracting this mean value from the true values, so that it is clear if the station values are higher or lower than normal. This means that we do not need to take

differences in elevation or topography into account when comparing neighbours, as we are not comparing actual values, but rather deviations from the mean value.

All stations which are within the DLS distance are investigated and their anomalised values noted. We then calculate the weighted median value from these stations to take into account the decay in the correlation with increasing distance. We use the median to reduce the sensitivity to outliers.

If the station value is greater than 7.5 median-absolute-deviations away from the weighted median value (this corresponds to about 5 standard deviations if the distribution is Gaussian, but is a robust measure of the spread of the distribution), then there is low confidence in the veracity of this value and so it is removed from the data.

To present the data, the individual stations are gridded on a $3.75^\circ \times 2.5^\circ$ grid, matching the output from HadCM3. To determine the value of each grid box, the DLS is used to calculate which stations can reasonably contribute to the value. The value of each station is then weighted using the DLS to obtain a final grid box value. At least three stations need to have valid data and be near enough (within 1 DLS of the gridbox centre) to contribute in order for a value to be calculated for the grid point. As for the original HadEX, the HadCM3 land-sea mask is used. However, in three cases the mask has been adjusted as there are data over Tasmania, eastern Australia and Italy that would not be included otherwise (Figure 7).

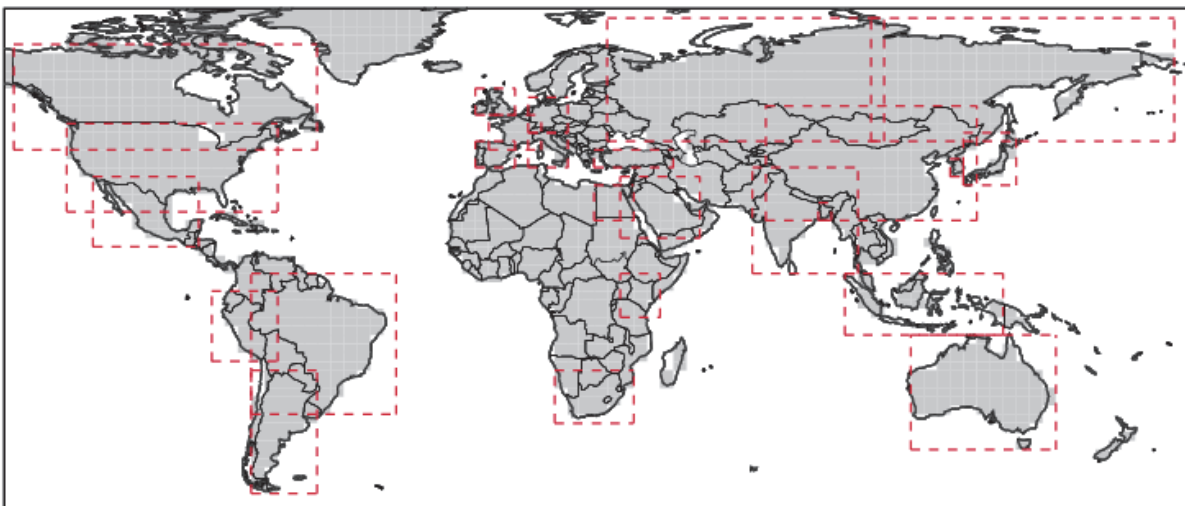


Figure 7. Land Sea mask used for gridding the station data and regional areas allocated to each country as described in Table 2.

Presentation of extremes of temperature and precipitation

Indices are displayed as regional gridded maps of decadal trends and regional average time-series with decadal trends where appropriate. Trends are fitted using the median of pairwise slopes method (Sen 1968, Lanzante 1996). Trends are considered to be significantly different from a zero trend if the 5th to 95th percentiles of the pairwise slopes do not encompass zero. This is shown by a black dot in the centre of the grid-box or by a solid line on time-series plots. This infers that there is high confidence in the sign (positive or negative) of the sign. Confidence in the trend magnitude can be inferred by the spread of the 5th to 95th percentiles of the pairwise slopes which is given for the regional average decadal trends. Trends are only calculated when there are data present for at least 50% of years in the period of record and for the updated data (not HadEX) there must be at least one year in each decade.

Due to the practice of data-interpolation during the gridding stage (using the DLS) there are values for some grid boxes when no actually station lies within the grid box. There is more confidence in grid boxes for which there are underlying data. For this reason, we identify those grid boxes which contain at least 3 stations by a black contour line on the maps. The DLS differs with region, season and index which leads to large differences in the spatial coverage. The indices, by their nature of being largely threshold driven, can be intermittent over time which also affects spatial and temporal coverage (see Table 3).

Each index (and each month for the indices for which there is monthly data) has a different DLS, and so the coverage between different indices and datasets can be different. The restrictions on having at least 20 years of data present for each input station, at least 50% of years in the period of record and at least one year in each decade for the trending calculation, combined with the DLS, can restrict the coverage to only those regions with a dense station network reporting reliably.

Each country has a rectangular region assigned as shown by the red dashed box on the map in Figure 7 and listed in Table 4, which is used for the creation of the regional average. This is sometimes identical to the attribution region shown in grey on the map in Figure 7. This region is again shown on the maps accompanying the time series of the regional averages as a reminder of the region and grid boxes used in the calculation. Regional averages are created by weighting grid box values by the cosine of their grid box centre latitude. To ensure consistency over time a regional average is only calculated when there are a sufficient number of grid boxes present. The full-period median number of grid-boxes present is calculated. For regions with a median of more than six grid-boxes there must be at least 80%

of the median number of grid boxes present for any one year to calculate a regional average. For regions with six or fewer median grid boxes this is relaxed to 50%. These limitations ensure that a single station or grid box which has a longer period of record than its neighbours cannot skew the timeseries trend. So sometimes there may be grid-boxes present but no regional average time series. The trends for the regional averages are calculated in the same way as for the individual grid boxes, using the median of pairwise slopes method (Sen 1968, Lanzante 1996). Confidence in the trend is also determined if the 5th to 95th percentiles of the pairwise slopes are of the same sign and thus inconsistent with a zero trend. As well as the trend in quantity per decade, we also show the full change in the quantity from 1960 to 2010 that this fitted linear trend implies.

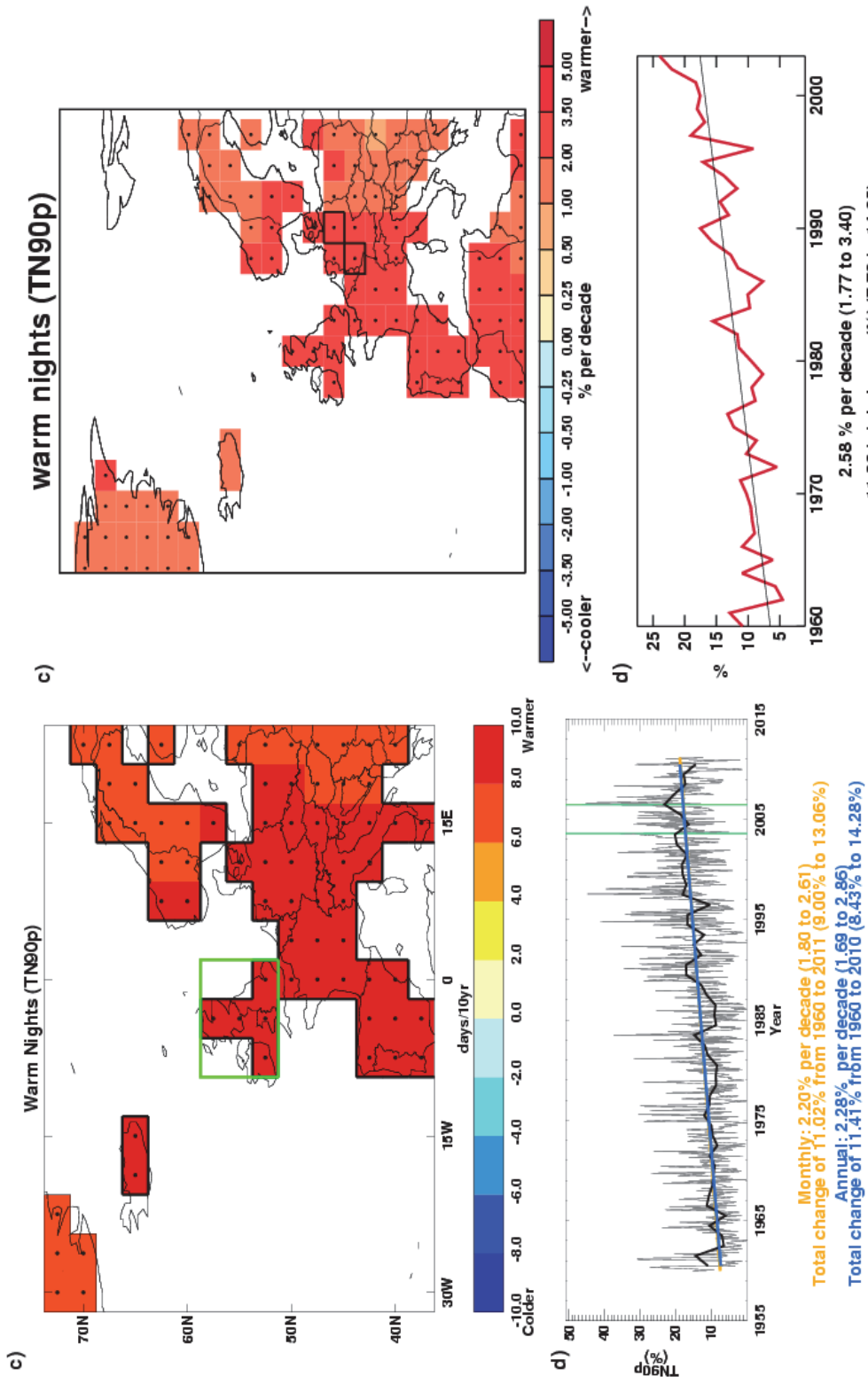


Figure 8. Examples of the plots shown in the data section. Left: From ECA&D data between 1960-2010 for the number of warm nights, and Right: from HadEX data (1960-2003) for the total precipitation. A full explanation of the plots is given in the text below.

The results are presented in the form of a map and a time series for each country and index. The map shows the grid box decadal trend in the index over the period for which there are data. High confidence, as determined above, is shown by a black dot in the grid box centre. To show the variation over time, the values for each year (and month if available) are shown in a time series for a regional average. The values of the indices have been normalised to a base period of 1961-1990 (except the Indian gridded data which use a 1971 to 1990 period), both in HadEX and in the new data acquired for this project. Therefore, for example, the percentage of nights exceeding the 90th percentile for a temperature is 10% for that period.

There are two influences on whether a grid box contains a value or not – the land-sea mask, and the decorrelation length scale. The land-sea mask is shown in Figure 7. There are grid boxes which contain some land but are mostly sea and so are not considered. The decorrelation length scale sets the maximum distance a grid box can be from stations before no value is assigned to it. Grid boxes containing three or more stations are highlighted by a thick border. This indicates regions where the value shown is likely to be more representative of the grid box area mean as opposed to a single station location.

On the maps for the new data there is a box indicating which grid boxes have been extracted to calculate the area average for the time series. This box is the same as shown in Figure 7 at the beginning of each country's document. These selected grid boxes are combined using area (cosine) weighting to calculate the regional average (both annual [thick lines] and monthly [thin lines] where available). Monthly (orange) and annual (blue) trends are fitted to these time series using the method described above. The decadal trend and total change over the period where there are data are shown with 5th to 95th percentile confidence intervals in parentheses. High confidence, as determined above, is shown by a solid line as opposed to a dotted one. The green vertical lines on the time series show the dates of some of the notable events outlined in each section.

Attribution

Regional distributions of seasonal mean temperatures in the 2000s are computed with and without the effect of anthropogenic influences on the climate. The analysis considers temperatures averaged over the regions shown in Figure 3. These are also identified as grey boxes on the maps in Figure 7. The coordinates of the regions are given in Table 5. The methodology combines information from observations and model simulations using the approach originally introduced in Christidis et al., 2010 and later extended in Christidis et al.,

2011, where more details can be found. The analysis requires spatial scales greater than about 2,500 km and for that reason the selected regions (Fig.9 and Table 5) are often larger than individual countries, or include several smaller countries in a single region (for example UK, Germany and France are grouped in one region).

Observations of land temperature come from the CRUTEM3 gridded dataset (Brohan et al., 2006) and model simulations from two coupled GCMs, namely the Hadley Centre HadGEM1 model (Martin et al., 2006) and version 3.2 of the MIROC model (K-1 Developers, 2004). The use of two GCMs helps investigate the sensitivity of the results to the model used in the analysis. Ensembles of model simulations from two types of experiments are used to partition the temperature response to external forcings between its anthropogenic and natural components. The first experiment (ALL) simulates the combined effect of natural and anthropogenic forcings on the climate system and the second (ANTHRO) includes anthropogenic forcings only. The difference of the two gives an estimate of the effect of the natural forcings (NAT). Estimates of the effect of internal climate variability are derived from long control simulations of the unforced climate. Distributions of the regional summer mean temperature are computed as follows:

- a) A global optimal fingerprinting analysis (Allen and Tett, 1999; Allen and Stott, 2003) is first carried out that scales the global simulated patterns (fingerprints) of climate change attributed to different combinations of external forcings to best match them to the observations. The uncertainty in the scaling that originates from internal variability leads to samples of the scaled fingerprints, i.e. several realisations that are plausibly consistent with the observations. The 2000-2009 decade is then extracted from the scaled patterns and two samples of the decadal mean temperature averaged over the reference region are then computed with and without human influences, which provide the Probability Density Functions (PDFs) of the decadal mean temperature attributable to ALL and NAT forcings.
- b) Model-derived estimates of noise are added to the distributions to take into account the uncertainty in the simulated fingerprints.
- c) In the same way, additional noise from control model simulations is introduced to the distributions to represent the effect of internal variability in the annual values of the seasonal mean temperatures. The result is a pair of estimated distributions of the annual values of the seasonal mean temperature in the region with and without the effect of human activity on the climate. The temperatures throughout the analysis are expressed as anomalies relative to period 1961-1990.

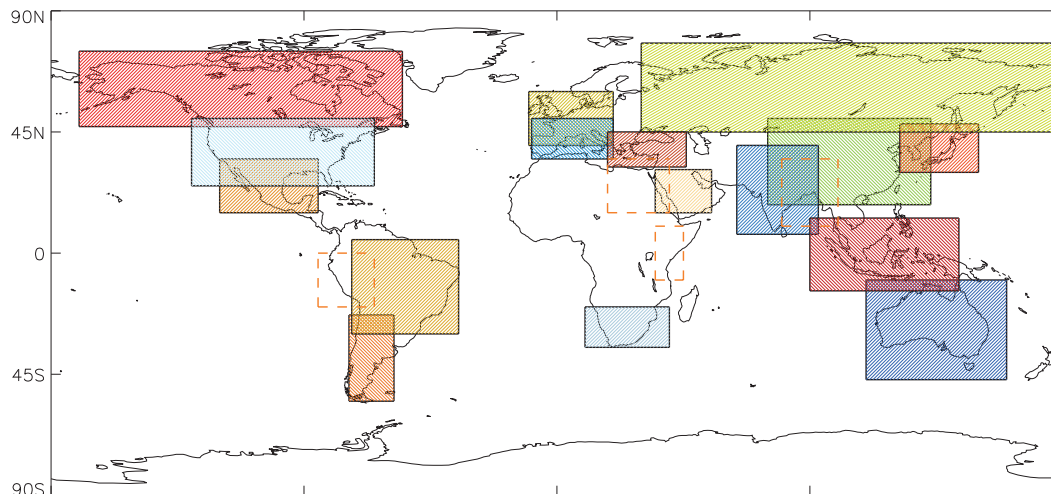


Figure 9. The regions used in the attribution analysis. Regions marked with dashed orange boundaries correspond to non-G20 countries that were also included in the analysis

Region	Region Coordinates
Argentina	74-58W, 55-23S
Australia	110-160E, 47-10S
Bangladesh	80-100E, 10-35N
Brazil	73-35W, 30S-5N
Canada-Alaska	170-55W, 47-75N
China	75-133E, 18-50N
Egypt	18-40E, 15-35N
France-Germany-UK	10W-20E, 40-60N
India	64-93E, 7-40N
Indonesia	90-143E, 14S-13N
Italy-Spain	9W-20E, 35-50N
Japan-Republic of Korea	122-150E, 30-48N
Kenya	35-45E, 10S-10N
Mexico	120-85W, 15-35N
Peru	85-65W, 20-0S
Russia	30-185E, 45-78N
Saudi Arabia	35-55E, 15-31N
South Africa	10-40E, 35-20S
Turkey	18-46E, 32-45N

Table 5. The coordinates of the regions used in the attribution analysis

References

- ALEXANDER, L. V., ZHANG, X., PETERSON, T. C., CAESAR, J., GLEASON, B., KLEIN TANK, A. M. G., HAYLOCK, M., COLLINS, D., TREWIN, B., RAHIMZADEH, F., TAGIPOUR, A., RUPA KUMAR, K., REVADEKAR, J., GRIFFITHS, G., VINCENT, L., STEPHENSON, D. B., BURN, J., AGUILAR, E., BRUNET, M., TAYLOR, M., NEW, M., ZHAI, P., RUSTICUCCI, M. and VAZQUEZ-AGUIRRE, J. L. 2006. Global observed changes in daily climate extremes of temperature and precipitation. *J. Geophys. Res.* 111, D05109. doi:10.1029/2005JD006290.
- ALLEN, M. R., TETT S. F. B. 1999. Checking for model consistency in optimal fingerprinting. *Clim Dyn* 15: 419-434
- ALLEN M. R., STOTT P. A. 2003. Estimating signal amplitudes in optimal fingerprinting, part I: theory. *Clim Dyn* 21: 477-491
- BROHAN, P., KENNEDY, J.J., HARRIS, I., TETT, S.F.B. and JONES, P.D. 2006. Uncertainty estimates in regional and global observed temperature changes: a new dataset from 1850. *J. Geophys. Res.* 111, D12106. doi:10.1029/2005JD006548.
- BULYGINA, O., N. N. KORSHUNOVA, AND V. N. RAZUVAEV. 2003. Regional Climates Asia, Russia, in State of the Climate in 2002. *Bulletin of the American Meteorological Society* S48–S50.
- BULYGINA, O. 2004. Regional Climate Asia, Russia, in State of the Climate in 2003. *Bulletin of the American Meteorological Society* S55–S57.
- BULYGINA, O. N., N. N. KORSHUNOVA, and V. N. RAZUVAEV. 2006. Regional Climates Asia, Russia, in State of the Climate in 2005. *Bulletin of the American Meteorological Society* S71-S73.
- BULYGINA, O. N., N. N. KORSHUNOVA, and V. N. RAZUVAEV. 2007. Regional Climates Asia, west and central Asia, in State of the Climate in 2006. *Bulletin of the American Meteorological Society* S94-S97.
- BULYGINA, O. N., N. N. KORSHUNOVA, and V. N. RAZUVAEV. 2008. Regional Climates Asia, Russia, in State of the Climate in 2007. *Bulletin of the American Meteorological Society* 89 (7), S131-S133.

BULYGINA, O. N., N. N. KORSHUNOVA, and N. RAZUVAEV. 2009. Regional Climates Asia, Russia, in State of the Climate in 2008. *Bulletin of the American Meteorological Society* 90 (8), S153-S155.

BULYGINA, O. N., N. N. KORSHUNOVA, and N. RAZUVAEV. 2010. Regional Climates Asia, Russia, in State of the Climate in 2009. *Bulletin of the American Meteorological Society* 91 (7), S170-S174.

CHRISTIDIS N., STOTT. P A., ZWIERS, F. W., SHIOGAMA, H., NOZAWA, T. 2010. Probabilistic estimates of recent changes in temperature: a multi-scale attribution analysis. *Clim Dyn* 34: 1139-1156

CHRISTIDIS, N., STOTT, P. A., ZWIERS, F. W., SHIOGAMA, H., NOZAWA, T. 2011. The contribution of anthropogenic forcings to regional changes in temperature during the last decade. *Climate Dynamics* in press.

DURRE, I, MENNE, MJ, GLEASON, BE, HOUSTON, TG, VOSE, RS, 2010. Comprehensive Automated Quality Assurance of Daily Surface Observations, *Journal of Applied Meteorology and Climatology*, 49, 8, 1615-1633

K-1 MODEL DEVELOPERS (2004) K-1 coupled GCM (MIROC) description, K-1 Tech Rep, H Hasumi and S Emori (eds), Centre for Clim Sys Res, Univ of Tokyo

KLEIN TANK, A.M.G. et al. 2002. Daily dataset of 20th-century surface air temperature and precipitation series for the European Climate Assessment. *Int. J. of Clim.* 22, 1441-1453.

LANZANTE, J. R. 1996. Resistant, robust and non-parametric techniques for the analysis of climate data: theory and examples, including applications to historical radiosonde station data. *Int. J. Clim.* 16, 1197–226.

MAIER, F., A. OBREGÓN, P. BISSOLLI, C. ACHBERGER , J. J. KENNEDY, D. E. PARKER , O. BULYGINA, and N. KORSHUNOVA. 2011. Summer heat waves in Eastern Europe and western Russia in State of the Climate in 2010. *Bulletin of the American Meteorological Society* 92, S210.

MARTIN G.M., RINGER. M. A., POPE V. D., JONES, A., DEARDEN, C., HINTON, T. 2006. The physical properties of the atmosphere in the new Hadley Centre Global Environmental Model (HadGEM1). Part I: Model description and global climatology. *J Clim* 19: 1274-1301

SANCHEZ-LUGO, A., KENNEDY, J.J. and BERRISFORD, P. 2011. Global Climate, Surface Temperatures in State of the Climate 2010. *Bulletin of the American Meteorological Society* 92 (6), S36-S37.

SEN, P. K. 1968. Estimates of the regression coefficient based on Kendall's tau. *J. Am. Stat. Assoc.* 63, 1379–89.

UNFCCC – ПЯТОЕ НАЦИОНАЛЬНОЕ СООБЩЕНИЕ РОССИЙСКОЙ ФЕДЕРАЦИИ – Москва 2010 г. – Fifth national communication by the government of the Russian Federation to the United Nations Framework Convention on Climate Change – Russian Federation http://unfccc.int/resource/docs/natc/rus_nc5_resubmit.pdf direct translation – DdG 27 June 2011.

WAPLE, A. M., J. H. LAWRIMORE, M. S. HALPERT, G. D. BELL, W. HIGGINS, B. LYON, M. J. MENNE, K. L. GLEASON, R. C. SCHNELL, J. R. CHRISTY, W. THIAW, W. J. WRIGHT, M. J. SALINGER, L. ALEXANDER, R. S. STONE, and S. J. CAMARGO. 2002. Regional Climate Asia, Harsh Siberian Winter, in Climate Assessment for 2001. *Bulletin of the American Meteorological Society* S49–S50.

WMO WORLD METEOROLOGICAL ORGANIZATION. 2001. Statement on Status of the Global Climate in 2000, WMO-No. 920.

http://www.wmo.int/pages/prog/wcp/wcdmp/statement/wmostatement_en.html

WMO WORLD METEOROLOGICAL ORGANIZATION. 2002. Statement on Status of the Global Climate in 2001, WMO-No. 940.

http://www.wmo.int/pages/prog/wcp/wcdmp/statement/wmostatement_en.html

WMO WORLD METEOROLOGICAL ORGANIZATION. 2003. Statement on Status of the Global Climate in 2002, WMO-No. 949.

http://www.wmo.int/pages/prog/wcp/wcdmp/statement/wmostatement_en.html

WMO WORLD METEOROLOGICAL ORGANIZATION. 2004. Statement on Status of the Global Climate in 2003, WMO-No. 966.

http://www.wmo.int/pages/prog/wcp/wcdmp/statement/wmostatement_en.html

WMO WORLD METEOROLOGICAL ORGANIZATION. 2005. Statement on Status of the Global Climate in 2004, WMO-No. 983.

http://www.wmo.int/pages/prog/wcp/wcdmp/statement/wmostatement_en.html

WMO WORLD METEOROLOGICAL ORGANIZATION. 2006. Statement on Status of the Global Climate in 2005, WMO-No. 998.

http://www.wmo.int/pages/prog/wcp/wcdmp/statement/wmostatement_en.html

WMO WORLD METEOROLOGICAL ORGANIZATION. 2007. Statement on Status of the Global Climate in 2006, WMO-No. 1016.

http://www.wmo.int/pages/prog/wcp/wcdmp/statement/wmostatement_en.html

WMO WORLD METEOROLOGICAL ORGANIZATION. 2008. Statement on Status of the Global Climate in 2007, WMO-No. 1031.

http://www.wmo.int/pages/prog/wcp/wcdmp/statement/wmostatement_en.html

WMO WORLD METEOROLOGICAL ORGANIZATION. 2009. Statement on Status of the Global Climate in 2008, WMO-No. 1039.

http://www.wmo.int/pages/prog/wcp/wcdmp/statement/wmostatement_en.html

WMO WORLD METEOROLOGICAL ORGANIZATION. 2011. Statement on Status of the Global Climate in 2010, WMO-No. 1074.

http://www.wmo.int/pages/prog/wcp/wcdmp/statement/wmostatement_en.html

Acknowledgements

Data for this work were taken from the GHCND database (Durre et al. 2010). We thank Lisa Alexander and Markus Donat (University of New South Wales) for their help and advice.

Chapter 2 – Climate Change Projections

Introduction

Climate models are used to understand how the climate will evolve over time and typically represent the atmosphere, ocean, land surface, cryosphere, and biogeochemical processes, and solve the equations governing their evolution on a geographical grid covering the globe. Some processes are represented explicitly within climate models, large-scale circulations for instance, while others are represented by simplified parameterisations. The use of these parameterisations is sometimes due to processes taking place on scales smaller than the typical grid size of a climate model (a Global Climate Model (GCM) has a typical horizontal resolution of between 250 and 600km) or sometimes to the current limited understanding of these processes. Different climate modelling institutions use different plausible representations of the climate system, which is why climate projections for a single greenhouse gas emissions scenario differ between modelling institutes. This gives rise to “climate model structural uncertainty”.

In response to a proposed activity of the World Climate Research Programme's (WCRP's; <http://www.wcrp-climate.org/>) Working Group on Coupled Modelling (WGCM), the Program for Climate Model Diagnosis and Intercomparison (PCMDI; <http://www-pcmdi.llnl.gov/>) volunteered to collect model output contributed by leading climate modelling centres around the world. Climate model output from simulations of the past, present and future climate was collected by PCMDI mostly during the years 2005 and 2006, and this archived data constitutes phase 3 of the Coupled Model Intercomparison Project (CMIP3). In part, the WGCM organised this activity to enable those outside the major modelling centres to perform research of relevance to climate scientists preparing the IPCC Fourth Assessment Report (AR4). This unprecedented collection of recent model output is commonly known as the “CMIP3 multi-model dataset”. The GCMs included in this dataset are referred to regularly throughout this review, although not exclusively.

The CMIP3 multi-model ensemble has been widely used in studies of regional climate change and associated impacts. Each of the constituent models was subject to extensive testing by the contributing institute, and the ensemble has the advantage of having been constructed from a large pool of alternative model components, therefore sampling alternative structural assumptions in how best to represent the physical climate system. Being assembled on an opportunity basis, however, the CMIP3 ensemble was not designed to represent model uncertainties in a systematic manner, so it does not, in isolation, support

robust estimates of the risk of different levels of future climate change, especially at a regional level.

Since CMIP3, a new (CMIP5) generation of coupled ocean-atmosphere models has been developed, which is only just beginning to be available and is being used for new projections for the IPCC Fifth Assessment Report (AR5).

These newer models typically feature higher spatial resolution than their CMIP3 counterparts, including in some models a more realistic representation of stratosphere-troposphere interactions. The CMIP5 models also benefit from several years of development in their parameterisations of small scale processes, which, together with resolution increases, are expected to result in a general improvement in the accuracy of their simulations of historical climate, and in the credibility of their projections of future changes. The CMIP5 programme also includes a number of comprehensive Earth System Models (ESMs) which explicitly simulate the earth's carbon cycle and key aspects of atmospheric chemistry, and also contain more sophisticated representations of aerosols compared to CMIP3 models.

The CMIP3 results should be interpreted as a useful interim set of plausible outcomes. However, their neglect of uncertainties, for instance in carbon cycle feedbacks, implies that higher levels of warming outside the CMIP3 envelope cannot be ruled out. In future, CMIP5 coupled model and ESM projections can be expected to produce improved advice on future regional changes. In particular, ensembles of ESM projections will be needed to provide a more comprehensive survey of possible future changes and their relative likelihoods of occurrence. This is likely to require analysis of the CMIP5 multi-model ESM projections, augmented by larger ensembles of ESM simulations in which uncertainties in physical and biogeochemical feedback processes can be explored more systematically, for example via ensembles of model runs in which key aspects of the climate model are slightly adjusted. Note that such an exercise might lead to the specification of wider rather than narrower uncertainties compared to CMIP3 results, if the effects of representing a wider range of earth system processes outweigh the effects of refinements in the simulation of physical atmosphere-ocean processes already included in the CMIP3 models.

Climate projections

The Met Office Hadley Centre is currently producing perturbed parameter ensembles of a single model configuration known as HadCM3C, to explore uncertainties in physical and biogeochemical feedback processes. The results of this analysis will become available in the next year and will supplement the CMIP5 multi-model ESM projections, providing a more comprehensive set of data to help progress understanding of future climate change.

However, many of the studies covered in the chapter on climate impacts have used CMIP3 model output. For this reason, and because it is still the most widely used set of projections available, the CMIP3 ensemble output for temperature and precipitation, for the A1B emission scenario, for Russia and the surrounding region is shown below.

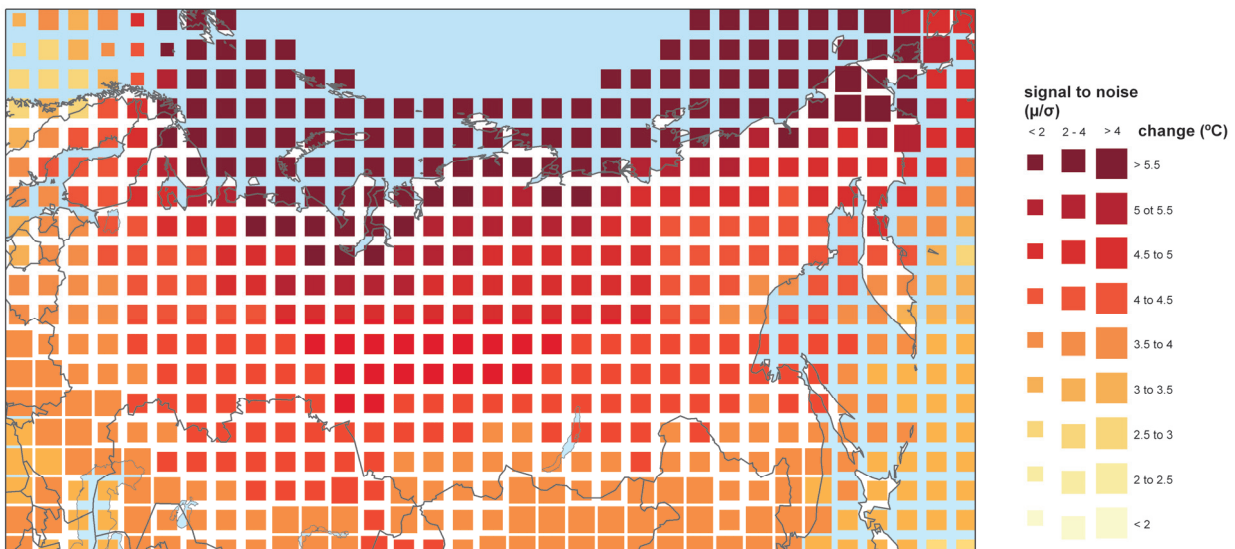


Figure 1. Percentage change in average annual temperature by 2100 from 1960-1990 baseline climate, averaged over 21 CMIP3 models. The size of each pixel represents the level of agreement between models on the magnitude of the change.

precipitation change ranges from an increase of 5% to a decrease of 5%. Ensemble agreement over the changes is high over most of the country, but more moderate in parts of the southwest.

Chapter 3 – Climate Change Impact Projections

Introduction

Aims and approach

This chapter looks at research on a range of projected climate change impacts, with focus on results for Russia. It includes projections taken from the AVOID programme, for some of the impact sectors.

The aim of this work is to take a ‘top down’ approach to assessing global impacts studies, both from the literature and from new research undertaken by the AVOID programme. This project covers 23 countries, with summaries from global studies provided for each of these. This global approach allows some level of comparison between countries, whilst presenting information on a scale most meaningful to inform international policy.

The literature covered in this chapter focuses on research published since the Fourth Assessment Report (AR4) of the Intergovernmental Panel on Climate Change (IPCC) and should be read in conjunction with IPCC AR4 WG1 and WG2 reports. For some sectors considered, an absence of research developments since the IPCC AR4, means earlier work is cited as this helps describe the current level of scientific understanding. This report focuses on assessing scientific research about climate change impacts within sectors; it does not present an integrated analysis of climate change adaptation policies.

Some national and sub-national scale literature is reported to a limited extent to provide some regional context.

Impact sectors considered and methods

This report reviews the evidence for the impact of climate change on a number of sectors, for Russia. The following sectors are considered in turn in this report:

- Crop yields
- Food security
- Water stress and drought
- Pluvial flooding and rainfall
- Fluvial flooding
- Tropical cyclones (where applicable)

- Coastal regions

Supporting literature

Literature searches were conducted for each sector with the Thomson Reuters Web of Science (WoS., 2011) and Google Scholar academic search engines respectively. Furthermore, climate change impact experts from each of the 23 countries reviewed were contacted. These experts were selected through a combination of government nomination and from experts known to the Met Office. They were asked to provide literature that they felt would be of relevance to this review. Where appropriate, such evidence has been included. A wide range of evidence was considered, including; research from international peer-reviewed journal papers; reports from governments, non-governmental organisations, and private businesses (e.g. reinsurance companies), and research papers published in national journals.

For each impact sector, results from assessments that include a global- or regional-scale perspective are considered separately from research that has been conducted at the national- or sub-national-scale. The consideration of global- and regional-scale studies facilitates a comparison of impacts across different countries, because such studies apply a consistent methodology for each country. While results from national- and sub-national-scale studies are not easily comparable between countries, they can provide a level of detail that is not always possible with larger-scale studies. However, the national- and sub-national scale literature included in this project does not represent a comprehensive coverage of regional-based research and cannot, and should not, replace individual, detailed impacts studies in countries. The review aims to present an up-to-date assessment of the impact of climate change on each of the sectors considered.

AVOID programme results

Much of the work in this report is drawn from modelling results and analyses coming out of the AVOID programme. The AVOID programme is a research consortium funded by DECC and Defra and led by the UK Met Office and also comprises the Walker Institute at the University of Reading, the Tyndall Centre represented through the University of East Anglia, and the Grantham Institute for Climate Change at Imperial College. The expertise in the AVOID programme includes climate change research and modelling, climate change impacts in natural and human systems, socio-economic sciences, mitigation and technology.

The unique expertise of the programme is in bringing these research areas together to produce integrated and policy-relevant results. The experts who work within the programme were also well suited to review the literature assessment part of this report. In this report the modelling of sea level rise impacts was carried out for the AVOID programme by the University of Southampton.

The AVOID programme uses the same emissions scenarios across the different impact sectors studied. These are a business as usual (IPCC SRES A1B) and an aggressive mitigation (the AVOID A1B-2016-5-L) scenario. Model output for both scenarios was taken from more than 20 GCMs and averaged for use in the impact models. The impact models are sector specific, and frequently employ further analytical techniques such as pattern scaling and downscaling in the crop yield models.

Data and analysis from AVOID programme research is provided for the following impact sectors:

- Crop yields
- Water stress and drought
- Fluvial flooding
- Coastal regions

Uncertainty in climate change impact assessment

There are many uncertainties in future projections of climate change and its impacts. Several of these are well-recognised, but some are not. One category of uncertainty arises because we don't yet know how mankind will alter the climate in the future. For instance, uncertainties in future greenhouse gas emissions depends on the future socio-economic pathway, which, in turn, depends on factors such as population, economic growth, technology development, energy demand and methods of supply, and land use. The usual approach to dealing with this is to consider a range of possible future scenarios.

Another category of uncertainties relate to our incomplete understanding of the climate system, or an inability to adequately model some aspects of the system. This includes:

- Uncertainties in translating emissions of greenhouse gases into atmospheric concentrations and radiative forcing. Atmospheric CO₂ concentrations are currently rising at approximately 50% of the rate of anthropogenic emissions, with the remaining 50% being offset by a net uptake of CO₂ into the oceans and land

biosphere. However, this rate of uptake itself probably depends on climate, and evidence suggests it may weaken under a warming climate, causing more CO₂ to remain in the atmosphere, warming climate further. The extent of this feedback is highly uncertain, but it not considered in most studies. The phase 3 of the Coupled Model Intercomparison Project (CMIP3), which provided the future climate projections for the IPCC Fourth Assessment Report (AR4), used a single estimate of CO₂ concentration rise for each emissions scenario, so the CMIP3 projections (which were used in most studies presented here, including AVOID) do not account for this uncertainty.

- Uncertainty in climate response to the forcing by greenhouse gases and aerosols. One aspect of this is the response of global mean temperature (“climate sensitivity”), but a more relevant aspect for impacts studies is the response of regional climates, including temperature, precipitation and other meteorological variables. Different climate models can give very different results in some regions, while giving similar results in other regions. Confidence in regional projections requires more than just agreement between models: physical understanding of the relevant atmospheric, ocean and land surface processes is also important, to establish whether the models are likely to be realistic.
- Additional forcings of regional climate. Greenhouse gas changes are not the only anthropogenic driver of climate change; atmospheric aerosols and land cover change are also important, and unlike greenhouse gases, the strength of their influence varies significantly from place to place. The CMIP3 models used in most impacts studies generally account for aerosols but not land cover change.
- Uncertainty in impacts processes. The consequences of a given changes in weather or climatic conditions for biophysical impacts such as river flows, drought, flooding, crop yield or ecosystem distribution and functioning depend on many other processes which are often poorly-understood, especially at large scales. In particular, the extent to which different biophysical impacts interact with each other has been hardly studied, but may be crucial; for example, impacts of climate change on crop yield may depend not only on local climate changes affecting rain-fed crops, but also remote climate changes affecting river flows providing water for irrigation.
- Uncertainties in non-climate effects of some greenhouse gases. As well as being a greenhouse gas, CO₂ exerts physiological influences on plants, affecting photosynthesis and transpiration. Under higher CO₂ concentrations, and with no

other limiting factors, photosynthesis can increase, while the requirements of water for transpiration can decrease. However, while this has been extensively studied under experimental conditions, including in some cases in the free atmosphere, the extent to which the ongoing rise in ambient CO₂ affects crop yields and natural vegetation functioning remains uncertain and controversial. Many impacts projections assume CO₂ physiological effects to be significant, while others assume it to be non-existent. Studies of climate change impacts on crops and ecosystems should therefore be examined with care to establish which assumptions have been made.

In addition to these uncertainties, the climate varies significantly through natural processes from year-to-year and also decade-to-decade, and this variability can be significant in comparison to anthropogenic forcings on shorter timescales (the next few decades) particularly at regional scales. Whilst we can characterise the natural variability it will not be possible to give a precise forecast for a particular year decades into the future.

A further category of uncertainty in projections arises as a result of using different methods to correct for uncertainties and limitations in climate models. Despite being painstakingly developed in order to represent current climate as closely as possible, current climate models are nevertheless subject to systematic errors such as simulating too little or too much rainfall in some regions. In order to reduce the impact of these, '*bias correction*' techniques are often employed, in which the climate model is a source of information on the *change* in climate which is then applied to the observed present-day climate state (rather than using the model's own simulation of the present-day state). However, these bias-corrections typically introduce their own uncertainties and errors, and can lead to inconsistencies between the projected impacts and the driving climate change (such as river flows changing by an amount which is not matched by the original change in precipitation). Currently, this source of uncertainty is rarely considered

When climate change projections from climate models are applied to climate change impact models (e.g. a global hydrological model), the climate model structural uncertainty carries through to the impact estimates. Additional uncertainties include changes in future emissions and population, as well as parameterisations within the impact models (this is rarely considered). Figure 1 highlights the importance of considering climate model structural uncertainty in climate change impacts assessment. Figure 1 shows that for 2°C prescribed global-mean warming, the magnitude of, and sign of change in average annual runoff from present, simulated by an impacts model, can differ depending upon the GCM that provides the climate change projections that drive the impact model. This example also shows that

the choice of impact model, in this case a global hydrological model (GHM) or catchment-scale hydrological model (CHM), can affect the magnitude of impact and sign of change from present (e.g. see IPSL CM4 and MPI ECHAM5 simulations for the Xiangxi). To this end, throughout this review, the number of climate models applied in each study reviewed, and the other sources of uncertainty (e.g. emissions scenarios) are noted. Very few studies consider the application of multiple impacts models and it is recommended that future studies address this.

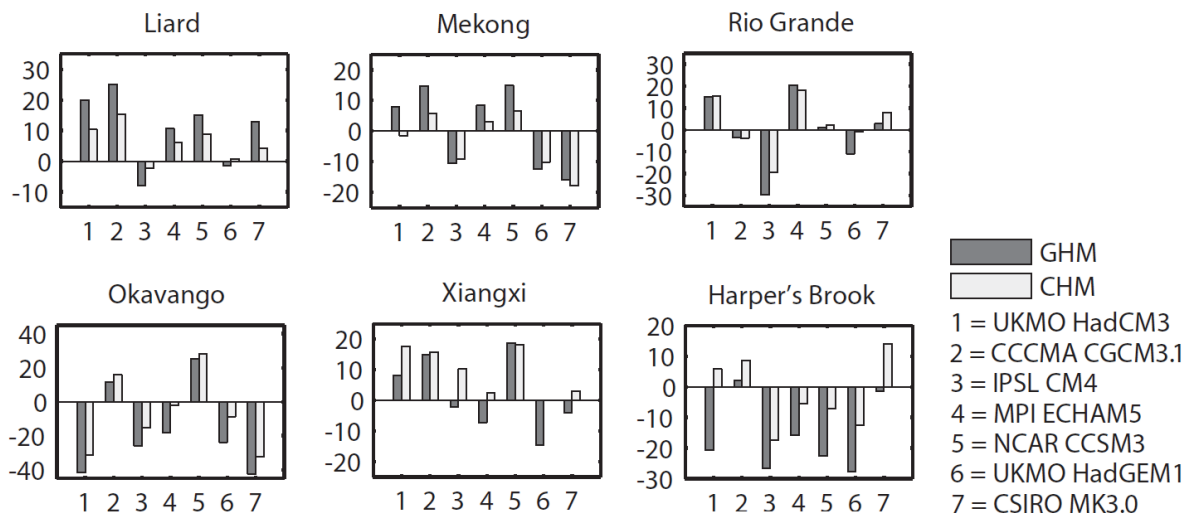


Figure 1. Change in average annual runoff relative to present (vertical axis; %), when a global hydrological model (GHM) and a catchment-scale hydrological model (CHM) are driven with climate change projections from 7 GCMs (horizontal axis), under a 2°C prescribed global-mean warming scenario, for six river catchments. The figure is from Gosling et al. (2011).

A key uncertainty in climate projections for Russia includes the extent of the Arctic sea ice retreat. Following a record minima in 2007, Arctic summer sea ice extent recovered back to the long-term trend line in 2009 (Fetterer et al., 2009), although estimates of thickness suggest that it is significantly thinner as a result of being largely composed of thin first year ice. It has been argued that the decline in 2007 was not particularly unusual in the context of the observational record (Notz, 2009), especially given that variability might be expected to increase as the sea ice thins (Goosse et al., 2009, Notz, 2009). However, abrupt reductions in future Arctic summer sea ice extent are seen in projections from several GCMs included in the CMIP3 multi-model dataset (Holland et al., 2006). Although there remains uncertainty, it is still considered likely that sea ice decline could be reversible (Notz, 2009), although some consequences of a temporary, but complete, seasonal loss of sea ice (e.g. for biodiversity) might be irreversible.

Methods combining observational constraints with model projections suggest that summer sea ice may disappear earlier than simulated by many (but not all) CMIP3 multi-model dataset models reported in the IPCC AR4, probably before the end of the century under a

mid-range non-mitigation emission scenario (Boe et al., 2009, Wang and Overland, 2009). However, although model skill has improved, caution is advised in interpreting such results, given remaining imperfections in the models. CMIP3 multi-model dataset models reported in the IPCC AR4 show large uncertainty, in terms of differences in contemporary sea ice mass budgets, partly due to a lack of relevant observations to validate the models (Holland et al., 2010) although some models, such as HadGEM2, are now able to simulate many aspects of the observed long-term trend and interannual variability. Despite uncertainty over the timing of routinely ice-free summer Arctic conditions, it is still thought very likely that this could occur with a 4°C global-mean warming. Amstrup et al. (2010) applied a GCM to show that more Arctic sea-ice could be retained with greenhouse gas mitigation relative to a business-as-usual scenario, but the model did not reveal thresholds leading to irreversible ice loss.

Zhang et al. (2010) simulated that a summer ice-free Arctic is likely by the mid-2040s, if Arctic surface air temperatures increase by 4°C by 2050 and climate variability is similar to the past relatively warm two decades. If the temperature increase is reduced to 2°C, a summer ice free Arctic could be unlikely before 2050. Because of enhanced winter ice growth, arctic winter ice extent remains nearly stable and therefore appears to be a less sensitive climate indicator. Projections for the different SRES emissions scenarios considered by Zhang et al. (2010) are displayed in Table 1.

Scenario	Mean ice extent (10^{12} m^2)	Mean ice volume (10^{12} m^3)
HC	6.8 (100)	13.0 (100)
A2	1.9 (28)	1.0 (8)
A1	3.3 (49)	1.6 (12)
B2	4.2 (62)	2.7 (21)
B1	5.5 (81)	3.8 (29)

Table 1. Simulated September Arctic mean ice extent and mean ice volume for the 1978-2009 time horizon (HC) and the 2010-2050 time horizon under four emissions scenarios. Values in parentheses are corresponding changes in percentage of the 1978-2009 mean September ice extent and volume. Data is from Zhang et al. (2010).

Summary of findings for each sector

Crop yields

- Quantitative crop yield projections under climate change scenarios for Russia vary greatly across studies due to the application of different models, assumptions and emissions scenarios.
- Whilst a definitive conclusion on the impact of climate change on crop yields in Russia cannot be drawn, the majority of global- and regional-scale studies included in this report project a decrease in the yield of wheat, Russia's major crop, as a consequence of climate change.
- Studies from the AVOID programme suggest a mixed outcome, with some areas of cultivated land becoming more suitable for agriculture, and other areas becoming less suitable, as a result of climate change.
- Important knowledge gaps and key uncertainties include the quantification of yield increases due to CO₂ fertilisation, the quantification of yield reductions due to ozone damage and the extent to which crop diseases might affect crop yields with climate change.

Food security

- Russia is currently a country with extremely low levels of undernourishment. The majority of global- and regional-scale studies included here project that although negatively affected, the country is unlikely to face severe food security issues over the next 40 years as a consequence of climate change.
- National-scale assessments are consistent in showing that climate change could have a negative impact on food security in Russia.
- One study concluded that Russia's economy could present a high vulnerability to the impact of climate change on fisheries by the 2050s. Another projected that the 10-year averaged maximum catch potential from 2005 to 2055 could see around a 20% increase under the A1B emission scenario.

Water stress and drought

- Global-scale studies included here show that the west of Russia is the most vulnerable region of the country to water stress. For the rest of the country and particularly the east, vulnerability is presently low.
- A number of global-scale studies included here project an increase in water availability across Russia as a whole with climate change, although there is regional variation, with an increase in water stress possible for the west of the country.
- However, recent simulations from the AVOID programme show consensus across models for little change in the population exposed to increased or decreased water stress with climate change.

Pluvial flooding and rainfall

- Recent studies suggest that winter precipitation could increase for Russia under climate change, and there is consistency across different climate models in this change.
- There is less agreement across climate models for precipitation changes in summer, however.
- Increases in precipitation from extreme storm events are also possible with climate change, although such projections cannot be translated directly into flood projections without detailed local-scale impact models, incorporating topography and hydrology.

Fluvial flooding

- Recent studies have suggested that flood magnitudes for Central and Eastern Siberia and the Russian Far East may increase with climate change, but decrease in European Russia and West Siberia, due to smaller maximum rates of snowmelt runoff.
- Results from simulations by the AVOID programme, that applied climate change projections from 21 climate models, show a high level of agreement among models that flood risk for Russia as a whole could decrease with climate change throughout the 21st century.

- Although most studies present a useful indicator of exposure to flood risk with climate change, none of them account for the effect that hydropower reservoirs, present in most large rivers, can have on the height of the annual flood peak, which can be substantial. Also, few studies have investigated the occurrence of ice dams and the potential resultant flooding with climate change.

Tropical cyclones

- Russia is not impacted by tropical cyclones.

Coastal regions

- There is very little work on the impact of climate change on Russia's coastal regions.
- However one study estimates that the population exposure to sea level rise (SLR) could increase from 189,000 in present to 226,000 under un-mitigated A1B emissions in 2070. Relative to A1B an aggressive mitigation policy could avoid an exposure of around 28,000 people by 2070. The study estimated that population exposure to sea level rise (SLR) could increase from 189,000 in present to 226,000 under un-mitigated A1B emissions in 2070; an aggressive mitigation scenario could avoid an exposure of around 28,000 people, relative to un-mitigated climate change in 2070.
- Nevertheless, further studies on the impact of climate change on Russia's coastal regions could improve understanding.

Crop yields

Headline

Crop yield projections under climate change scenarios for Russia vary greatly across studies due to the application of different models, assumptions and emissions scenarios. The majority of studies focus on wheat and potatoes but the wide range in impact estimates precludes a robust conclusion on the impact of climate change on crop yields in Russia.

Results from the AVOID programme for Russia indicate that the balance of impacts is more towards increasing rather than decreasing suitability in 2030 in both scenarios. However, as the 21st century progresses, the balance shifts more towards decreasing suitability, with this shift being small under the mitigation scenario but larger under A1B, partly because of smaller areas showing increasing suitability but mainly because larger areas undergo declining suitability.

Supporting literature

Introduction

The impacts of climate change on crop productivity are highly uncertain due to the complexity of the processes involved. Most current studies are limited in their ability to capture the uncertainty in regional climate projections, and often omit potentially important aspects such as extreme events and changes in pests and diseases. Importantly, there is a lack of clarity on how climate change impacts on drought are best quantified from an agricultural perspective, with different metrics giving very different impressions of future risk. The dependence of some regional agriculture on remote rainfall, snowmelt and glaciers adds to the complexity - these factors are rarely taken into account, and most studies focus solely on the impacts of local climate change on rain-fed agriculture. However, irrigated agricultural land produces approximately 40-45 % of the world's food (Doll and Siebert 2002), and the water for irrigation is often extracted from rivers which can depend on climatic conditions far from the point of extraction. Hence, impacts of climate change on crop productivity often need to take account of remote as well as local climate changes. Indirect impacts via sea-level rise, storms and diseases have also not been quantified. Perhaps most seriously, there is high uncertainty in the extent to which the direct effects of CO₂ rise on plant physiology will interact with climate change in affecting productivity. Therefore, at present, the aggregate impacts of climate change on large-scale agricultural productivity cannot be reliably

quantified (Gornall et al, 2010). This section summarises findings from a range of post IPCC AR4 assessments to inform and contextualise the analysis performed by AVOID programme for this project. The results from the AVOID work are discussed in the next section.

Wheat, sugar beet, potatoes and cereals (maize, barley, oats and rye) are Russia's most important crops (see Table 2) (FAO, 2008).

Harvested area (ha)		Quantity (Metric ton)		Value (\$1000)	
Wheat	26000000	Wheat	63700000	Wheat	6670000
Barley	9420000	Sugar beet	28900000	Potatoes	2820000
Sunflower seed	5980000	Potatoes	28800000	Sunflower seed	1540000
Oats	3400000	Barley	23100000	Sugar beet	1310000
Rye	2130000	Sunflower seed	7350000	Tomatoes	459000
Potatoes	2100000	Maize	6680000	Apples	421000
Maize	1730000	Oats	5830000	Vegetables fresh (nes) ¹	416000

¹ nes = not elsewhere specified or included

Table 2. The top 7 crops by harvested area, quantity and value according to the FAO (2008) in Russia. Crops that feature in all lists are shaded green; crops that feature in two top 7 lists are shaded amber. Data is from FAO (2008) and has been rounded down to three significant figures.

A number of global impact model studies looking at crop yield which include results for some of the main crops in Russia have been conducted. They apply a variety of methodological approaches, including using different climate model inputs and treatment of other factors that might affect yield, such as impact of increased CO₂ in the atmosphere on plant growth and adaption of agricultural practises to changing climate conditions. These different models, assumptions and emissions scenarios mean that there are a range of crop yield projections for Russia.

Important knowledge gaps and key uncertainties which are applicable to Russia as well as at the global scale, include: the quantification of yield increases due to CO₂ fertilisation and yield reductions due to ozone damage (Ainsworth and McGrath, 2010, Iglesias et al., 2009), and the extent crop diseases could affect crop yields with climate change (Luck et al., 2011).

Most crop simulation models do not include the direct effect of extreme temperatures on crop development and growth, thus only changes in mean climate conditions are considered to affect crop yields for the studies included here.

Assessments that include a global or regional perspective

Recent Past

Crop yield changes could be due to a variety of factors, which might include, but not be confined to, a changing climate. In order to assess the impact of recent climate change

(1980-2008) on wheat, maize, rice and soybean, Lobell et al. (2011) looked at how the overall yield trend in these crops changed in response to changes in climate over the period studied. The study was conducted at the global-scale but national estimates for Russia were also calculated. Lobell et al. (2011) divided the climate-induced yield trend by the overall yield trend for 1980–2008, to produce a simple metric of the importance of climate relative to all other factors. The ratio produced indicates the influence of climate on the productivity trend. So for example a value of -0.1 represents a 10% reduction in yield gain due to climate change, compared to the increase that could have been achieved without climate change, but with technology and other gains. This can also be expressed as 10 years of climate trend being equivalent to the loss of roughly 1 year of technology gains. For Russia, maize, soybean and wheat yield were impacted adversely, relative to what would have been achieved without the climate trends (see Table 3).

Crop	Trend
Maize	-0.2 to -0.1
Rice	0.0 to 0.1
Wheat	-0.3 to -0.2
Soybean	-0.2 to -0.1

Table 3. The estimated net impact of climate trends for 1980-2008 on crop yields in Russia. Climate-induced yield trend divided by overall yield trend. Data is from Lobell et al. (2011).

Climate change studies

Several recent studies have applied climate projections from Global Climate Models (GCMs) to crop models to assess the global-scale impact of climate change on crop yields (Iglesias and Rosenzweig, 2009, Tatsumi et al., 2011, Fischer, 2009). Most of these studies include impact estimates at the national-scale for Russia, which are presented in this section. The process of CO₂ fertilisation of some crops is usually included in most climate impact studies of yields. However, other gases can influence crop yield and are not always included in impacts models. An example of this is ozone (O₃) and so a study which attempts to quantify the potential impact on crop yield of changes in ozone in the atmosphere is also included (Avnery et al. 2011). In addition to these studies, the AVOID programme analysed the patterns of climate change for 21 GCMs, to establish an index of 'climate suitability' of agricultural land. Climate suitability is not directly equivalent to crop yields, but is a means of looking at a standard metric across all the countries including in this project, and of assessing the level of agreement on variables that affect crop production, between all 21 GCMs.

Iglesias and Rosenzweig (2009) repeated an earlier study presented by Parry et al. (2004) by applying climate projections from the HadCM3 GCM (instead of HadCM2, which was

applied by Parry et al. (2004)), under seven SRES emissions scenarios and for three future time periods. This study used a globally consistent crop simulation methodologies and climate change scenarios, and weighted the model site results by their contribution to regional and national, and rain-fed and irrigated production. The study also applied a quantitative estimation of physiological CO₂ effects on crop yields and considered the effect of adaptation by assessing the country or regional potential for reaching optimal crop yield. The results from the study for Russia are presented in Table 4 and Table 5. The simulations showed that relative to the baseline (1970-2000) yield levels, crop yield losses were projected for each of the crops with climate change for all time horizons. Under all emissions scenarios (except A1FI) and B1a, wheat yield was estimated to increase between 2050 and 2080; the declining yield trend for maize on the other hand was not reversed.

Scenario	Year	Wheat	Maize
A1FI	2020	-3.19	-6.19
	2050	-4.56	-11.56
	2080	-5.07	-15.07
A2a	2020	-3.16	-6.16
	2050	-3.38	-10.38
	2080	-0.41	-11.41
A2b	2020	-2.89	-5.89
	2050	-4.37	-11.37
	2080	-2.70	-13.70
A2c	2020	-1.89	-4.89
	2050	-3.92	-10.92
	2080	-1.04	-12.04
B1a	2020	-5.57	-8.57
	2050	-3.29	-8.29
	2080	-5.82	-11.82
B2a	2020	-5.85	-8.85
	2050	-4.33	-9.33
	2080	-2.99	-9.99
B2b	2020	-4.09	-7.09
	2050	-7.48	-12.48
	2080	-4.71	-11.71

Table 4. Wheat and maize yield changes (%) in Russia relative to baseline scenario (1970-2000) for different emission scenarios and future time periods. Some emissions scenarios were run in an ensemble simulation (e.g. A2a, A2b, A2c). Data is from Iglesias and Rosenzweig (2009).

	Wheat		Maize	
	Up	Down	Up	Down
Baseline to 2020	0	7	0	7
Baseline to 2050	0	7	0	7
Baseline to 2080	0	7	0	7
2020 to 2050	2	5	1	6
2050 to 2080	5	2	1	6

Table 5. The number of emission scenarios that predict yield gains (“Up”) or yield losses (“Down”) for wheat and maize in Russia between two points in time. Data is from Iglesias and Rosenzweig (2009).

Tatsumi et al. (2011) applied an improved version of the GAEZ crop model (iGAEZ) to simulate crop yields on a global scale for wheat, potato, cassava, soybean, rice, sweet potato, maize, green beans. The impact of global warming on crop yields from the 1990s to 2090s was assessed by projecting five GCM outputs under the SRES A1B scenario and comparing the results for crop yields as calculated using the iGAEZ model for the period of 1990-1999. The results for Russia are displayed in Table 6 and suggest a general decline in yields of all crops modelled, except for rice.

Wheat	Potato	Cassava	Soybean	Rice	Sweet potato	Maize	Green beans
-8.28	-9.24	-	-10.73	11.45	-	-11.5	-

Table 6. Average change in yield (%), during 1990s-2090s in Russia. Data is from Tatsumi et al. (2011).

Fischer (2009) projected global ‘production potential’ changes for 2050 using the GAEZ (Global Agro-Ecological Zones) crops model with climate change scenarios from the HadCM3 and CSIRO GCMs respectively, under SRES A2 emissions. The impacts of future climate on crop yields of rain-fed cereals in Russia (relative to yield realised under current climate) are presented in Table 7. Contrary to the previous studies these results suggest an increase in the crop yield potential, especially for maize and sorghum.

	CO ₂ fert.	2020s		2050s		2080s	
		CSIRO	HADCM3	CSIRO	HADCM3	CSIRO	HADCM3
Rain-fed wheat	Yes	4	3	4	5	-15	-1
	No	1	n/a	-2	n/a	-23	n/a
Rain-fed maize	Yes	64	54	79	67	69	63
	No	61	n/a	73	n/a	62	n/a
Rain-fed cereals	Yes	n/a	5	n/a	9	n/a	6
	No	n/a	n/a	n/a	n/a	n/a	n/a
Rain-fed sorghum	Yes	60	n/a	75	n/a	70	n/a
	No	57	n/a	68	n/a	62	n/a

Table 7. Impacts of climate change on the production potential in Russia of rain-fed cereals in current cultivated land (% change with respect to yield realised under current climate), with two GCMs and with and without CO₂ fertilisation (“CO₂ fert.”) under SRES A2 emissions. Data is from Fischer (2009).

In addition to the studies looking at the effect of changes in climate and CO₂ concentrations on crop yield, Avnery et al. (2011) investigated the effects of ozone surface exposure on crop yield losses for soybeans, maize and wheat under the SRES A2 and B1 scenarios respectively. Two metrics of ozone exposure were investigated; seasonal daytime (08:00-19:59) mean O₃ (“M12”) and accumulated O₃ above a threshold of 40 ppbv (“AOT40”). The effect of the ozone exposure was considered in isolation from climate and other changes. The results for Russia are presented in Table 8.

	A2		B1	
	M12	AOT40	M12	AOT40
Soybeans	-	-	-	-
Maize	6-8	2-4	4-6	0-2
Wheat	2-4	15-20	0-2	8-10

Table 8. National relative crop yield losses (%) for 2030 under A2 and B1 emission scenarios according to the M12 (seasonal daytime (08:00–19:59) mean) and AOT40 (accumulated O₃ above a threshold of 40 ppbv) metrics of O₃ exposure. Data is from Avnery et al. (2011).

National-scale or sub-national scale assessments

Climate change studies

In this section we present results from recent studies that have produced national or sub-national scale projections of future crop yields in Russia.

Alcamo et al. (2007a) assessed the impact of climate change on Russian agriculture by applying climate projections from two GCMs under SRES A2 and B2 emissions scenarios. The authors also accounted for the frequency (and spatial heterogeneity) of extreme climate events. The simulations suggested that decreased crop production in some Russian regions

could be compensated by increased production in others, thus resulting in relatively small average changes (see Table 9). However, the frequency of food production shortfall years (a year in which potential production of the most important crops in a region is below 50% of its average climate normal production) doubled in many of the main crop growing areas in the 2020s, and tripled in the 2070s.

	2020				2070			
	A2		B2		A2		B2	
	Grain	Potato	Grain	Potato	Grain	Potato	Grain	Potato
ECHAM4	112	96	101	105	95	96	95	97
HadCM3	94	106	91	122	90	104	88	104

Table 9. Climate-related potential crop production (calculated from crop yield) in Russia, expressed as percentage of current mean potential crop production (average annual production from 1961 to 1990 = 100%). Grain included wheat and rye. Data is from Alcamo et al. (2007a).

Dronin and Kirilenko (2008) also assessed the impact of climate change on Russian crop production. The authors applied the same GCMs and emissions scenarios as Alcamo et al. (2007a) and showed that crop production declined in the 2020s and 2070s from baseline levels (see Figure 2). However, the authors did not consider the potential yield increases in regions that currently do not produce wheat or the CO₂ fertilisation effect.

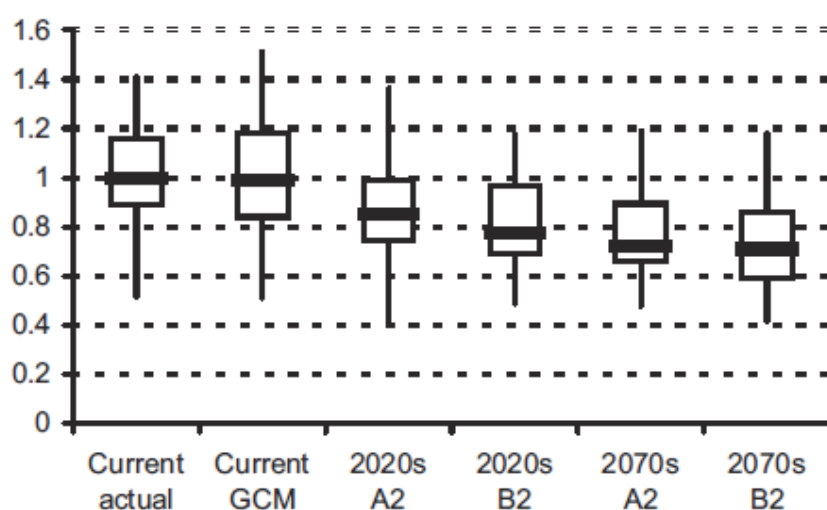


Figure 2. Russian wheat production change (as a proportion of current (1961-1990) production) under HADCM3 and ECHAM4 runs (the range across GCMs is included in the errorbars), employing SRES A2 and B2 emission scenarios and the GAEZ-R crop model. Minimum, first quartile, mean, third quartile, and maximum annual yield are shown. 'Current actual' represents observed production as reported by the Russian National Statistics Committee (GosComStat) whereas 'Current GCM' represents wheat production as estimated by GAEZ-R simulations. Figure is from Dronin and Kirilenko (2008).

AVOID programme results

To further quantify the impact of climate change on crops, the AVOID programme simulated the effect of climate change on the suitability of land for crop cultivation for all countries reviewed in this literature assessment based upon the patterns of climate change from 21 GCMs (Warren et al., 2010). This ensures a consistent methodological approach across all countries and takes consideration of climate modelling uncertainties.

Methodology

The effect of climate change on the suitability of land for crop cultivation is characterised here by an index which defines the percentage of cropland in a region with 1) a decrease in suitability or 2) an increase in suitability. A threshold change of 5% is applied here to characterise decrease or increase in suitability. The crop suitability index is calculated at a spatial resolution of $0.5^{\circ} \times 0.5^{\circ}$, and is based on climate and soil properties (Ramankutty et al., 2002). The baseline crop suitability index, against which the future changes are measured, is representative conditions circa 2000. The key features of the climate for the crop suitability index are temperature and the availability of water for plants, and changes in these were derived from climate model projections of future changes in temperature and precipitation, with some further calculations then being used to estimate actual and potential evapotranspiration as an indicator of water availability. It should be noted that changes in atmospheric CO_2 concentrations can decrease evapotranspiration by increasing the efficiency of water use by plants (Ramankutty et al., 2002), but that aspect of the index was not included in the analysis here. Increased CO_2 can also increase photosynthesis and improve yield to a small extent, but again these effects are not included. Exclusion of these effects may lead to an overestimate of decreases in suitability.

The index here is calculated only for grid cells which contain cropland circa 2000, as defined in the global crop extent data set described by Ramankutty et al. (2008) which was derived from satellite measurements. It is assumed that crop extent does not change over time. The crop suitability index varies significantly for current croplands across the world (Ramankutty et al., 2002), with the suitability being low in some current cropland areas according to this index. Therefore, while climate change clearly has the potential to decrease suitability for cultivation if temperature and precipitation regimes become less favourable, there is also scope for climate change to increase suitability in some existing cropland areas if conditions become more favourable in areas where the suitability index is not at its maximum value of 1. It should be noted that some areas which are not currently croplands may already be suitable for cultivation or may become suitable as a result of future climate change, and may

become used as croplands in the future either as part of climate change adaptation or changes in land use arising for other reasons. Such areas are not included in this analysis.

Results

Crop suitability was estimated under the pattern of climate change from 21 GCMs with two emissions scenarios; 1) SRES A1B and 2) an aggressive mitigation scenario where emissions follow A1B up to 2016 but then decline at a rate of 5% per year thereafter to a low emissions floor (denoted A1B-2016-5-L). The application of 21 GCMs is an attempt to quantify the uncertainty due to climate modelling, although it is acknowledged that only one crop suitability impacts model is applied. Simulations were performed for the years 2030, 2050, 2080 and 2100. The results for Russia are presented in Figure 3.

Under all the climate projections, some existing cropland areas become less suitable for cultivation while other existing cropland areas become more suitable. The areas of increased and decreased suitability differ considerably according to the climate model used, and these differences between models increase into the future, especially in the A1B scenario.

In both scenarios, between 39% and 62% of current Russian croplands become more suitable for cultivation by 2030. In the mitigation scenario, the range of projected areas undergoing increased suitability becomes larger through the 21st century, with the lowest projection falling slightly to 37% while the highest projection rises to 69% - however, the mean of all model projections remains similar over time. However, for the A1B scenario, the difference between model projections of areas of increased suitability becomes rather larger, ranging from 22% to 73% by 2100 with the mean projection falling from 47% in 2030 to 40% in 2100. For both scenarios, between 3% and 43% of current Russian croplands are projected to undergo declining suitability by 2030. By 2100 this rises to 10%-50% under the mitigation scenario and 15%-75% under A1B.

So, for Russia, the balance of impacts is more towards increasing rather than declining suitability in 2030 in both scenarios. However, as the 21st century progresses, the balance shifts more towards declining suitability, with this shift being small under the mitigation scenario but larger under A1B, partly because of smaller areas showing increasing suitability but mainly because larger areas undergo declining suitability.

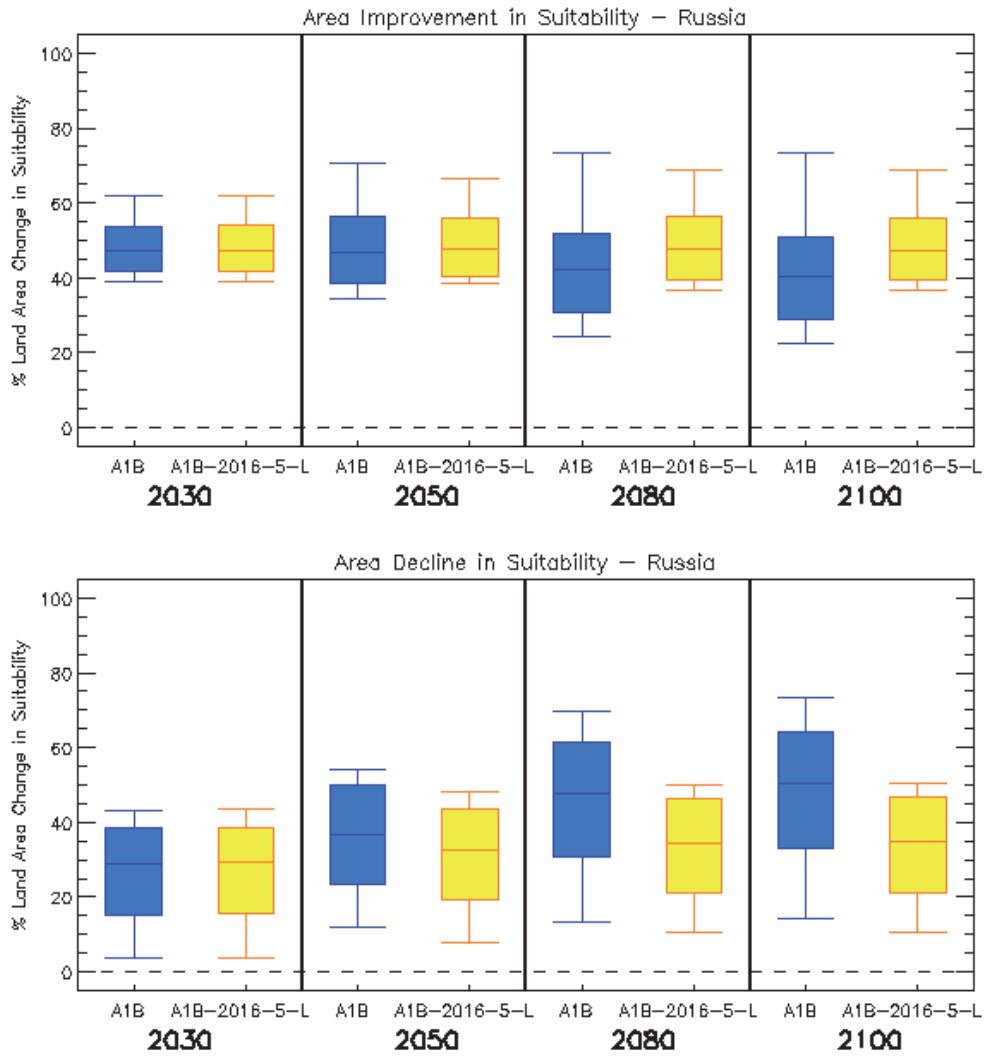


Figure 3. Box and whisker plots for the impact of climate change on increased crop suitability (top panel) and decreased crop suitability (bottom panel) for Russia, from 21 GCMs under two emissions scenarios (A1B and A1B-2016-5-L), for four time horizons. The plots show the 25th, 50th, and 75th percentiles (represented by the boxes), and the maximum and minimum values (shown by the extent of the whiskers).

Food security

Headline

There is no consensus across studies regarding the impact of climate change on food security for Russia. A number of global-scale assessments suggest that food security may not be an issue with climate change and that Russia might be able to export food due to surplus. A different global-scale assessment suggests that Russia may need to limit food exports to avoid major food insecurity under climate change, however. National-scale assessments are consistent in showing that climate change could have a negative impact on food security in Russia.

Supporting literature

Introduction

Food security is a concept that encompasses more than just crop production, but is a complex interaction between food availability and socio-economic, policy and health factors that influence access to food, utilisation and stability of food supplies. In 1996 the World Food Summit defined food security as existing 'when all people, at all times, have physical and economic access to sufficient, safe and nutritious food to meet their dietary needs, and their food preferences are met for an active and healthy life'. As such this section cannot be a comprehensive analysis of all the factors that are important in determining food security, but does attempt to assess a selection of the available literature on how climate change, combined with projections of global and regional population and policy responses, may influence food security.

With regards to food security Russia is presently a country of very low concern, relative to other countries across the globe. According to FAO statistics (FAO, 2010) Russia has extremely low rates of undernourishment (less than 5% of the population). However, a number of global studies disagree about the effect of climate change on food security in Russia in the future. These differences are in part, due to the application of different climate models, crops models and food security models. Additional uncertainties concern the response of capture fisheries to climate change. These uncertainties call for a comprehensive assessment of the impact of climate change on food security in Russia.

Assessments that include a global or regional perspective

Several recent studies have analysed food security under climate change across the globe. Wu et al. (2011) simulated crop yields with the GIS-based Environmental Policy Integrated Climate (EPIC) model. This was combined with crop areas simulated by a crop choice decision model to calculate total food production and per capita food availability across the globe, which was used to represent the status of food availability and stability. The study focussed on the SRES A1 scenario and applied climate change simulations for the 2000s (1991–2000) and 2020s (2011–2020). The climate simulations were performed by MIROC (Model for Interdisciplinary Research on Climate) version 3.2., which means the effects of climate model uncertainty were not considered. Downscaled population and GDP data from the International Institute for Applied Systems Analysis (IIASA) were applied in the simulations. Wu et al. (2011) concluded that Russia is not likely to face severe food insecurity in the next 20 years

However, the results presented by Wu et al. (2011) are in stark contrast to the results of a study presented by Arnell et al. (2010) who demonstrated how important adaptation measures could be for Russia, if major food security issues are to be avoided under climate change. The study considered the impacts of global climate change and mitigation policy on food security for eleven countries. The study applied climate change patterns from the HadCM3 GCM and explored food security under two emissions scenarios; a business as usual scenario (SRES A1B) and four mitigations scenarios where emissions peak in 2030 and subsequently reduce at 2% per year to a high emissions floor (referred to as 2030-2-H) or 5% per year to a low emissions floor (2030-5-L), or where they peak in 2016 and subsequently reduce at 2% per year to a high emissions floor (referred to as 2016-2-H) or 5% per year to a low emissions floor (2016-5-L). The study also considered a series of structural adjustments that could be made in the future to adapt to food security issues, including that 1) if there is a shortfall of any per-capita food availability due to crop yield and/or population changes, then original (baseline) food amounts are made up by reducing or removing export amounts; and 2) if, after the above adjustments, there is still a shortfall, then the amount of crops going to animal feed is reduced or removed to try to make up to the original (baseline) food amounts. The model simulations presented by Arnell et al. (2010) characterise the numbers of people *exposed to undernourishment* in the absence of increased crop production and imports, not actual numbers of undernourished people. The results are presented in Figure 4. Arnell et al. (2010) estimated that exposure to undernourishment could increase in Russia by 2050 as the population increases by 15% under A1B and crop yields fall by up to 44%. Without structural adjustments, over 95% of the population in Russia could be exposed to undernourishment under any given emissions

scenarios from 2050 onwards. However, with structural adjustments incorporated into the simulations, this is reduced to around 8-10% for any given scenario. Moreover, this highlights that structural adjustments within Russia are comparatively more effective at improving food security than the global climate change mitigation considered here.

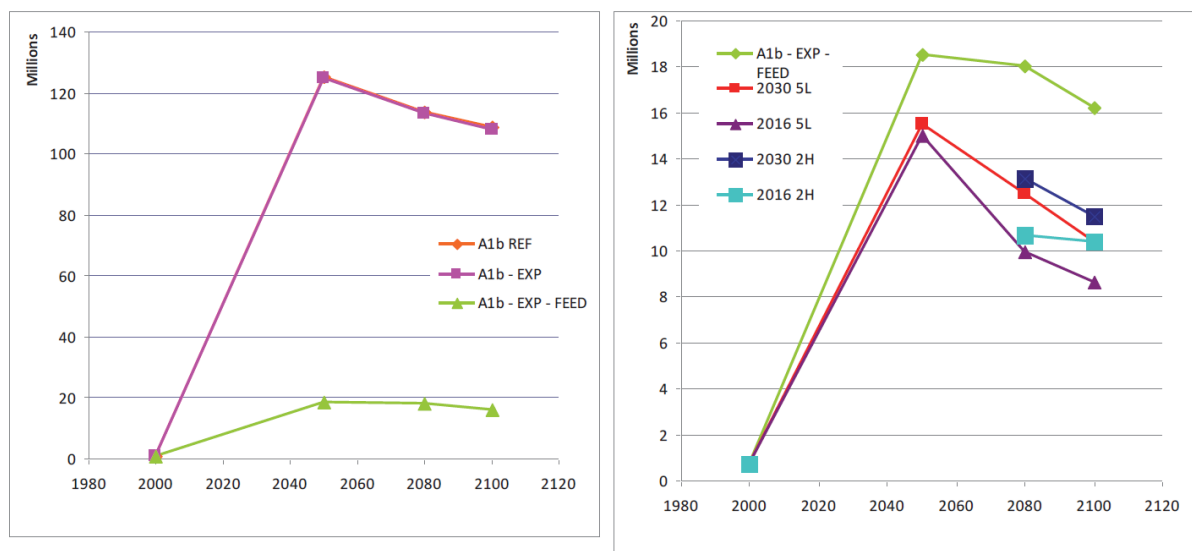


Figure 4. Total projected population exposed to undernourishment in Russia. The left panel shows total exposure under the A1B emissions scenario (“A1b REF”), plus the A1B scenario with exports reduced or removed (“A1b-EXP”) and the A1B scenario with exports removed and allocation to feed reduced or removed (“A1b-EXP-FEED”). The right panel shows the total exposure under the A1b-EXP-FEED and three mitigation scenarios. The figure is from Arnell et al. (2010).

A more optimistic outlook for Russia is suggested by Falkenmark et al. (2009), which supports the conclusions of Wu et al. (2011). The study presents an analysis of water constraints and opportunities for global food production on current croplands and assesses five main factors:

- 1) how far improved land and water management might go towards achieving global food security,
- 2) the water deficits that would remain in regions currently experiencing water scarcity and which are aiming at food self-sufficiency,
- 3) how the water deficits above may be met by importing food,
- 4) the cropland expansion required in low income countries without the needed purchasing power for such imports, and
- 5) the proportion of that expansion pressure which will remain unresolved due to potential lack of accessible land.

Similar to the study presented by Wu et al. (2011), there is no major treatment of modelling uncertainty; simulations were generated by only the LPJml dynamic global vegetation and water balance model (Gerten et al. 2004) with population growth and climate change under the SRES A2 emission scenario. Falkenmark et al. (2009) summarise the impacts of future improvements (or lack thereof) in water productivity for each country across the globe and show that this generates either a deficit or a surplus of water in relation to food water requirements in each country. These can be met either by trade or by horizontal expansion (by converting other terrestrial ecosystems to crop land). The study estimated that in 2050 around one third of the world's population will live in each of three regions: those that export food, those that import food, and those that have to expand their croplands at the expense of other ecosystems because they do not have enough purchasing power to import their food. The simulations demonstrated that Russia was a food exporting country in 2050.

The International Food Policy Research Institute (IFPRI) have produced a report and online tool that describes the possible impact of climate change on two major indicators of food security; 1) the number of children aged 0-5 malnourished, and 2) the average daily kilocalorie availability (Nelson et al., 2010, IFPRI, 2010). The study considered three broad socio-economic scenarios; 1) a 'pessimistic' scenario, which is representative of the lowest of the four GDP growth rate scenarios from the Millennium Ecosystem Assessment GDP scenarios and equivalent to the UN high variant of future population change, 2) a 'baseline' scenario, which is based on future GDP rates estimated by the World Bank and a population change scenario equivalent to the UN medium variant, and 3) an 'optimistic' scenario that is representative of the highest of the four GDP growth rate scenarios from the Millennium Ecosystem Assessment GDP scenarios and equivalent to the UN low variant of future population change. Nelson et al. (2010) also considered climate modelling and emission uncertainty and included a factor to account for CO₂ fertilisation in their work. The study applied two GCMs, the CSIRO GCM and the MIROC GCM, and forced each GCM with two SRES emissions scenarios (A1B and B1). They also considered a no climate change emissions scenario, which they called 'perfect mitigation' (note that in most other climate change impact studies that this is referred to as the baseline). The perfect mitigation scenario is useful to compare the effect of climate change against what might have happened without, but is not a realistic scenario itself. Estimates for both indicators of food security from 2010 to 2050, for Russia, are presented in Table 10 and Table 11. Figure 5 displays the effect of climate change, calculated by comparing the 'perfect mitigation' scenario with each baseline, optimistic and pessimistic scenario. The results indicate that during 2010-2050, average daily kilocalorie availability increases under the optimistic and baseline scenarios. However, climate change has the effect of mitigating this improvement;

by 2050 climate change is attributable for up to around a 9% decline in kilocalorie availability (Figure 5). Child malnourishment increases by at least around 100,000 during 2010-2050. Whilst this increase is partly attributable to socioeconomic conditions, climate change is attributable for up to a 28% increase in malnourishment in 2050 (Figure 5). This implies that Russia could face food security issues with climate change and serves to support the findings presented by Arnell et al. (2010), in this respect, although it should be noted that kilocalorie availability remains high in 2050. Figure 6 and Figure 7 show how the changes projected for Russia compare with the projections for the rest of the globe (IFPRI, 2010).

Scenario	2010	2050
Baseline CSI A1B	2959	3131
Baseline CSI B1	2963	3154
Baseline MIR A1B	2944	3054
Baseline MIR B1	2955	3114
Baseline Perfect Mitigation	3002	3350
Pessimistic CSI A1B	2885	2699
Pessimistic CSI B1	2889	2717
Pessimistic MIR A1B	2871	2633
Pessimistic MIR B1	2878	2667
Pessimistic Perfect Mitigation	2927	2876
Optimistic CSI A1B	2956	3254
Optimistic CSI B1	2960	3272
Optimistic MIR A1B	2941	3169
Optimistic MIR B1	2948	3207
Optimistic Perfect Mitigation	2999	3476

Table 10. Average daily kilocalorie availability simulated under different climate and socioeconomic scenarios, for Russia (IFPRI, 2010).

Scenario	2010	2050
Baseline CSI A1B	0.41	0.66
Baseline CSI B1	0.41	0.65
Baseline MIR A1B	0.42	0.7
Baseline MIR B1	0.41	0.67
Baseline Perfect Mitigation	0.38	0.55
Pessimistic CSI A1B	0.46	1.02
Pessimistic CSI B1	0.46	1.01
Pessimistic MIR A1B	0.47	1.07
Pessimistic MIR B1	0.47	1.04
Pessimistic Perfect Mitigation	0.43	0.91
Optimistic CSI A1B	0.41	0.52
Optimistic CSI B1	0.41	0.51
Optimistic MIR A1B	0.42	0.55
Optimistic MIR B1	0.42	0.54
Optimistic Perfect Mitigation	0.39	0.43

Table 11. Number of malnourished children (aged 0-5; millions) simulated under different climate and socioeconomic scenarios, for Russia (IFPRI, 2010).

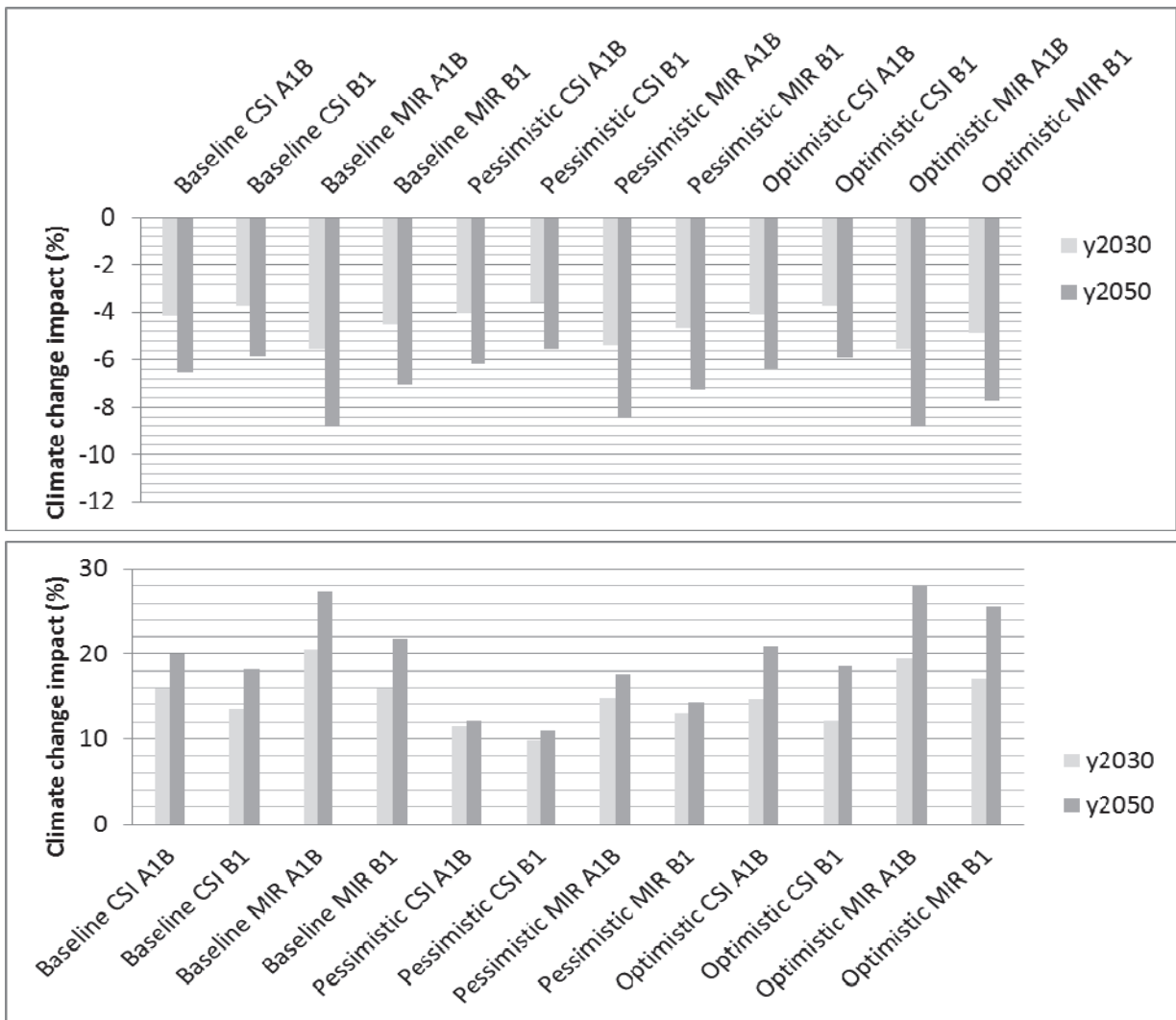


Figure 5. The impact of climate change on average daily kilocalorie availability (top panel) and number of malnourished children (bottom) in Russia (IFPRI, 2010).

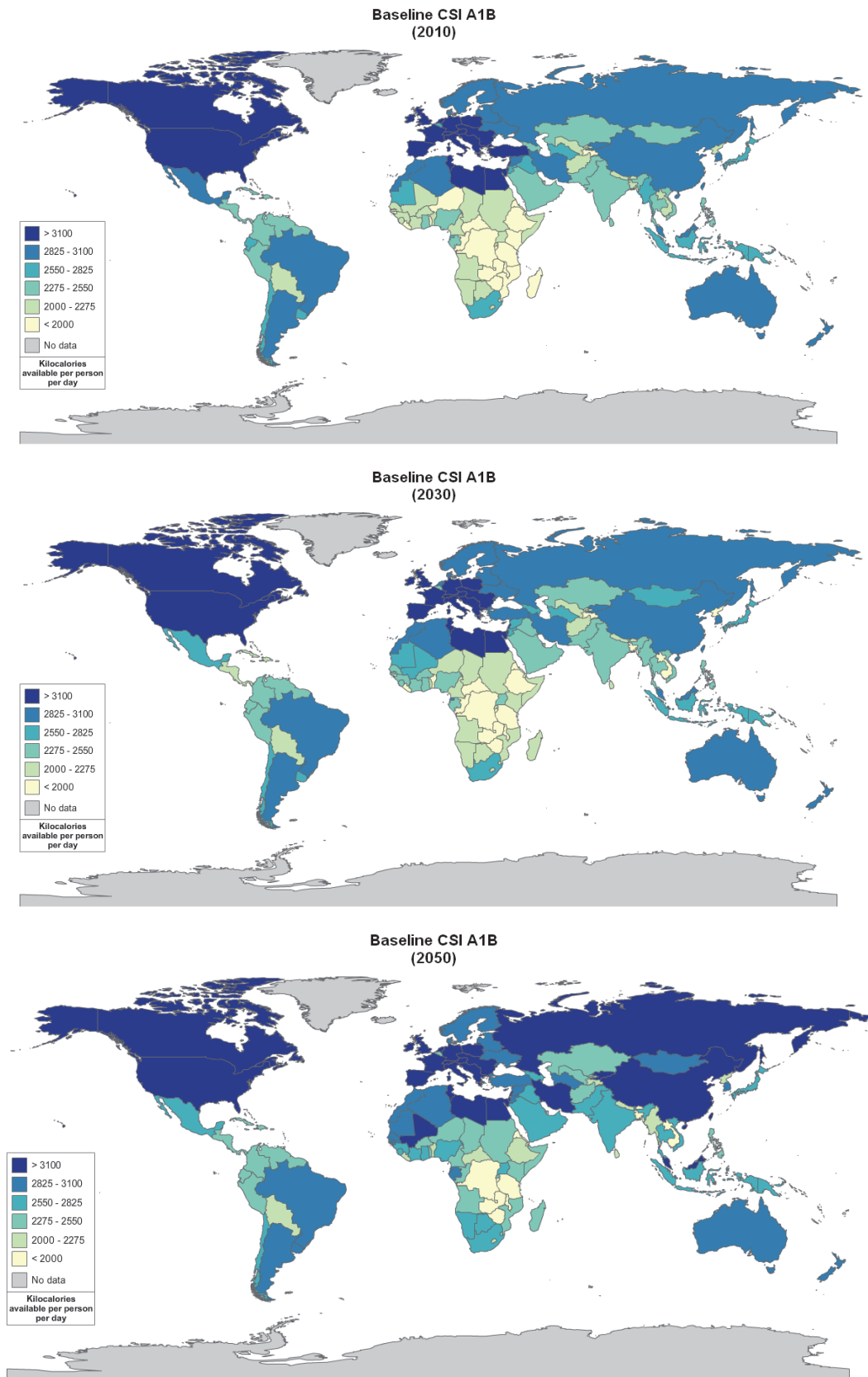


Figure 6. Average daily kilocalorie availability simulated by the CSIRO GCM (CSI) under an A1B emissions scenario and the baseline socioeconomic scenario, for 2010 (top panel), 2030 (middle panel) and 2050 (bottom panel). The figure is from IFPRI (IFPRI, 2010). The changes show the combination of both climate change and socio-economic changes.

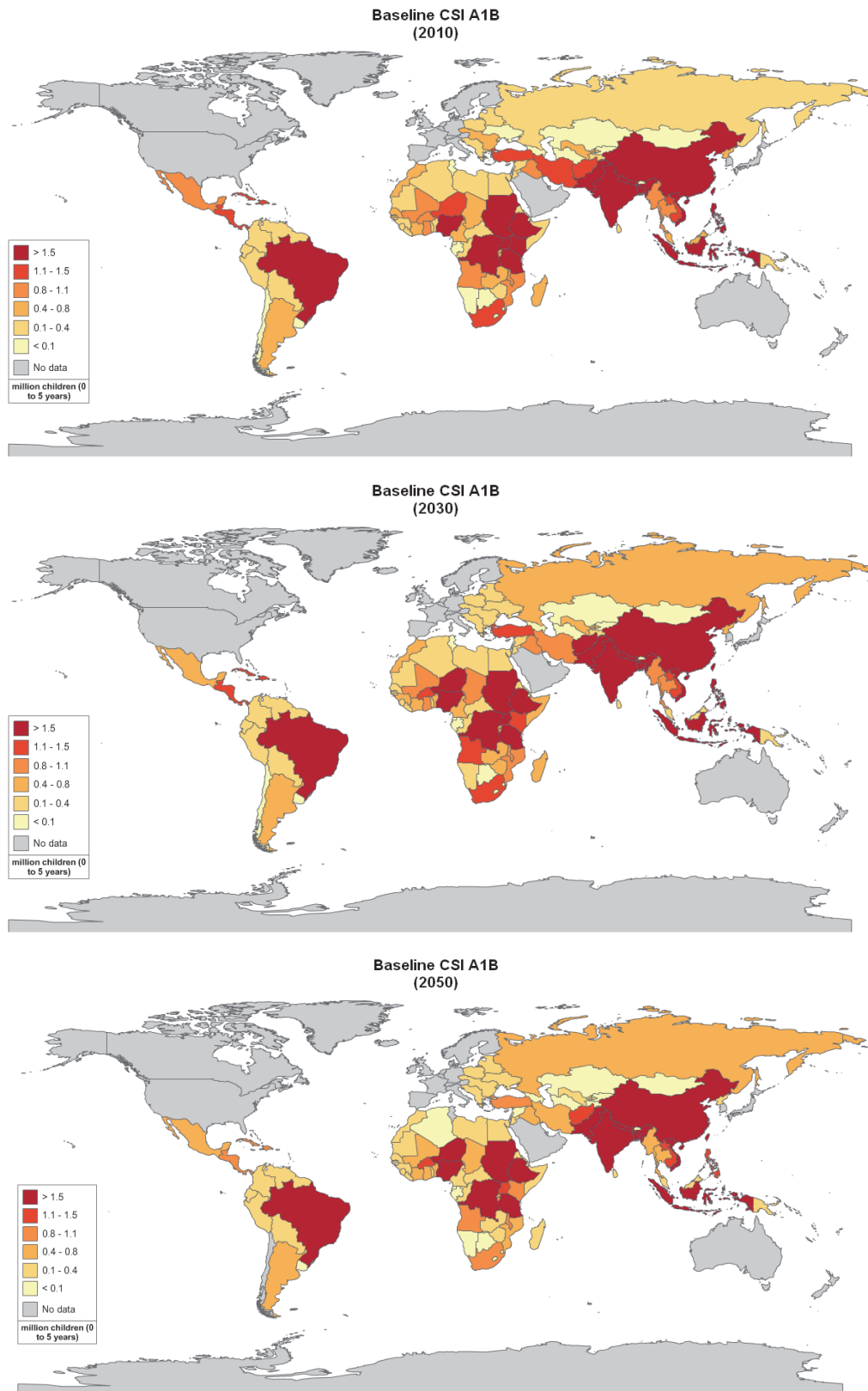


Figure 7. Number of malnourished children (aged 0-5; millions) simulated by the CSIRO GCM (CSI) under an A1B emissions scenario and the baseline socioeconomic scenario, for 2010 (top panel), 2030 (middle panel) and 2050 (bottom panel). The figure is from IFPRI (IFPRI, 2010). The changes show the combination of both climate change and socio-economic changes.

It is important to note that up until recently, projections of climate change impacts on global food supply have tended to focus solely on production from terrestrial biomes, with the large contribution of animal protein from marine capture fisheries often ignored. However, recent studies have attempted to address this knowledge gap (Allison et al., 2009, Cheung et al., 2010). In addition to the direct affects of climate change, changes in the acidity of the oceans, due to increases in CO₂ levels, could also have an impact of marine ecosystems, which could also affect fish stocks. However, this relationship is complex and not well understood, and studies today have not been able to begin to quantify the impact of ocean acidification on fish stocks.

Allison et al. (2009) conducted a global analysis that compares the vulnerability of 132 national economies to potential climate change impacts on their capture fisheries. The study considered a country's vulnerability to be a function of the combined effect of projected climate change, the relative importance of fisheries to national economies and diets, and the national societal capacity to adapt to potential impacts and opportunities. Climate change projections from a single GCM under two emissions scenarios (SRES A1FI and B2) were used in the analysis. It should be noted, however, that results from studies that have applied only a single climate model or climate change scenario should be interpreted with caution. This is because they do not consider other possible climate change scenarios which could result in a different impact outcome, in terms of magnitude and in some cases sign of change. Allison et al. (2009) concluded that Russia's fisheries presented a high vulnerability to climate change, which reflects its relatively important fishing fleets, high level of exposure to predicted climate change and relatively low adaptive capacity. Other countries that presented high vulnerability included some in Central and Western Africa (e.g. Malawi, Guinea, Senegal, and Uganda), Peru and Colombia in north-western South America, and four tropical Asian countries (Bangladesh, Cambodia, Pakistan, and Yemen) (see Figure 8).

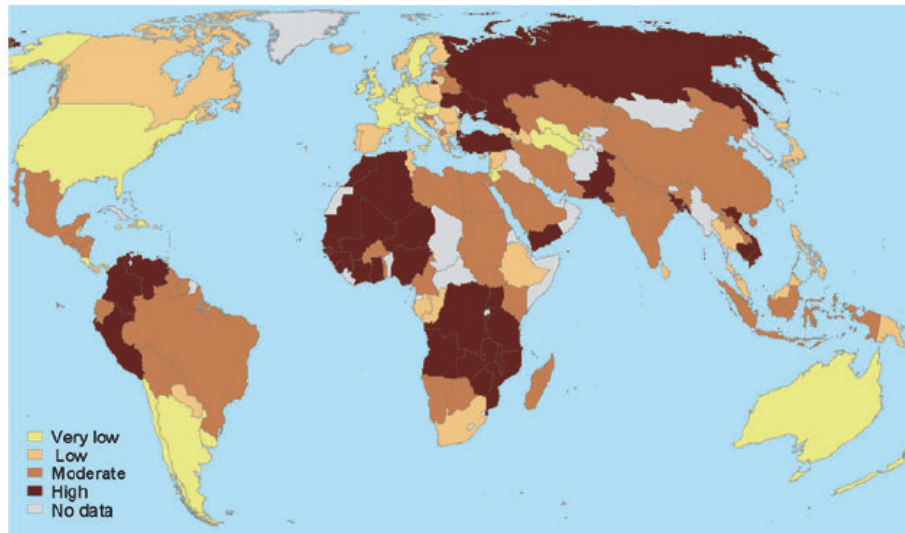


Figure 8. Vulnerability of national economies to potential climate change impacts on fisheries under SRES B2 (Allison et al., 2009). Colours represent quartiles with dark brown for the upper quartile (highest index value), yellow for the lowest quartile, and grey where no data were available.

Cheung et al. (2010) considered marine capture fisheries at the global scale for several countries. The study projected changes in global catch potential for 1066 species of exploited marine fish and invertebrates from 2005 to 2055 under climate change scenarios. Cheung et al. (2010) found that climate change may lead to large-scale redistribution of global catch potential, with an average of 30–70% increase in high-latitude regions and a decline of up to 40% in the tropics. The simulations were based on climate simulations from a single GCM (GFDL CM2.1) under a SRES A1B emissions scenario (CO₂ concentration at 720ppm in 2100) and a stable-2000 level scenario (CO₂ concentration maintains at year 2000 level of 365 ppm). The limitations of applying a single climate model have been noted previously. The results presented by Cheung et al. (2010) for Russia are in stark contrast to those presented for Russian marine fisheries by Allison et al. (2009). The projected change in the 10-year averaged maximum catch potential from 2005 to 2055 was around a 20% increase under A1B, whereas under the stabilisation scenario the increase was around 2%, based upon 75 exploited species included in the analysis. Figure 9 demonstrates how this compares with projected changes for other countries across the globe.

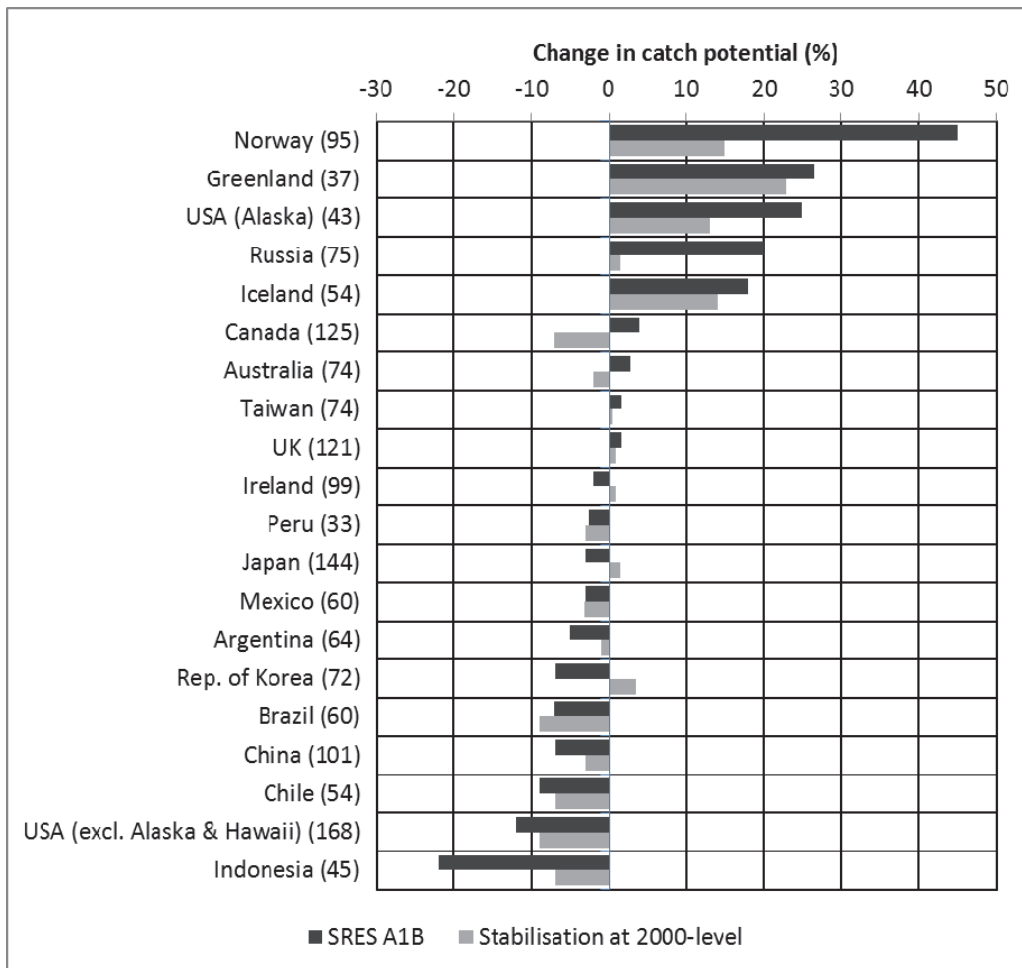


Figure 9. Projected changes in the 10-year averaged maximum catch potential from 2005 to 2055. The numbers in parentheses represent the numbers of exploited species included in the analysis. Adapted from Cheung et al. (2010).

National-scale or sub-national scale assessments

Climate change studies

Recent national-scale studies, presented by Dronin and Kirilenko (2008, 2011) support the more pessimistic outlooks for food security in Russia under climate change, which are presented by some global studies (Allison et al., 2009, Arnell et al., 2010, IFPRI, 2010, Nelson et al., 2010). Dronin and Kirilenko (2008, 2011) analysed the impact of climate change on cereal production in Russia and found that the general perception of a beneficiary effect of a warmer climate is unlikely to be true, primarily due to increasing risk of droughts in the most important agricultural areas of Russia. The studies applied two GCMs and the average of two emissions scenarios (SRES A2 and B2) in 2020 and 2070, and they considered to main market forces; 1) the ‘Fortress Market’ scenario, which assumes that a number of production regions tend to restrict their sales, holding a considerable amount of grain surplus for their internal consumption; and 2) an ‘Open Market’ scenario that assumes

that the production regions are able to sell the available harvested grain without administrative restrictions. The study assessed how climate change affected national food stress, where food stress was taken as number of events when the amount of available grain (i.e. the grain locally grown or purchased from other regions) in an administrative region drops to 70% of the present-day level, per century. The analyses of Dronin and Kirilenko (2008, 2011) highlights that an increase in area under agriculture (referred to as a shift in agriculture) and/or an adoption of an 'Open Market' over a "Fortress Market" can only partially alleviate the negative consequences of climate change. For example, Table 12 shows food stresses (events per century) for the 'Fortress Market' and 'Open Market' scenarios, for 17 geographic regions in Russia, for the baseline (no climate change) and the 2020s and 2070s (average of A2 and B2 scenarios). Dronin and Kirilenko (2011) explain these negative impacts of climate change by arguing that in crop producing regions, there is little land suitable for agriculture which is not already converted into arable. In consuming regions of the north, land reserve is also not very significant, as large areas are unsuitable for agriculture due to inferior soils, existing land use or prohibitive terrain. They also note that current trends render these optimistic projections of land use shift unrealistic. Moreover, Dronin and Kirilenko (2011) note that the territories newly becoming available for grain production due to increasing temperatures are subject to rural depopulation and widespread abandonment of agricultural lands; up to 40% of agriculture lands in the 1980s are now vacant.

Region	Fortress Market					Open Market		
	Baseline	No shift in agriculture		Shift in agriculture		Baseline	2020	2070
		2020	2070	2020	2070			
C. Black	3	2	5	0	5	3	3	10
N.	0	0	2	0	0	0	0	7
Lower	10	20	32	20	28	10	13	17
S–W	3	0	5	0	3	10	20	20
Middle	3	8	17	7	13	0	0	5
Volga-	10	15	23	12	15	10	28	38
S–E Siberia	13	7	0	5	0	10	7	12
Baikal	20	47	55	38	48	20	40	53
N.	3	3	17	2	13	17	38	50
North	10	13	27	10	18	0	0	0
North–West	10	33	53	25	50	10	5	12
Central	3	10	20	5	8	7	3	12
Western	0	2	0	0	0	0	0	0
Eastern	13	38	55	28	50	10	7	12
Far East	10	30	53	23	45	10	7	12
North East	10	33	53	27	50	3	3	10
Urals	7	5	12	3	10	3	3	10
Mean	7	13	22	10	17	6	8	14

Table 12. Food stresses (events per century) for the ‘Fortress Market’ and ‘Open Market’ scenarios, for 17 geographic regions in Russia, for the baseline (no climate change) and the 2020s and 2070s (mean of A2 and B2 scenarios). Adapted from Dronin and Kirilenko (2008, 2011).

Similarly, Alcamo et al. (2007a) simulated adverse impacts of climate change on Russian food security, which further add support to global studies that suggest the same (Allison et al., 2009, Arnell et al., 2010, IFPRI, 2010, Nelson et al., 2010). This study applied two climate models (ECHAM4 and HadCM3), driven by two emissions scenarios (SRES A2 and B2) to investigate how food production shortfalls occurred under climate change. Food production shortfalls were taken as a year in which potential production of the most important crops in a region were below 50% of its average climate normal production, taking into account production in food-exporting regions. Table 13 shows that the frequency of shortfalls in five or more of the main crop growing regions in the same year is around 2 years per decade under climate normal conditions but could increase up to 5–6 years per decade in the 2070s, depending on the scenario and climate model. Alcamo et al. (2007a) estimate that there are currently around 50 million people living in regions that experience one or more shortfalls per decade and that this number could increase up to 82–139 million in the 2070s (with the range due to different climate scenarios, climate models, and population projections).

Number of years per decade with shortfalls in 5 or more regions				
Climate normal (1961-1990)	2020s A2	2070s A2	2020s B2	2070s B2
2	3-4	6	3	5-6
Number of years per decade with shortfalls in 8 or more regions				
Climate normal (1961-1990)	2020s A2	2070s A2	2020s B2	2070s B2
0	1-2	3-4	1	2-3

Table 13. The number of years per decade in which food production shortfalls occur in several of the main crop growing regions of Russia simultaneously. The ranges are due to differences in climate scenarios from HADCM3 and ECHAM climate models. Adapted from Alcamo et al. (2007a).

Water stress and drought

Headline

Numerous studies that have applied rigorous methods and made some account for emissions and climate modelling uncertainty indicate that water availability could increase with climate change for Russia as a whole. There is regional variation in these projections, however. The west of Russia is vulnerable to water stress in the present climate, and here, water stress could increase with climate change. However, for the rest of the country and particularly the east, vulnerability is presently low and water availability could increase in these regions with climate change.

Results from the AVOID programme for Russia show consensus across GCMs towards little change in the population exposed to increased or decreased water stress with climate change.

Supporting literature

Introduction

For the purposes of this report droughts are considered to be extreme events at the lower bound of climate variability; episodes of prolonged absence or marked deficiency of precipitation. Water stress is considered as the situation where water stores and fluxes (e.g. groundwater and river discharge) are not replenished at a sufficient rate to adequately meet water demand and consumption.

A number of impact model studies looking at water stress and drought for the present (recent past) and future (climate change scenario) have been conducted. These studies are conducted at global or national scale and include the application of global water 'availability' or 'stress' models driven by one or more climate change scenario from one or more GCM. The approaches variously include other factors and assumptions that might affect water availability, such as the impact of changing demographics and infrastructure investment, etc. These different models (hydrological and climate), assumptions and emissions scenarios mean that there are a range of water stress projections Russia. This section summarises findings from these studies to inform and contextualise the analysis performed by the AVOID programme for this project. The results from the AVOID work and discussed in the next section.

Important knowledge gaps and key uncertainties which are applicable to Russia as well as at the global-scale, include; the appropriate coupling of surface water and groundwater in hydrological models, including the recharge process, improved soil moisture and evaporation dynamics, inclusion of water quality, inclusion of water management (Wood et al. 2011) and further refinement of the down-scaling methodologies used for the climate driving variables (Harding et al. 2011).

Assessments that include a global or regional perspective

Recent Past

Recent research presented by Vörösmarty et al. (2010) describes the calculation of an 'Adjusted Human Water Security Threat' (HWS) indicator. The indicator is a function of the cumulative impacts of 23 biophysical and chemical drivers simulated globally across 46,517 grid cells representing 99.2 million km². With a digital terrain model at its base, the calculations in each of the grid boxes of this model take account of the multiple pressures on the environment, and the way these combine with each other, as water flows in river basins. The level of investment in water infrastructure is also considered. This infrastructure measure (the *investment benefits factor*) is based on actual existing built infrastructure, rather than on the financial value of investments made in the water sector, which is a very unreliable and incomplete dataset. The analysis described by Vörösmarty et al. (2010) represents the current state-of-the-art in applied policy-focussed water resource assessment. In this measure of water security, the method reveals those areas where this is lacking, which is a representation of human water stress. One drawback of this method is that no analysis is provided in places where there is 'no appreciable flow', where rivers do not flow, or only do so for such short periods that they cannot be reliably measured. This method also does not address places where water supplies depend wholly on groundwater or desalination, being piped in, or based on wastewater reuse. It is based on what is known from all verified peer reviewed sources about surface water resources as generated by natural ecosystem processes and modified by river and other hydraulic infrastructure (Vorosmarty et al., 2010).

Here, the present day HWS is mapped for Russia. The model applied operates at 50km resolution, so, larger countries appear to have smoother coverage than smaller countries, but all are mapped and calculated on the same scale, with the same data and model, and thus comparisons between places are legitimate. It is important to note that this analysis is a comparative one, where each place is assessed *relative* to the rest of the globe. In this way, this presents a realistic comparison of conditions across the globe. As a result of this,

however, some places may seem to be less stressed than may be originally considered. One example is Australia, which is noted for its droughts and long dry spells, and while there are some densely populated cities in that country where water stress is a real issue, for most of the country, *relative to the rest of the world*, the measure suggests water stress (as measured by HWS defined by Vörösmarty et al. (2010)), is not a serious problem.

Figure 10 presents the results of this analysis for Russia. Russia has vast resources of water in the north and east, largely unused to any major degree. This results in a low threat to human water security, and a low level of water stress. In the west and south, on the other hand, many areas face extreme threats to their water security, and water stress is particularly high in areas with an industrial or agricultural legacy.

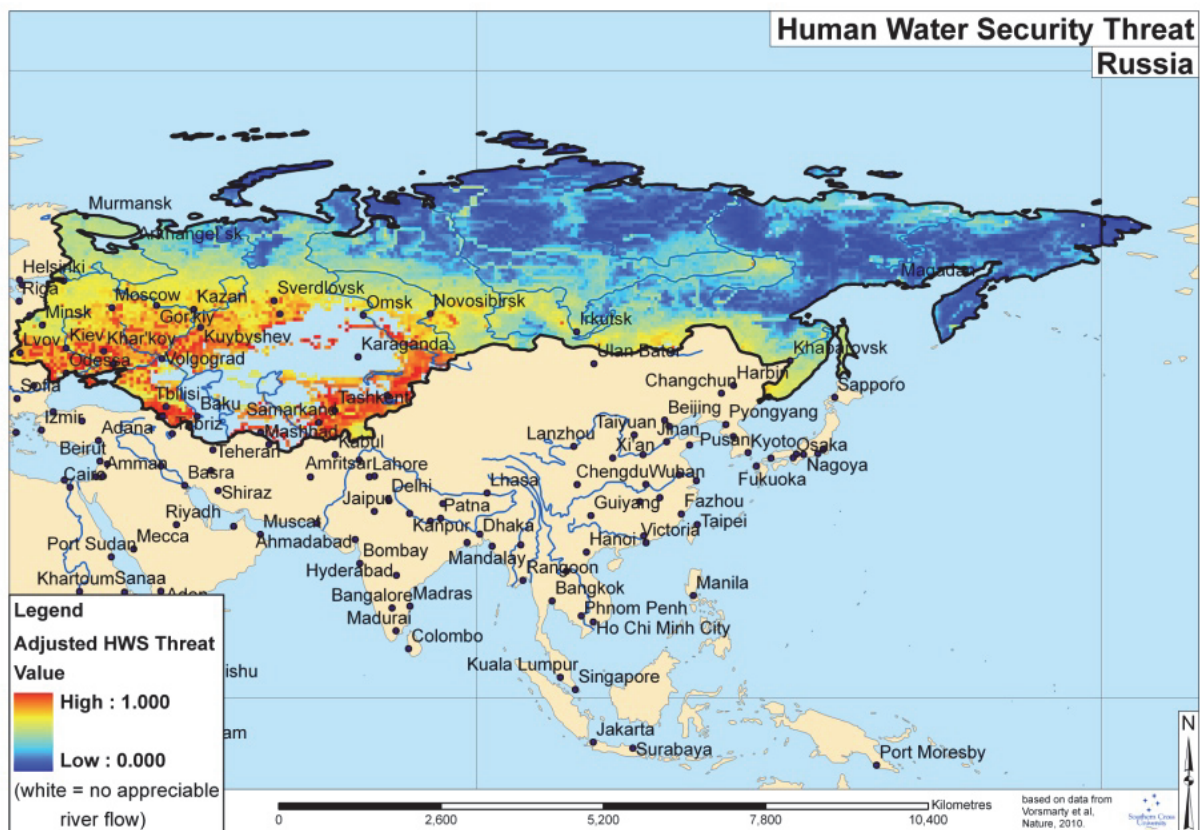


Figure 10. Present Adjusted Human Water Security Threat (HWS) for Russia, calculated following the method described by Vörösmarty et al. (2010).

Smakhtin et al. (2004) present a first attempt to estimate the volume of water required for the maintenance of freshwater-dependent ecosystems at the global scale. This total environmental water requirement (EWR) consists of ecologically relevant low-flow and high-flow components. The authors argue that the relationship between water availability, total use and the EWR may be described by the water stress indicator (WSI). If WSI exceeds 1.0,

the basin is classified as “environmentally water scarce”. In such a basin, the discharge has already been reduced by total withdrawals to such levels that the amount of water left in the basin is less than EWR. Smaller index values indicate progressively lower water resources exploitation and lower risk of “environmental water scarcity.” Basins where WSI is greater than 0.6 but less than 1.0 are arbitrarily defined as heavily exploited or “environmentally water stressed” and basins where WSI is greater than 0.3 but less than 0.6 are defined as moderately exploited. In these basins, 0-40% and 40-70% of the utilizable water respectively is still available before water withdrawals come in conflict with the EWR. Environmentally “safe” basins are defined as those where WSI is less than 0.3. The global distribution of WSI for the 1961-1990 time horizon is shown in Figure 11. The results show that for the basins considered, parts of western Russia present a medium to high vulnerability to water stress, whereas the east presents very low vulnerability. The pattern is similar to that presented in Figure 10 and is further supported by a study presented by Shiklomanov et al. (2011) that showed despite large water resources, the distribution relative to demand in Russia is uneven; the annual per capita availability ranges from 3,440m³ in central regions to 278,000m³ in the far east of the country, implying that no region is under particular water stress when assessed at this scale. To this end, the authors argue that supply demand problems are not expected to increase as per capita water availability increases by 12-14% through the 21st century.

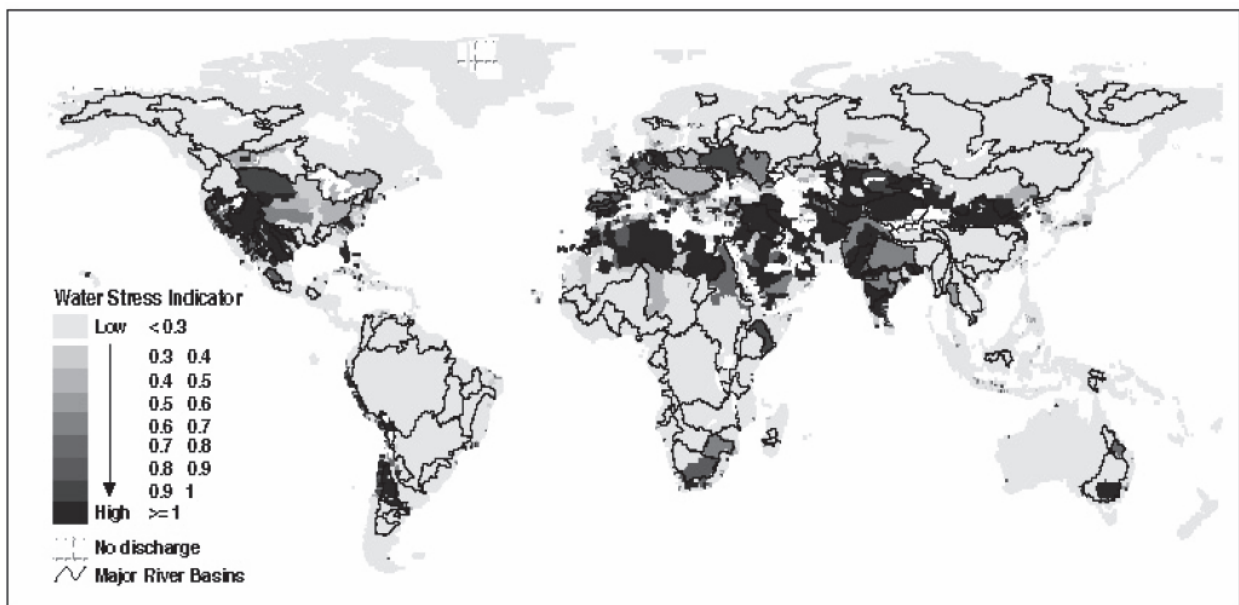


Figure 11. A map of the major river basins across the globe and the water stress indicator (WSI) for the 1961-1990 time horizon. The figure is from Smakhtin et al. (2004).

Climate Change Studies

Rockstrom et al. (2009) applied the LPJml vegetation and water balance model (Gerten et al. 2004) to assess green-blue water (irrigation and infiltrated water) availability and requirements. The authors applied observed climate data from the CRU TS2.1 gridded dataset for a present-day simulation, and climate change projections from the HadCM2 GCM under the SRES A2 scenario to represent the climate change scenario for the year 2050. The study assumed that if water availability was less than $1,300\text{m}^3/\text{capita}/\text{year}$, then the country was considered to present insufficient water for food self-sufficiency. The simulations presented by Rockstrom et al. (2009) should not be considered as definitive, however, because the study only applied one climate model, which means climate modelling uncertainty was overlooked. The results from the two simulations are presented in Figure 12. Rockstrom et al. (2009) found that globally in 2050 and under the SRES A2 scenario, around 59% of the world's population could be exposed to "blue water shortage" (i.e. irrigation water shortage), and 36% exposed to "green water shortages" (i.e. infiltrated rain shortage). For Russia, Rockstrom et al. (2009) found that blue-green water availability was well above the $1,300\text{m}^3/\text{capita}/\text{year}$ threshold in present and under climate change. This is largely supportive of the conclusions of Shiklomanov et al. (2011) for Russia.

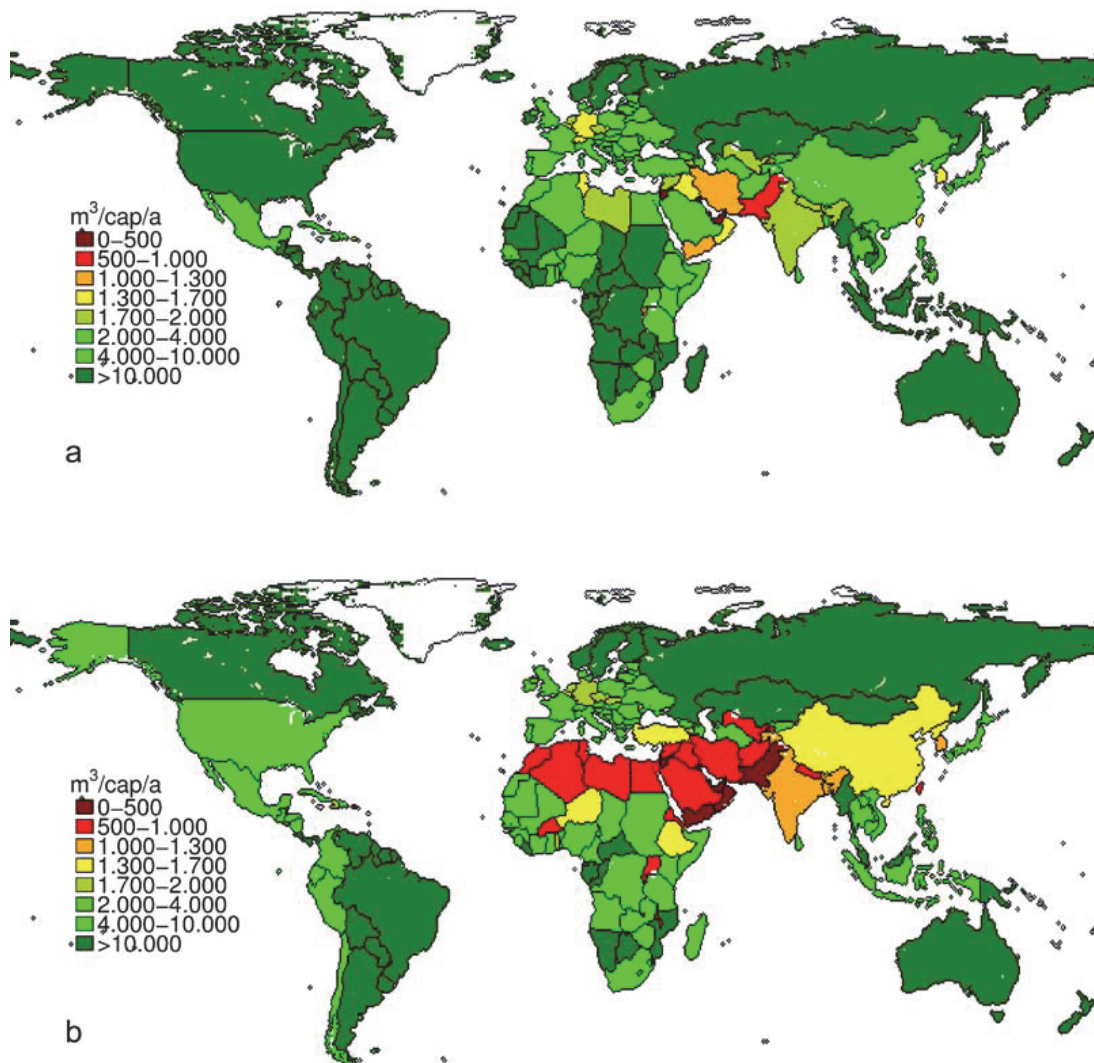


Figure 12. Simulated blue-green water availability ($m^3/capita/year$) for present climate (top panel) and including both demographic and climate change under the SRES A2 scenario in 2050 (bottom panel). The study assumed that if water availability was less than $1,300m^3/capita/year$, then the country was considered to present insufficient water for food self-sufficiency. The figure is from Rockstrom et al. (2009).

Doll (2009) presents updated estimates of the impact of climate change on groundwater resources by applying a new version of the WaterGAP hydrological model. The study accounted for the number of people affected by changes in groundwater resources under climate change relative to present (1961-1990). To this end, the study provides an assessment of the vulnerability of humans to decreases in available groundwater resources (GWR). This indicator was termed the “Vulnerability Index” (VI), defined as; $VI = -\% \text{ change GWR} * \text{Sensitivity Index (SI)}$. The SI component was a function of three more specific sensitivity indicators that include an indicator of water scarcity (calculated from the ratio between consumptive water use to low flows), an indicator for the dependence upon groundwater supplies, and an indicator for the adaptive capacity of the human system. Doll (2009) applied climate projections from two GCMs (ECHAM4 and HadCM3) to WaterGAP,

for two scenarios (SRES A2 and B2), for the 2050s. Figure 13 presents each of these four simulations respectively. There is variation across scenarios and GCMs. However, for Russia, all simulations are generally consistent in showing no GWR decrease with climate change, implying no changing vulnerability to decreases in groundwater resources as a result of climate change.

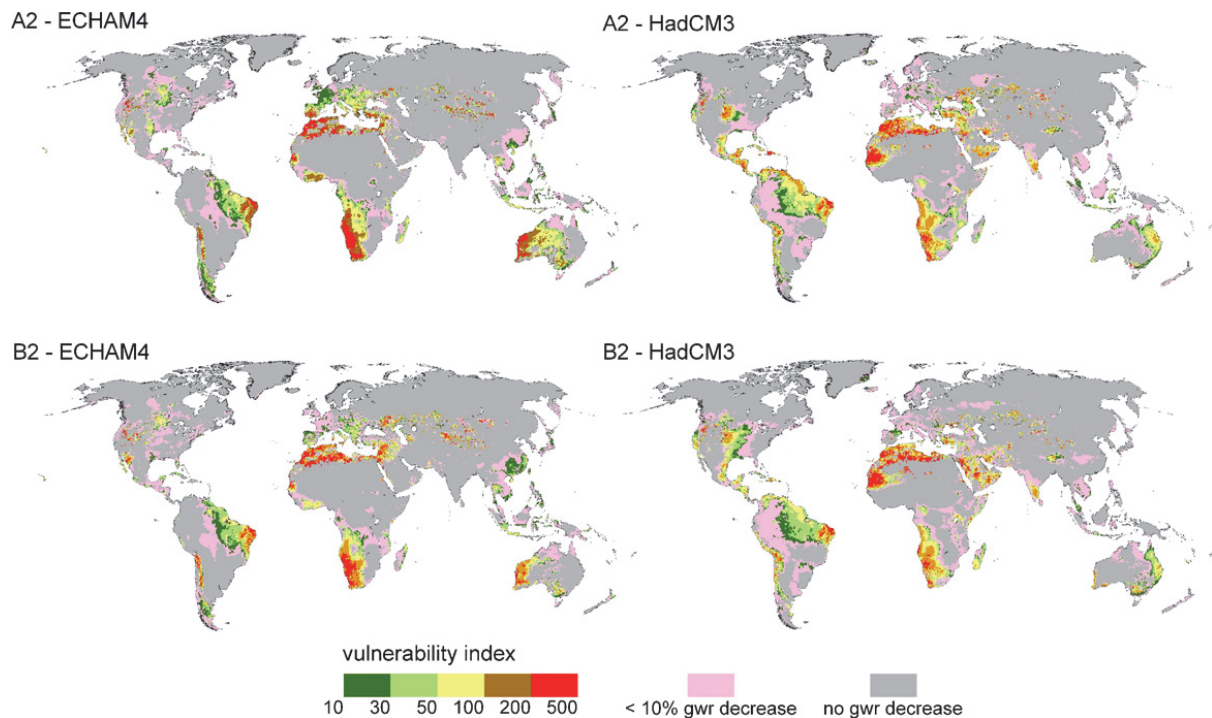


Figure 13. Vulnerability index (VI) showing human vulnerability to climate change induced decreases of renewable groundwater resources (GWR) by the 2050s under two emissions scenarios for two GCMs. VI is only defined for areas with a GWR decrease of at least 10% relative to present (1961-1990). The figure is from Doll (2009).

Fung et al. (2011) applied climate change scenarios for prescribed global-mean warming of 2°C and 4°C respectively, from two ensembles; 1) an ensemble of 1518 (2°C world) and 399 (4°C) members from the ClimatePrediction.net (CPDN) experiments, and 2) an ensemble of climate projections from 22 GCMs included in the CMIP3 multi-model dataset. The climate projections were applied to the MacPDM global hydrological model (Gosling and Arnell, 2011) and population projections followed the UNPOP60 population scenario. Fung et al. (2011) calculated a water stress index (WSI) based upon resources per capita, similar to the method applied by Rockstrom et al. (2009). Results from the simulations are presented in Figure 14. There was consensus across models that water stress decreases with climate change across much of eastern Russia, whilst it increases in parts of western Russia.

It should be noted that the estimates of drying across the globe that are presented by Fung et al. (2011) could be over-estimated slightly. This is because the MacPDM hydrological model is an offline model; i.e. it is not coupled to an ocean-atmosphere GCM. Therefore the

dynamical effects of vegetation changes in response to water availability are not simulated. Recent work has highlighted that increased plant water use efficiency under higher CO₂ may ameliorate future increased drought to some extent, but not completely (Betts et al., 2007).

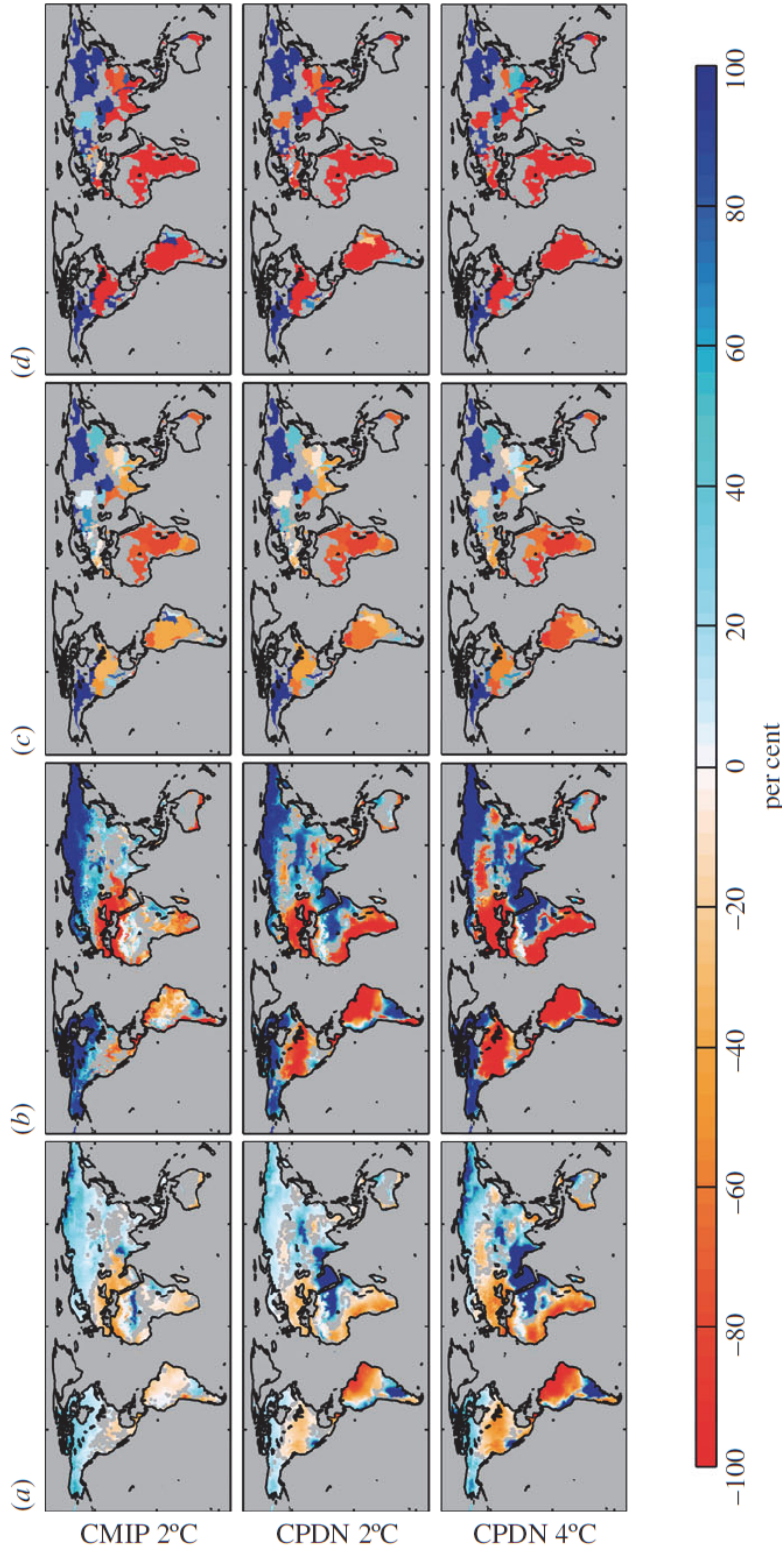


Figure 14. For a 2°C and 4°C rise in temperature and UNPOP60 population scenario compared with the baseline period (1961-1990): (a) spatial pattern of ensemble-average changes in mean annual run-off (DMAR), (b) model consensus on direction of change in water stress, (c) ensemble-average change in water stress (DWSI) and (d) model consensus on the direction of change in water stress. For the model consensus, red and therefore negative values represent the percentage of models showing a negative change in the respective parameter and for blue, positive values, represent the percentage of models showing a positive change. For DMAR and DWSI, colour classification spans from -100% to 100% (this means that high positive values of DMAR and DWSI are effectively filtered out in these plots), whereas for consensus, colour classification spans from -100% to 100%. For plots of DMAR and consensus for the direction of change in run-off, grey land areas represent where DMAR is less than natural variability. For DWSI and consensus for direction of change in water stress, only 112 major river basins are plotted (Greenland has been excluded from the analysis). The figure is from Fung et al. (2011).

The IPCC AR4 (2007a) noted that decreasing rain and increasing temperatures have caused droughts in recent decades, and they reported that 27 major droughts in the 20th century have been observed.

A report compiled by the World Bank (2009) applied climate change projections from 8 GCMs under the A1B emissions scenario to investigate precipitation changes under climate change. The report showed that the number of consecutive dry days could increase relative to present in western Russia by the 2050s, but decrease across much of the rest of the country (see Figure 15).

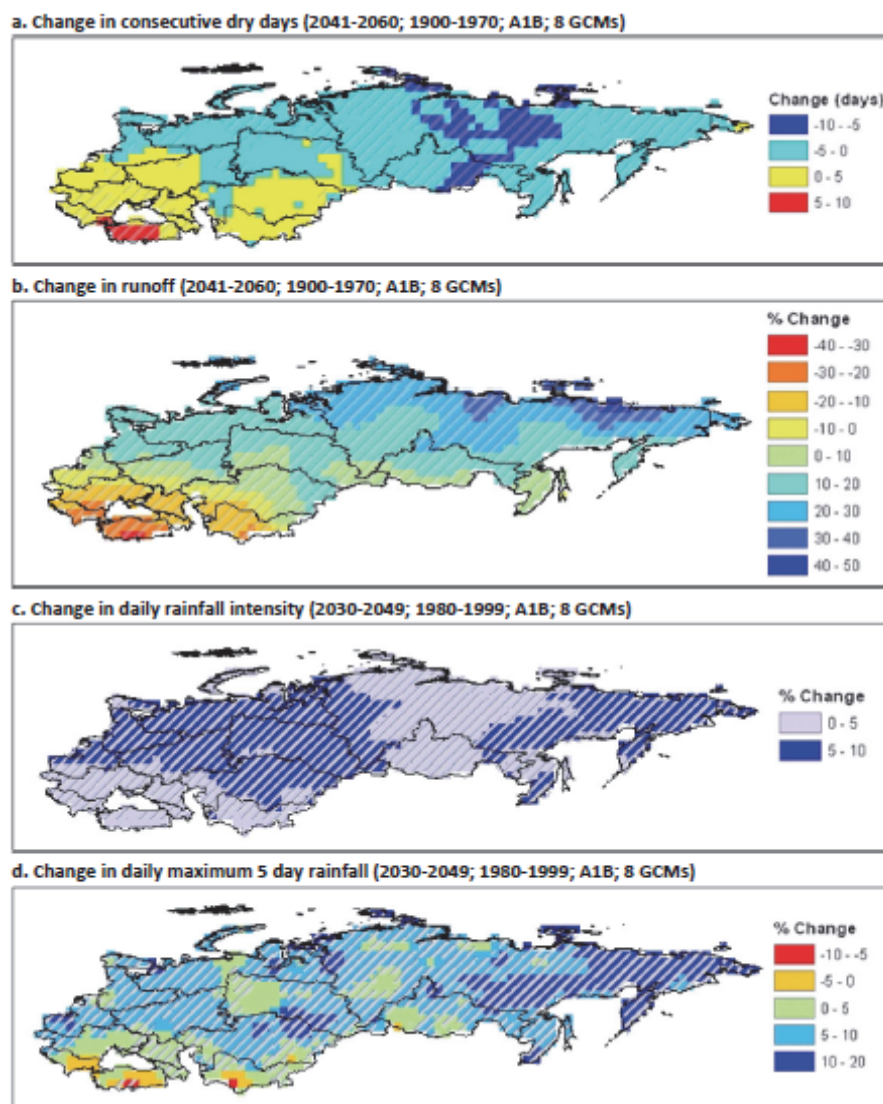


Figure 15. Ensemble-mean changes in consecutive dry days (a), runoff (b), daily rainfall intensity (c), and daily maximum 5-day rainfall (d), from 8GCMs under the A1B emissions scenario, for the time horizons noted in each panel. The figure is from World Bank (2009) and (Westphal, 2008).

National-scale or sub-national scale assessments

Climate change studies

The Report of the centralized in-depth review of the fourth national communication of the Russian Federation (UNFCCC, 2009) highlights an observed increasing aridity in some central and eastern regions and an increase in the frequency of droughts. Moreover, a comprehensive report presented by Roshydromet (2008) applied climate projections for Russia for the 21st century and showed that in terms of annual river runoff, further decreases in regions which currently suffer from water shortages could occur. In general, Roshydromet (2008) found that southern rivers could see decreases in runoff as a result of decreases in precipitation and increases in evaporation.

A national-scale assessment of water stress in present climate and under climate change scenarios presented by Alcamo et al. (2007b) supports several global-scale assessments that include information for Russia, which show that present day vulnerability to water stress is located in the west of the country and that under climate change Russia could experience an increase in water availability (Doll, 2009, Rockstrom et al., 2009). Alcamo et al. (2007b) applied climate change projections from two GCMs (HadCM3 and ECHAM) to the WaterGAP hydrological model under the SRES A2 scenario for the 2070s (see Figure 16). Increases in water availability were greatest in the east under climate change. Small decreases in water availability were simulated for parts of far-western Russia but overall, water availability increased over the country with climate change.

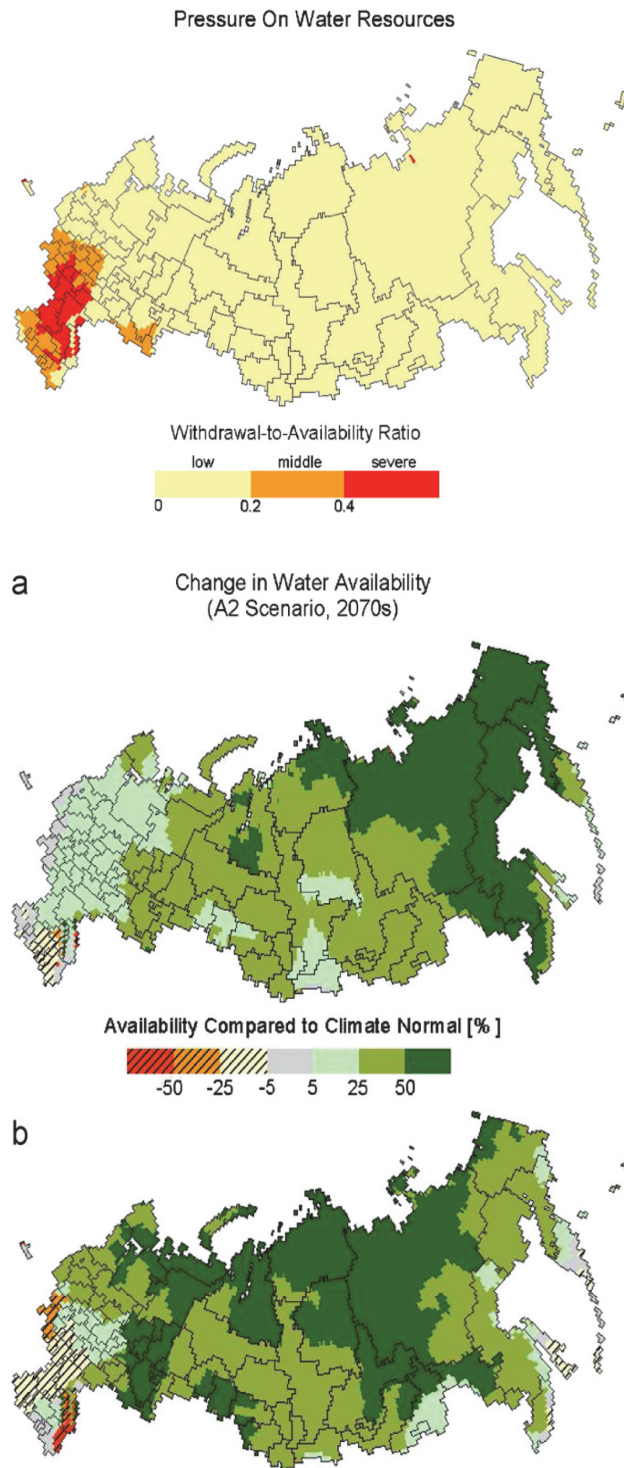


Figure 16. The top panel displays the current water stress in Russia as indicated by the withdrawals-to-availability ratio (w.t.a.) computed by the WaterGAP hydrological model (water withdrawals data from 1995 and water availability based on average during climate normal period (1961–1990)). The other two panels show changes in water availability between the current climate and 2070s, computed by WaterGAP for the A2 scenario, with the HadCM3 GCM (middle panel) and ECHAM GCM (bottom panel). The figure is from Alcamo et al. (2007b).

AVOID Programme Results

To further quantify the impact of climate change on water stress and the inherent uncertainties, the AVOID programme calculated water stress indices for all countries reviewed in this literature assessment based upon the patterns of climate change from 21 GCMs (Warren et al., 2010), following the method described by Gosling et al. (2010) and Arnell (2004). This ensures a consistent methodological approach across all countries and takes consideration of climate modelling uncertainties.

Methodology

The indicator of the effect of climate change on exposure to water resources stress has two components. The first is the number of people within a region with an *increase in exposure to stress*, calculated as the sum of 1) people living in water-stressed watersheds with a significant reduction in runoff due to climate change and 2) people living in watersheds which become water-stressed due to a reduction in runoff. The second is the number of people within a region with a *decrease in exposure to stress*, calculated as the sum of 1) people living in water-stressed watersheds with a significant increase in runoff due to climate change and 2) people living in watersheds which cease to be water-stressed due to an increase in runoff. It is not appropriate to calculate the net effect of “increase in exposure” and “decrease in exposure”, because the consequences of the two are not equivalent. A water-stressed watershed has an average annual runoff less than 1000m³/capita/year, a widely used indicator of water scarcity. This indicator may underestimate water stress in watersheds where per capita withdrawals are high, such as in watersheds with large withdrawals for irrigation.

Average annual runoff (30-year mean) is simulated at a spatial resolution of 0.5x0.5° using a global hydrological model, MacPDM ([Gosling and Arnell, 2011](#)), and summed to the watershed scale. Climate change has a “significant” effect on average annual runoff when the change from the baseline is greater than the estimated standard deviation of 30-year mean annual runoff: this varies between 5 and 10%, with higher values in drier areas.

The pattern of climate change from 21 GCMs was applied to MacPDM, under two emissions scenarios; 1) SRES A1B and 2) an aggressive mitigation scenario where emissions follow A1B up to 2016 but then decline at a rate of 5% per year thereafter to a low emissions floor (denoted A1B-2016-5-L). Both scenarios assume that population changes through the 21st century following the SRES A1 scenario as implemented in IMAGE 2.3 ([van Vuuren et al., 2007](#)). The application of 21 GCMs is an attempt to quantify the uncertainty due to climate

modelling, although it is acknowledged that only one impacts model is applied (MacPDM). Simulations were performed for the years 2030, 2050, 2080 and 2100. Following Warren et al. (2010), changes in the population affected by increasing or decreasing water stress represent the additional percentage of population affected due to climate change, not the absolute change in the percentage of the affected population relative to present day.

The results for Russia are presented in Figure 17 and they show consensus across GCMs towards little change in the population exposed to increased or decreased water stress with climate change.

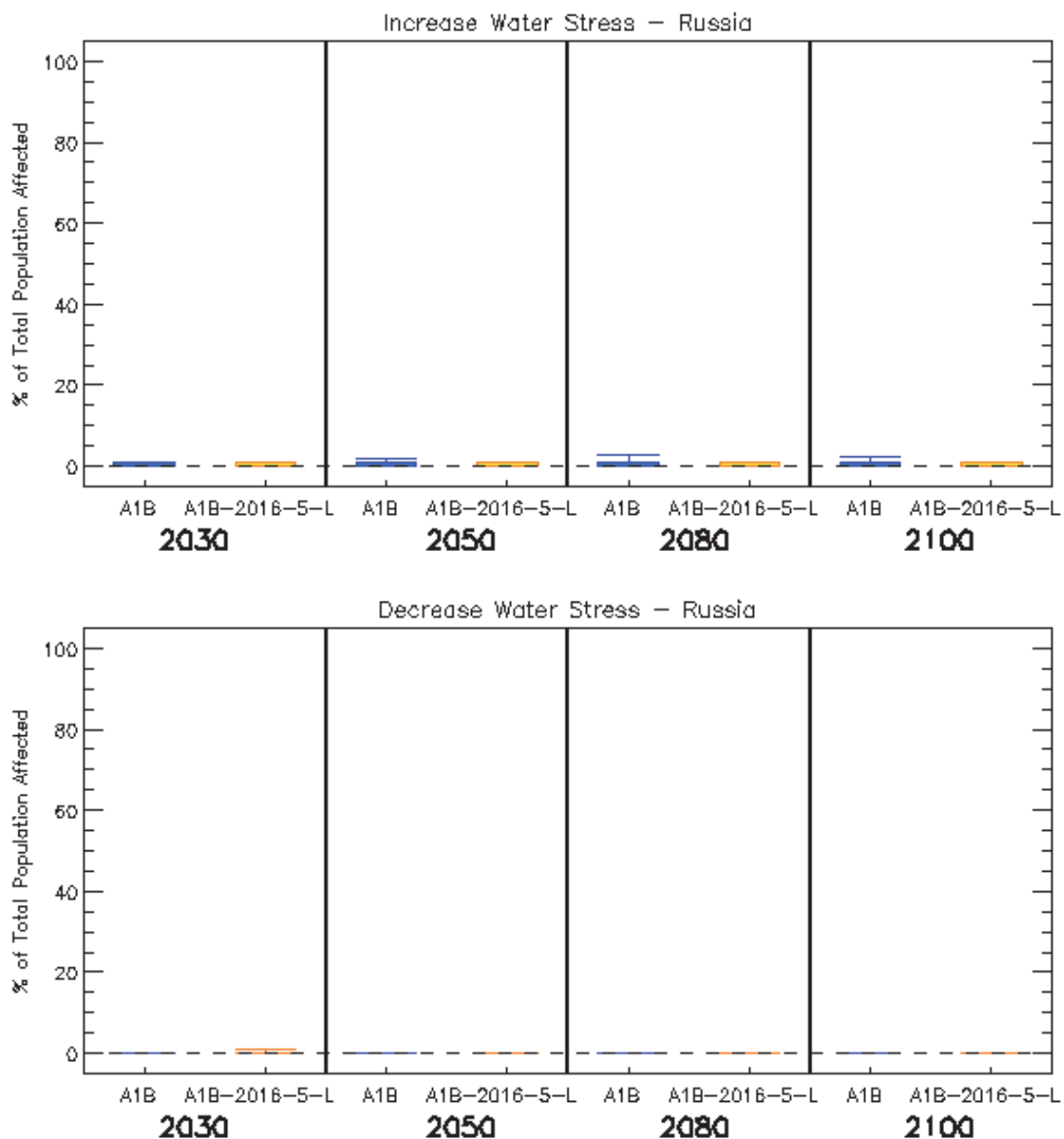


Figure 17. Box and whisker plots for the impact of climate change on increased water stress (top panel) and decreased water stress (bottom panel) in Russia, from 21 GCMs under two emissions scenarios (A1B and A1B-2016-5-L), for four time horizons. The plots show the 25th, 50th, and 75th percentiles (represented by the boxes), and the maximum and minimum values (shown by the extent of the whiskers).

Pluvial flooding and rainfall

Headline

Recent studies suggest that winter precipitation could increase for Russia, under climate change, and there is consistency across different GCMs in this change. There is less agreement across GCMs for precipitation changes in summer, however. Increases in precipitation from extreme storm events are also possible with climate change, although such projections cannot be translated directly into flood projections; detailed local-scale impact models, incorporating topography and specifics of hydrology, are needed here.

Supporting literature

Introduction

Pluvial flooding can be defined as flooding derived directly from heavy rainfall, which results in overland flow if it is either not able to soak into the ground or exceeds the capacity of artificial drainage systems. This is in contrast to fluvial flooding, which involves flow in rivers either exceeding the capacity of the river channel or breaking through the river banks, and so inundating the floodplain. Pluvial flooding can occur far from river channels, and is usually caused by high intensity, short-duration rainfall events, although it can be caused by lower intensity, longer-duration events, or sometimes by snowmelt. Changes in mean annual or seasonal rainfall are unlikely to be good indicators of change in pluvial flooding; changes in extreme rainfall are of much greater significance. However, even increases in daily rainfall extremes will not necessarily result in increases in pluvial flooding, as this is likely to be dependent on the sub-daily distribution of the rainfall as well as local factors such as soil type, antecedent soil moisture, land cover (especially urbanisation), capacity and maintenance of artificial drainage systems etc. It should be noted that both pluvial and fluvial flooding can potentially result from the same rainfall event.

Assessments that include a global or regional perspective

Climate change studies

The IPCC AR4 (2007b) noted an increase in annual precipitation with climate change for the North Asia region, with a high consistency amongst CMIP3 multi-model dataset models. The

IPCC AR4 (2007a) also noted an observed increase in heavy rains in western Russia and decrease in Siberia, and an increase in number of days with over 10mm rain. The report also stated that surface runoff could increase by 50-70% in Siberia.

Washington et al. (2009) investigated climate change projections from an aggressive mitigation scenario (CO₂ stabilisation in 2100 at around 450ppm) compared with a non-mitigation scenario (CO₂ concentrations around 740ppm in 2100) at the global-scale. The authors found that both scenarios simulated increases in precipitation with climate change, but the increases were greater with the non-mitigation scenario. Increases in precipitation of 10-20% due to climate change could be avoided by 2080-2099 in eastern regions of Russia under the mitigation scenario, relative to the non-mitigation scenario. Avoided changes in precipitation over the majority of the country were in the region of 0-10%, however.

A report compiled by the World Bank (2009) notes that there has been a significant increasing trend in annual precipitation for most of Russia, with the exception of the Central and Volga sub-regions and Baltic Russia. The study applied climate change projections from 8 GCMs under the A1B emissions scenario to investigate precipitation changes under climate change. The report showed that throughout the entire Europe and Central Asia Region, the GCMs projected that precipitation intensity could increase, ranging from 2–6% (see Figure 15). This may not seem a large change, but these are mean values and depending on local hydrology and topography, this increase in precipitation intensity could have implications for flood management. Most GCMs simulated an increase in precipitation from extreme storm events (2–9% increase in the maximum amount of precipitation over a 5-day period). The projections for extreme precipitation cannot be translated directly into flood projections however; detailed local-scale impact models, incorporating topography and specifics of hydrology, are needed for this.

National-scale or sub-national scale assessments

Climate change studies

A number of recent studies support the conclusions from the IPCC AR4 (2007b, 2007a). The report of the centralized in-depth review of the fourth national communication of the Russian Federation, (UNFCCC, 2009) highlights projected vulnerability from an increase in runoff in winter and summer for Russia, excluding the south-western regions, and an overall increase in flood risk. A comprehensive report by Roshydromet (2008) showed that observed annual precipitation in Russia increased by 7.2mm per decade over the period 1976-2006, but with considerable regional variations, with increases in spring precipitation in western and north-

eastern parts of Siberia, and the European parts of Russia. Indices of extreme precipitation change suggested a weak increase in the number of days with heavy precipitation, and also a decrease in the duration of dry periods (Roshydromet, 2008). The authors analysed climate change projections from the ensemble mean of 16 GCMs under the SRES A2 emissions scenario. They found that for the 2041-2060 time horizon, winter precipitation could increase for most of Russia and there was high agreement across the 16 GCMs here, whilst in summer the sign of the change depended on the region (see Figure 18).

Roshydromet (2008) noted that during the summer, convective precipitation could increase over most regions, but against a background of large inter-model variability. Likewise, Sillmann and Roeckner (2008) show increases across northern parts of Russia in heavy precipitation indices during the 21st century, with larger changes under A1B than under the B2 scenario.

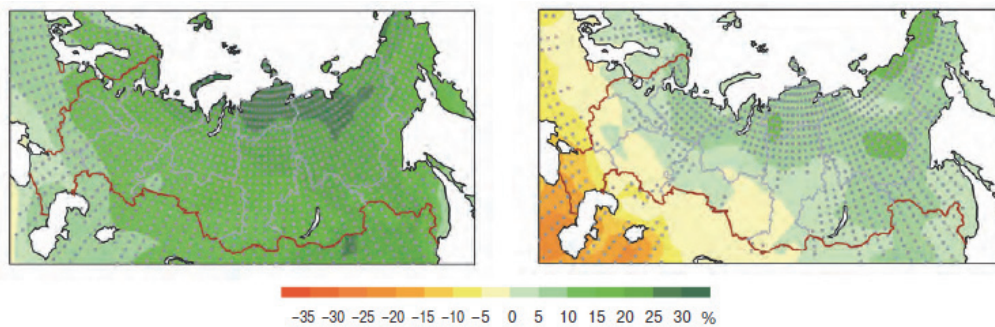


Figure 18. Changes (%) in precipitation for Russia and adjoining regions from the ensemble mean of 16 GCMs under the A2 emissions scenario for winter (left panel) and summer (right panel), for the 2041-2060 time horizon, relative to 1980-1999. Dots denote the areas where two thirds of the GCMs show changes of the same sign. The figure is from Roshydromet (2008).

Fluvial flooding

Headline

Recent studies have suggested that flood magnitudes in Central and Eastern Siberia and the Russian Far East may increase with climate change, but decrease in European Russia and West Siberia, due to smaller maximum rates of snowmelt runoff. Results from simulations by the AVOID programme, that applied climate change projections from 21 climate models, show a high level of agreement among models that flood risk for Russia as a whole could decrease with climate change throughout the 21st century. It is important to note that whilst the studies reviewed here present a useful indicator of exposure to flood risk with climate change, none of them took into account the effect that hydropower reservoirs, present in most large rivers, can have on the height of the annual flood peak, which can be substantial. Also, few studies have investigated the occurrence of ice dams and the resultant flooding with climate change.

Supporting literature

Introduction

This section summarises findings from a number of post IPCC AR4 assessments on river flooding in Russia to inform and contextualise the analysis performed by the AVOID programme for this project. The results from the AVOID work are discussed in the next section.

Fluvial flooding involves flow in rivers either exceeding the capacity of the river channel or breaking through the river banks, and so inundating the floodplain. A complex set of processes is involved in the translation of precipitation into runoff and subsequently river flow (routing of runoff along river channels). Some of the factors involved are; the partitioning of precipitation into rainfall and snowfall, soil type, antecedent soil moisture, infiltration, land cover, evaporation and plant transpiration, topography, groundwater storage. Determining whether a given river flow exceeds the channel capacity, and where any excess flow will go, is also not straightforward, and is complicated by the presence of artificial river embankments and other man-made structures for example. Hydrological models attempt to simplify and conceptualise these factors and processes, to allow the simulation of runoff

and/or river flow under different conditions. However, the results from global-scale hydrological modelling need to be interpreted with caution, especially for smaller regions, due to the necessarily coarse resolution of such modelling and the assumptions and simplifications this entails (e.g. a 0.5° grid corresponds to landscape features spatially averaged to around 50-55km for mid- to low-latitudes). Such results provide a consistent, high-level picture, but will not show any finer resolution detail or variability. Smaller-scale or catchment-scale hydrological modelling can allow for more local factors affecting the hydrology, but will also involve further sources of uncertainty, such as in the downscaling of global climate model data to the necessary scale for the hydrological models. Furthermore, the application of different hydrological models and analysis techniques often makes it difficult to compare results for different catchments.

Annual discharge from Eurasian rivers to the Arctic Ocean has been showing a rapid increase over the past few decades, with an unprecedented river flow volume in 2007 (Shiklomanov and Lammers, 2009). However, Shiklomanov et al. (2007) found no evidence of widespread ongoing trends in extreme discharge. The most consistent changes were a decrease in spring maximum discharge across southern Central Siberia, and increases in extreme discharge in the Lena river basin. In slight contrast, Semenov (2011) reported an increase in flooding events in the first decade of the 21st century in several Russian river basins, including the Volga and Ob. Shiklomanov et al. (2007) also found a significant shift to an earlier spring snowmelt runoff peak, which has been confirmed by other studies (Tan et al., 2011).

Assessments that include a global or regional perspective

Climate change studies

With climate change, a general increase in river discharge towards the Arctic Ocean is possible (Kattsov et al., 2007). However, very few studies have specifically assessed potential changes in flood risk across the Russian Federation under climate change scenarios.

A global modelling study presented by Hirabayashi et al. (2008), which analysed climate change simulations from a single GCM under the A1B emissions scenario, projected little change in flood frequency in the next few decades (2001-2030) in the western part of Russia. In parts of Central Siberia on the other hand, the return period of what was a 100-year flood event in the 20th century was projected to decrease to less than 40 years. By the end of the century (2071-2100) this trend was reinforced. In Central and Eastern Siberia and the

Russian Far East (with the exception of Kamchatka) a widespread decrease in the return period of a 100-year flood was projected, to less than 40 years, suggesting a strong increase in the occurrence of extreme discharge levels. In European Russia and West Siberia on the other hand, a widespread increase in the return period was found, suggesting fewer large flood events. For Northern European Russia these findings were confirmed by Dankers and Feyen (2008) and Dankers and Feyen (2009); both studies found a general decrease in the 100-year flood level in this area of 20-40% with climate change towards the end of the 21st century.

The decrease in extreme discharges for these regions of Russia can be attributed to a reduction in the length of the snow season and consequently a lower runoff peak during the spring snowmelt season. Further to the east, however, the increase in precipitation during the winter months is large enough to compensate for the shorter snow season, leading to higher snow accumulation and consequently higher peak runoff in spring in major Eurasian rivers such as the Yenisey and Lena. With the simulations presented by Hirabayashi et al. (2008), the return period of a 20th century 100-year flood reduced to 33 years in the Yenisey, 20 years in the Amur, 6 years in the Kolyma and less than 6 years in the Lena. The latter number would mean that by the end of the century extreme and currently rare floods could occur 18 times more frequently than in the past. In West Siberia and European Russia however, the return period of the 100-year flood level was projected to increase to 162 years in the Ob, 671 years in the Volga and over 2000 years in the Dniepr rivers, suggesting a strong decrease in flood hazard. In all rivers except the Amur the annual runoff peak was also expected to occur earlier, by between about half and one month. It should be noted, however, that results from studies that have applied only a single climate model or climate change scenario should be interpreted with caution. This is because they do not consider other possible climate change scenarios which could result in a different impact outcome, in terms of magnitude and in some cases sign of change. Nevertheless, similar patterns were also reported by Nohara et al. (2006), who applied 19 GCMs under the A1B emission scenario for the end of the 21st century (2081-2100). They found a wide spread of responses in some rivers, such as the Volga and Amur, suggesting large modelling uncertainty.

It is important to note that whilst the studies reviewed here present a useful indicator of exposure to flood risk with climate change, none of the studies took into account the effect that hydropower reservoirs, present in most large rivers, can have on the height of the annual flood peak, which can be substantial (Shiklomanov and Lammers, 2009). Also, few studies have investigated the occurrence of ice dams and the resultant flooding with climate change.

National-scale or sub-national scale assessments

Literature searches yielded no results for other national-scale or sub-national scale studies for this impact sector.

AVOID programme results

To quantify the impact of climate change on fluvial flooding and the inherent uncertainties, the AVOID programme calculated an indicator of flood risk for all countries reviewed in this literature assessment based upon the patterns of climate change from 21 GCMs (Warren et al., 2010). This ensures a consistent methodological approach across all countries and takes consideration of climate modelling uncertainties.

Methodology

The effect of climate change on fluvial flooding is shown here using an indicator representing the percentage change in average annual flood risk within a country, calculated by assuming a standardised relationship between flood magnitude and loss. The indicator is based on the estimated present-day (1961-1990) and future flood frequency curve, derived from the time series of runoff simulated at a spatial resolution of $0.5^{\circ} \times 0.5^{\circ}$ using a global hydrological model, MacPDM (Gosling and Arnell, 2011). The flood frequency curve was combined with a generic flood magnitude–damage curve to estimate the average annual flood damage in each grid cell. This was then multiplied by grid cell population and summed across a region, producing in effect a population-weighted average annual damage. Flood damage is thus assumed to be proportional to population in each grid cell, not the value of exposed assets, and the proportion of people exposed to flood is assumed to be constant across each grid cell (Warren et al., 2010).

The national values are calculated across major floodplains, based on the UN PREVIEW Global Risk Data Platform (preview.grid.unep.ch). This database contains gridded estimates, at a spatial resolution of 30 arc-seconds ($0.00833^{\circ} \times 0.00833^{\circ}$), of the estimated frequency of flooding. From this database the proportion of each $0.5^{\circ} \times 0.5^{\circ}$ grid cell defined as floodplain was determined, along with the numbers of people living in each $0.5^{\circ} \times 0.5^{\circ}$ grid cell in flood-prone areas. The floodplain data set does not include “small” floodplains, so underestimates actual exposure to flooding. The pattern of climate change from 21 GCMs was applied to MacPDM, under two emissions scenarios; 1) SRES A1B and 2) an aggressive mitigation scenario where emissions follow A1B up to 2016 but then decline at a rate of 5% per year thereafter to a low emissions floor (denoted A1B-2016-5-L). Both scenarios assume that

population changes through the 21st century following the SRES A1 scenario as implemented in IMAGE 2.3 (van Vuuren et al., 2007). The application of 21 GCMs is an attempt to quantify the uncertainty due to climate modelling, although it is acknowledged that only one impacts model is applied (MacPDM). Simulations were performed for the years 2030, 2050, 2080 and 2100. The result represents the change in flood risk due to climate change, not the change in flood risk relative to present day (Warren et al., 2010).

Results

The results for Russia are presented in Figure 19. By the 2030s, the models project a range of changes in mean fluvial flooding risk over Russia in both scenarios, with some models projecting increases, but the vast majority projecting decreases. The largest decrease projected for the 2030s is -45%, and the largest increase is nearly +15%. The mean projected change is about a 25% decrease in the average annual flood risk.

By 2100 differences in projections from the different models becomes greater, and this is more pronounced for the A1B scenario than the mitigation scenario. Under the mitigation scenario, a large majority of the models still project a lower flood risk (down to nearly -55%), but a few models project an increase. The mean of all projections is a decrease of about -25%, while the upper projection is approximately a +25% increase. Under the A1B scenario, more than three quarters of the models project a lower flood risk (down to -55%). The largest projected increase is approximately +30%, with the mean of all projections being a decrease in average annual flood risk of -25%.

So for Russia, the models show a greater tendency towards decreasing flood risk throughout the 21st century under both emissions scenarios, but the differences between the model projections are greater later in the century and particularly for A1B.

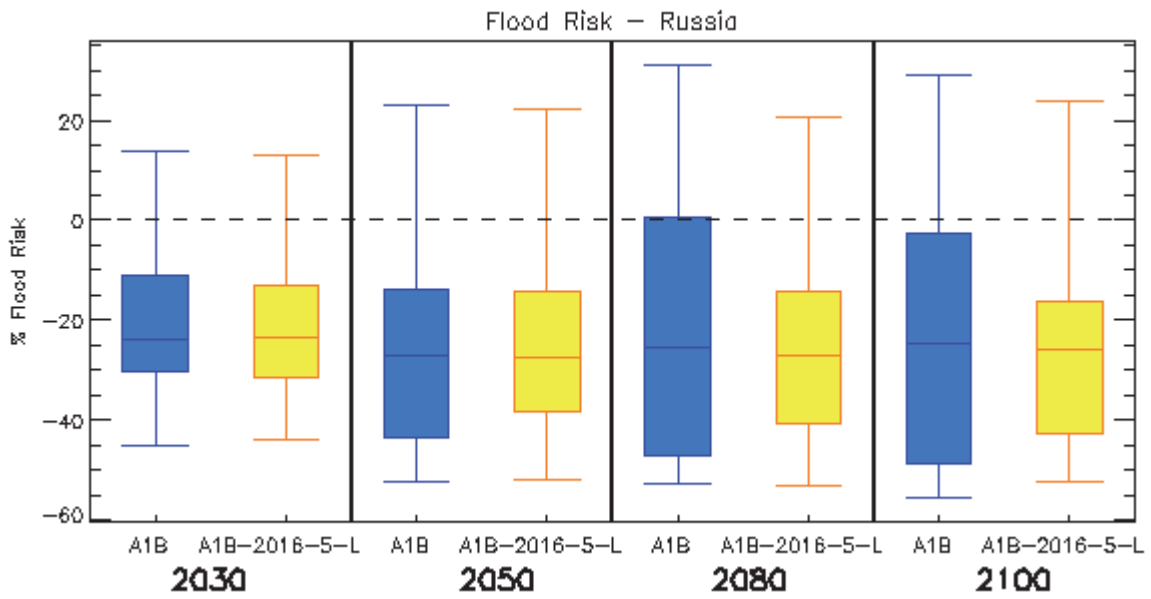


Figure 19. Box and whisker plots for the percentage change in average annual flood risk within Russia, from 21 GCMs under two emissions scenarios (A1B and A1B-2016-5-L), for four time horizons. The plots show the 25th, 50th, and 75th percentiles (represented by the boxes), and the maximum and minimum values (shown by the extent of the whiskers).

Tropical cyclones

This country is not impacted by tropical cyclones.

Coastal regions

Headline

There is very little work on the impact of climate change on Russia's coastal regions. However, one recently published study adds considerable knowledge to coverage in the IPCC AR4 and includes an estimate of the potential benefit of climate change mitigation. The study estimated that population exposure to sea level rise (SLR) could increase from 189,000 in present to 226,000 under un-mitigated A1B emissions in 2070; an aggressive mitigation scenario could avoid an exposure of around 28,000 people, relative to un-mitigated climate change in 2070. Nevertheless, further studies on the impact of climate change on Russia's coastal regions could improve understanding.

Assessments that include a global or regional perspective

The IPCC AR4 concluded that at the time, understanding was too limited to provide a best estimate or an upper bound for global SLR in the twenty-first century (IPCC, 2007b). However, a range of SLR, excluding accelerated ice loss effects was published, ranging from 0.19m to 0.59m by the 2090s (relative to 1980-2000), for a range of scenarios (SRES A1FI to B1). The IPCC AR4 also provided an illustrative estimate of an additional SLR term of up to 17cm from acceleration of ice sheet outlet glaciers and ice streams, but did not suggest this is the upper value that could occur. Although there are published projections of SLR in excess of IPCC AR4 values (Nicholls et al., 2011), many of these typically use semi-empirical methods that suffer from limited physical validity and further research is required to produce a more robust estimate. Linking sea level rise projections to temperature must also be done with caution because of the different response times of these two climate variables to a given radiative forcing change.

Nicholls and Lowe (2004) previously showed that mitigation alone would not avoid all of the impacts due to rising sea levels, adaptation would likely be needed too. Recent work by van Vuuren et al. (2011) estimated that, for a world where global mean near surface temperatures reach around 2°C by 2100, global mean SLR could be 0.49m above present levels by the end of the century. Their sea level rise estimate for a world with global mean temperatures reaching 4°C by 2100 was 0.71m, suggesting around 40% of the future increase in sea level to the end of the 21st century could be avoided by mitigation. A qualitatively similar conclusion was reached in a study by Pardaens et al. (2011), which

examined climate change projections from two GCMs. They found that around a third of global-mean SLR over the 21st century could potentially be avoided by a mitigation scenario under which global-mean surface air temperature is near-stabilised at around 2°C relative to pre-industrial times. Under their baseline business-as-usual scenario the projected increase in temperature over the 21st century is around 4°C, and the sea level rise range is 0.29-0.51m (by 2090-2099 relative to 1980-1999; 5% to 95% uncertainties arising from treatment of land-based ice melt and following the methodology used by the IPCC AR4). Under the mitigation scenario, global mean SLR in this study is projected to be 0.17-0.34m.

The IPCC 4th assessment (IPCCa) followed Nicholls and Lowe (2004) for estimates of the numbers of people affected by coastal flooding due to sea level rise. Nicholls and Lowe (2004) projected for the Former U.S.S.R. region that less than 100 thousand additional people per year could be flooded due to sea level rise by the 2080s relative to the 1990s for the SRES A2 Scenario (note this region also includes other countries, such as Ukraine and Bulgaria). However, it is important to note that this calculation assumed that protection standards increased as GDP increased, although there is no additional adaptation for sea level rise. More recently, Nicholls et al. (2011) also examined the potential impacts of sea level rise in a scenario that gave around 4°C of warming by 2100. Readings from Figure 3 from Nicholls et al. (2011) for the Commonwealth of Independent States region suggest that less an approximate 2 million additional people could be flooded for a 0.5 m SLR (assuming no additional protection). Nicholls et al. (2011) also looked at the consequence of a 2m SLR by 2100, however as we consider this rate of SLR to have a low probability we don't report these figures here.

There is little published on the impact of SLR on Russia's coast, although the issue is highlighted by a recent US government report, which notes that a combination of increased flooding from SLR and permafrost melting associated with climate change, threatens to undermine urban, industrial, and transportation infrastructure (National Intelligence Council, 2009). No quantitative impact estimates are provided, however.

Given this knowledge gap, the results from a study presented by Hanson et al. (2010) are highly informative, because they provide quantitative estimates of the impact of SLR for the Russian population, based upon a global-scale assessment. Hanson et al. (2010) investigated population exposure to global SLR, natural and human subsidence/uplift, and more intense storms and higher storm surges, for 136 port cities across the globe. Future city populations were calculated using global population and economic projections, based on the SRES A1 scenario up to 2030. The study accounted for uncertainty on future

urbanization rates, but estimates of population exposure were only presented for a rapid urbanisation scenario, which involved the direct extrapolation of population from 2030 to 2080. All scenarios assumed that new inhabitants of cities in the future will have the same relative exposure to flood risk as current inhabitants. The study is similar to a later study presented by Hanson et al. (2011) except here, different climate change scenarios were considered, and published estimates of exposure are available for more countries, including Russia. Future water levels were generated from temperature and thermal expansion data related to greenhouse gas emissions with SRES A1B (un-mitigated climate change) and under a mitigation scenario where emissions peak in 2016 and decrease subsequently at 5% per year to a low emissions floor (2016-5-L). Table 14 shows the aspects of SLR that were considered for various scenarios and Table 15 displays regional population exposure for each scenario in the 2030s, 2050s and 2070s. The result show that Russia is within the bottom third of counties most impacted by SLR.

Scenario		Water levels				
Code	Description	Climate			Subsidence	
		More intense storms	Sea-level change	Higher storm surges	Natural	Anthropogenic
FNC	Future city	V	x	x	X	x
FRSLC	Future City Sea-Level Change	V	V	x	V	x
FCC	Future City Climate Change	V	V	V	V	x
FAC	Future City All Changes	V	V	V	V	V

Table 14. Summary of the aspects of SLR considered by Hanson et al. (2010). 'V' denotes that the aspect was considered in the scenario and 'x' that it was not.

Rapid urbanisation projection																	
2030							2050							2070			
Country	Ports	Water level projection			Country	Ports	Water level projection			Country	Ports	Water level projection					
		FAC	FCC	FRSL C			FNC	FAC	FCC			FRSLC	FNC	FAC	FCC	FRSL C	FNC
CHINA	15	17,100	15,500	15,400	14,600	CHINA	15	23,000	19,700	18,700	17,400	CHINA	15	27,700	22,600	20,800	18,600
INDIA	6	11,600	10,800	10,300	9,970	INDIA	6	16,400	14,600	13,600	12,500	INDIA	6	20,600	17,900	15,600	13,900
US	17	8,990	8,960	8,830	8,460	US	17	11,300	11,200	10,800	9,970	US	17	12,800	12,700	12,100	10,700
JAPAN	6	5,260	4,610	4,430	4,390	JAPAN	6	6,440	5,280	5,000	4,760	JAPAN	6	7,800	5,970	5,580	5,070
INDONESIA	4	1,420	1,200	1,200	1,170	INDONESIA	4	2,110	1,610	1,610	1,500	INDONESIA	4	2,680	1,830	1,830	1,530
BRAZIL	10	833	833	833	802	BRAZIL	10	929	929	929	879	BRAZIL	10	940	940	940	864
UK	2	497	497	478	459	UK	2	609	609	564	521	UK	2	716	716	640	569
CANADA	2	459	433	422	405	CANADA	2	549	512	486	457	CANADA	2	614	585	545	489
REP OF KOREA	3	344	344	331	441	REP OF KOREA	3	361	361	341	318	REP OF KOREA	3	377	377	325	303
GERMANY	1	257	257	253	248	GERMANY	1	287	287	273	269	GERMANY	1	309	309	290	280
RUSSIA	1	177	177	177	177	RUSSIA	1	202	202	173	173	RUSSIA	1	226	226	197	169
AUSTRALIA	5	162	162	157	157	AUSTRALIA	5	197	197	191	181	AUSTRALIA	5	196	196	186	175
SAUDI ARABIA	1	24	24	24	22	SAUDI ARABIA	1	33	33	33	27	SAUDI ARABIA	1	38	38	38	29
SOUTH AFRICA	2	30	30	30	29	SOUTH AFRICA	2	28	28	28	27	SOUTH AFRICA	2	30	30	30	27
FRANCE	1	15	15	15	15	FRANCE	1	19	19	19	17	FRANCE	1	23	23	23	18
ITALY	1	2	2	2	2	ITALY	1	4	4	4	3	ITALY	1	6	6	6	4
MEXICO	0	0	0	0	0	MEXICO	0	0	0	0	0	MEXICO	0	0	0	0	0

Table 15. National estimates of population exposure (1,000s) for each water level projection (ranked according to exposure with the FAC (Future City All Changes) scenario) under a rapid urbanisation projection for the 2030s, 2050s and 2070s. Estimates for present day exposure and in the absence of climate change (for 2070 only) for comparison are presented in Table 16. Data is from Hanson et al. (2010) and has been rounded down to three significant figures.

By comparing the projections in Table 15 with the estimates for exposure in the absence of climate change that are presented in Table 16, the vulnerability of Russia to SLR is clear. For example, in present day there are around 189,000 people in Russia exposed to SLR and in the absence of climate change in the 2070s this decreases to around 169,000. With climate change in the 2070s, and under the FAC (Future City All Changes) scenario the exposed population is 226,000 under un-mitigated A1B emissions. This implies an incremental climate change impact of around 57,000 people. Hanson et al. (2010) also demonstrated that aggressive mitigation scenario could avoid an exposure of around 28,000 people in Russia, relative to un-mitigated climate change (see Table 16) in 2070.

Country	Ports	Population exposure				Exposure avoided
		Current	2070. Rapid urbanisation, FAC water level scenario			
			No climate change	A1B un-mitigated	Mitigated (2016-5-L)	
CHINA	15	8,740	18,600	27,700	26,500	1,140
UNITED STATES	17	6,680	10,700	12,800	12,300	505
RUSSIA	1	189	169	226	197	28
JAPAN	6	3,680	5,070	7,800	7,290	515
SOUTH AFRICA	2	24	27	30	29	0
INDIA	6	5,540	13,900	20,600	18,900	1,670
BRAZIL	10	555	864	940	926	14
MEXICO	0	0	0	0	0	0
CANADA	2	308	489	614	599	15
AUSTRALIA	5	99	175	196	190	6
INDONESIA	4	602	1,530	2,680	2,520	156
REP OF KOREA	3	294	303	377	343	34
UK	2	414	569	716	665	51
FRANCE	1	13	18	23	20	2
ITALY	1	2	4	6	6	0
GERMANY	1	261	280	309	295	15
SAUDI ARABIA	1	15	29	38	35	3

Table 16. Exposed population (1,000s) in present (current), and in the 2070s in the absence of climate change (no climate change), with unmitigated climate change (A1B un-mitigated), and mitigated climate change (mitigated 2016-5-L), under the rapid urbanisation and FAC (Future City All Changes) water level scenarios. The final column shows the potential avoided exposure, as a result of mitigation. Data is from Hanson et al. (2010) and has been rounded down to three significant figures.

To further quantify the impact of SLR and some of the inherent uncertainties, the DIVA model was used to calculate the number of people flooded per year for global mean sea level increases (Brown et al., 2011). The DIVA model (DINAS-COAST, 2006) is an integrated model of coastal systems that combines scenarios of water level changes with socio-economic information, such as increases in population. The study uses two climate scenarios; 1) the SRES A1B scenario and 2) a mitigation scenario, RCP2.6. In both cases an SRES A1B population scenario was used. The results are shown in Table 17.

	A1B		RCP	
	Low	High	Low	High
Additional people flooded (1000s)	90.44	359.74	60.49	215.21
Loss of wetlands area (% of country's total wetland)	30.01%	41.56%	24.72%	37.29%

Table 17. Number of additional people flooded (1000s), and percentage of total wetlands lost by the 2080s under the high and low SRES A1B and mitigation (RCP 2.6) scenarios (Brown et al., 2011).

National-scale or sub-national scale assessments

Literature searches yielded no results for national-scale or sub-national scale studies for this impact sector.

References

- AINSWORTH, E. A. & MCGRATH, J. M. 2010. Direct Effects of Rising Atmospheric Carbon Dioxide and Ozone on Crop Yields. *In: LOBELL, D. & BURKE, M. (eds.) Climate Change and Food Security*. Springer Netherlands.
- ALCAMO, J., DRONIN, N., ENDEJAN, M., GOLUBEV, G. & KIRILENKO, A. 2007a. A new assessment of climate change impacts on food production shortfalls and water availability in Russia. *Global Environmental Change*, 17, 429-444.
- ALCAMO, J., DRONIN, N., ENDEJAN, M., GOLUBEV, G. & KIRILENKOC, A. 2007b. A new assessment of climate change impacts on food production shortfalls and water availability in Russia. *Global Environmental Change-Human and Policy Dimensions*, 17, 429-444.
- ALCAMO, J., MORENO, J., NOVÁKY, B., BINDI, M., COROBOV, R., DEVOY, R., GIANNAKOPOULOS, C., MARTIN, E., OLESEN, J. & SHVIDENKO, A. 2007c. Europe. *In: PARRY, M. L., CANZIANI, O. F., PALUTIKOF, J. P., VAN DER LINDEN, P. J. & HANSON, C. E. (eds.) Climate Change 2007: Impacts, Adaptation and Vulnerability. Contribution of Working Group II to the Fourth Assessment Report of the Intergovernmental Panel on Climate Change*. Cambridge, UK: Cambridge University Press.
- ALLISON, E. H., PERRY, A. L., BADJECK, M.-C., NEIL ADGER, W., BROWN, K., CONWAY, D., HALLS, A. S., PILLING, G. M., REYNOLDS, J. D., ANDREW, N. L. & DULVY, N. K. 2009. Vulnerability of national economies to the impacts of climate change on fisheries. *Fish and Fisheries*, 10, 173-196.
- AMSTRUP, S. C., DEWEAVER, E. T., DOUGLAS, D. C., MARCOT, B. G., DURNER, G. M., BITZ, C. M. & BAILEY, D. A. 2010. Greenhouse gas mitigation can reduce sea-ice loss and increase polar bear persistence. *Nature*, 468, 955-U351.
- ARNELL, N., WHEELER, T., OSBORNE, T., ROSE, G., GOSLING, S., DAWSON, T., PENN, A. & PERRYMAN, A. 2010. The implications of climate policy for avoided impacts on water and food security. *Work stream 2, Report 6 of the AVOID programme (AV/WS2/D1/R06)*. London: Department for Energy and Climate Change (DECC).
- ARNELL, N. W. 2004. Climate change and global water resources: SRES emissions and socio-economic scenarios. *Global Environmental Change*, 14, 31-52.

AVNERY, S., MAUZERALL, D. L., LIU, J. F. & HOROWITZ, L. W. 2011. Global crop yield reductions due to surface ozone exposure: 2. Year 2030 potential crop production losses and economic damage under two scenarios of O₃ pollution. *Atmospheric Environment*, 45, 2297-2309.

BETTS, R. A., BOUCHER, O., COLLINS, M., COX, P. M., FALLOON, P. D., GEDNEY, N., HEMMING, D. L., HUNTINGFORD, C., JONES, C. D., SEXTON, D. M. H. & WEBB, M. J. 2007. Projected increase in continental runoff due to plant responses to increasing carbon dioxide. *Nature*, 448, 1037-1041.

BLOOM, A. A., PALMER, P. I., FRASER, A., REAY, D. S. & FRANKENBERG, C. 2010. Large-Scale Controls of Methanogenesis Inferred from Methane and Gravity Spaceborne Data. *Science*, 327, 322-325.

BOE, J. L., HALL, A. & QU, X. 2009. September sea-ice cover in the Arctic Ocean projected to vanish by 2100. *Nature Geoscience*, 2, 341-343.

BONAZZA, A., MESSINA, P., SABBIONI, C., GROSSI, C. M. & BRIMBLECOMBE, P. 2009a. Mapping the impact of climate change on surface recession of carbonate buildings in Europe. *Science of The Total Environment*, 407, 2039-2050.

BONAZZA, A., SABBIONI, C., MESSINA, P., GUARALDI, C. & DE NUNTIIS, P. 2009b. Climate change impact: Mapping thermal stress on Carrara marble in Europe. *Science of The Total Environment*, 407, 4506-4512.

BROWN, S., NICHOLLS, R., LOWE, J.A. and PARDAENS, A. (2011), Sea level rise impacts in 24 countries. Faculty of Engineering and the Environment and Tyndall Centre for Climate Change Research, University of Southampton.

CHAKRABORTY, S. & NEWTON, A. C. 2011. Climate change, plant diseases and food security: an overview. *Plant Pathology*, 60, 2-14.

CHEUNG, W. W. L., LAM, V. W. Y., SARMIENTO, J. L., KEARNEY, K., WATSON, R. E. G., ZELLER, D. & PAULY, D. 2010. Large-scale redistribution of maximum fisheries catch potential in the global ocean under climate change. *Global Change Biology*, 16, 24-35.

CIA 2011. World Factbook. US Central Intelligence Agency.

DANKERS, R., ANISIMOV, O., KOKOREV, V. & ET AL. 2010. Permafrost, soil-carbon balance and sustainability under climate change Research Programme, Final Report. *UK-Russia Climate Change Science Collaboration Project*.

DANKERS, R. & FEYEN, L. 2008. Climate change impact on flood hazard in Europe: An assessment based on high-resolution climate simulations. *Journal of Geophysical Research-Atmospheres*, 113.

DANKERS, R. & FEYEN, L. 2009. Flood hazard in Europe in an ensemble of regional climate scenarios. *Journal of Geophysical Research-Atmospheres*, 114.

DENMAN, K. E. A. 2007. Couplings between changes in the climate system and biogeochemistry. In: SOLOMON, S. E. A. (ed.) *Climate Change 2007: The Physical Science Basis. Contribution of Working Group I to the Fourth Assessment Report of the Intergovernmental Panel on Climate Change*. Cambridge, UK: Cambridge University Press.

DINAS-COAST Consortium. 2006 DIVA 1.5.5. Potsdam, Germany: Potsdam Institute for Climate Impact Research (on CD-ROM)

DLUGOKENCKY, E. J., BRUHWILER, L., WHITE, J. W. C., EMMONS, L. K., NOVELLI, P. C., MONTZKA, S. A., MASARIE, K. A., LANG, P. M., CROTWELL, A. M., MILLER, J. B. & GATTI, L. V. 2009. Observational constraints on recent increases in the atmospheric CH₄ burden. *Geophysical Research Letters*, 36, -.

DOLL, P. 2009. Vulnerability to the impact of climate change on renewable groundwater resources: a global-scale assessment. *Environmental Research Letters*, 4.

DOLL, P. & SIEBERT, S. 2002. Global modeling of irrigation water requirements. *Water Resources Research*. Vol: 38 Issue: 4. Doi: 10.1029/2001WR000355

DRONIN, N. & KIRILENKO, A. 2008. Climate change and food stress in Russia: what if the market transforms as it did during the past century? *Climatic Change*, 86, 123-150.

DRONIN, N. & KIRILENKO, A. 2011. Climate change, food stress, and security in Russia. *Regional Environmental Change*, 11, 167-178.

ELISEEV, A. V., MOKHOV, I. I., ARZHANOV, M. M., DEMCHENKO, P. F. & DENISOV, S. N. 2008. Interaction of the methane cycle and processes in wetland ecosystems in a climate model of intermediate complexity. *Izvestiya Atmospheric and Oceanic Physics*, 44, 139-152.

FALKENMARK, M., ROCKSTRÖM, J. & KARLBERG, L. 2009. Present and future water requirements for feeding humanity. *Food Security*, 1, 59-69.

FAO. 2008. *Food and Agricultural commodities production* [Online]. Available: <http://faostat.fao.org/site/339/default.aspx> [Accessed 1 June 2011].

- FAO. 2010. *Food Security country profiles* [Online]. Available: <http://www.fao.org/economic/ess/ess-fs/ess-fs-country/en/> [Accessed 1 Sept 2011].
- FETTERER, F., KNOWLES, K., MEIER, W. & SAVOIE, M. 2009. Sea Ice Index. Boulder, Colorado USA: National Snow and Ice Data Center.
- FISCHER, G. 2009. World Food and Agriculture to 2030/50: How do climate change and bioenergy alter the long-term outlook for food, agriculture and resource availability? *Expert Meeting on How to Feed the World in 2050*. Food and Agriculture Organization of the United Nations, Economic and Social Development Department.
- FISCHER, H., BEHRENS, M., BOCK, M., RICHTER, U., SCHMITT, J., LOULERGUE, L., CHAPPELLAZ, J., SPAHNI, R., BLUNIER, T., LEUENBERGER, M. & STOCKER, T. F. 2008. Changing boreal methane sources and constant biomass burning during the last termination. *Nature*, 452, 864-867.
- FSF 2010. Financial Standards Report Russia: Insurance Core Principles. Financial Standards Foundation.
- FUNG, F., LOPEZ, A. & NEW, M. 2011. Water availability in +2°C and +4°C worlds. *Philosophical Transactions of the Royal Society A: Mathematical, Physical and Engineering Sciences*, 369, 99-116.
- GEDNEY, N., COX, P. M. & HUNTINGFORD, C. 2004. Climate feedback from wetland methane emissions. *Geophysical Research Letters*, 31, -.
- GERTEN D., SCHAPHOFF S., HABERLANDT U., LUCHT W., SITCH S. 2004 . Terrestrial vegetation and water balance: hydrological evaluation of a dynamic global vegetation model *International Journal Water Resource Development* 286:249–270.
- GOOD, P., CAESAR, J., BERNIE, D., LOWE, J. A., VAN DER LINDEN, P., GOSLING, S. N., WARREN, R., ARNELL, N. W., SMITH, S., BAMBER, J., PAYNE, T., LAXON, S., SROKOSZ, M., SITCH, S., GEDNEY, N., HARRIS, G., HEWITT, H., JACKSON, L., JONES, C. D., O'CONNOR, F., RIDLEY, J., VELLINGA, M., HALLORAN, P. & MCNEALL, D. 2011. A review of recent developments in climate change science. Part I: Understanding of future change in the large-scale climate system. *Progress in Physical Geography*, 35, 281-296.
- GOOSSE, H., ARZEL, O., BITZ, C. M., DE MONTETY, A. & VANCOPPENOLLE, M. 2009. Increased variability of the Arctic summer ice extent in a warmer climate. *Geophysical Research Letters*, 36, -.

GORNALL, J., BETTS, R., BURKE, E., CLARK, R., CAMP, J., WILLETT, K., WILTSHIRE, A. 2010. Implications of climate change for agricultural productivity in the early twenty-first century. *Phil. Trans. R. Soc. B*, DOI: 10.1098/rstb.2010.0158

GOSLING, S., TAYLOR, R., ARNELL, N. & TODD, M. 2011. A comparative analysis of projected impacts of climate change on river runoff from global and catchment-scale hydrological models. *Hydrology and Earth System Sciences*, 15, 279–294.

GOSLING, S. N. & ARNELL, N. W. 2011. Simulating current global river runoff with a global hydrological model: model revisions, validation, and sensitivity analysis. *Hydrological Processes*, 25, 1129-1145.

GOSLING, S. N., BRETHERTON, D., HAINES, K. & ARNELL, N. W. 2010. Global hydrology modelling and uncertainty: running multiple ensembles with a campus grid. *Philosophical Transactions of the Royal Society A: Mathematical, Physical and Engineering Sciences*, 368, 4005-4021.

HANSON, S., NICHOLLS, R., RANGER, N., HALLEGATTE, S., CORFEE-MORLOT, J., HERWEIJER, C. & CHATEAU, J. 2011. A global ranking of port cities with high exposure to climate extremes. *Climatic Change*, 104, 89-111.

HANSON, S., NICHOLLS, R., S, H. & CORFEE-MORLOT, J. 2010. The effects of climate mitigation on the exposure of worlds large port cities to extreme coastal water levels. London, UK.

HARDING, R., BEST, M., BLYTH, E., HAGEMANN, D., KABAT, P., TALLAKSEN, L.M., WARNAARS, T., WIBERG, D., WEEDON, G.P., van LANEN, H., LUDWIG, F., HADDELAND, I. 2011. Preface to the “Water and Global Change (WATCH)” special collection: Current knowledge of the terrestrial global water cycle. *Journal of Hydrometeorology*, DOI: 10.1175/JHM-D-11-024.1

HIRABAYASHI, Y., KANAE, S., EMORI, S., OKI, T. & KIMOTO, M. 2008. Global projections of changing risks of floods and droughts in a changing climate. *Hydrological Sciences Journal-Journal Des Sciences Hydrologiques*, 53, 754-772.

HOLLAND, M. M., BITZ, C. M. & TREMBLAY, B. 2006. Future abrupt reductions in the summer Arctic sea ice. *Geophysical Research Letters*, 33, -.

HOLLAND, M. M., SERREZE, M. C. & STROEVE, J. 2010. The sea ice mass budget of the Arctic and its future change as simulated by coupled climate models. *Climate Dynamics*, 34, 185-200.

HUGELIUS, G. & KUHR, P. 2009. Landscape partitioning and environmental gradient analyses of soil organic carbon in a permafrost environment. *Global Biogeochemical Cycles*, 23, -.

IFPRI. 2010. *International Food Policy Research Institute (IFPRI) Food Security CASE maps. Generated by IFPRI in collaboration with StatPlanet*. [Online]. Available: www.ifpri.org/climatechange/casemaps.html [Accessed 21 June 2010].

IGLESIAS, A., GARROTE, L., QUIROGA, S. & MONEO, M. 2009. Impacts of climate change in agriculture in Europe. PESETA-Agriculture study. *JRC Scientific and Technical Reports*.

IGLESIAS, A. & ROSENZWEIG, C. 2009. Effects of Climate Change on Global Food Production under Special Report on Emissions Scenarios (SRES) Emissions and Socioeconomic Scenarios: Data from a Crop Modeling Study. Palisades, NY: Socioeconomic Data and Applications Center (SEDAC), Columbia University.

IPCC 2007a. Climate Change 2007: Impacts, Adaptation and Vulnerability. Contribution of Working Group II to the Fourth Assessment Report of the Intergovernmental Panel on Climate Change. *In*: PARRY, M. L., CANZIANI, O. F., PALUTIKOF, J. P., VAN DER LINDEN, P. J. & HANSON, C. E. (eds.). Cambridge, UK.

IPCC 2007b. Climate Change 2007: The Physical Science Basis. Contribution of Working Group I to the Fourth Assessment Report of the Intergovernmental Panel on Climate Change *In*: SOLOMON, S., QIN, D., MANNING, M., CHEN, Z., MARQUIS, M., AVERYT, K. B., TIGNOR, M. & MILLER, H. L. (eds.). Cambridge, United Kingdom and New York, NY, USA.

IPCC 2007c. Summary for Policymakers. *In*: PARRY, M. L., CANZIANI, O. F., PALUTIKOF, J. P., VAN DER LINDEN, P. J. & HANSON, C. E. (eds.) *Climate Change 2007: Impacts, Adaptation and Vulnerability. Contribution of Working Group II to the Fourth Assessment Report of the Intergovernmental Panel on Climate Change*. Cambridge: Cambridge University Press.

ISE, T., DUNN, A. L., WOFSY, S. C. & MOORCROFT, P. R. 2008. High sensitivity of peat decomposition to climate change through water-table feedback. *Nature Geoscience*, 1, 763-766.

JORGENSON, M. T., SHUR, Y. L. & PULLMAN, E. R. 2006. Abrupt increase in permafrost degradation in Arctic Alaska. *Geophysical Research Letters*, 33, -.

KATTSOV, V. M., WALSH, J. E., CHAPMAN, W. L., GOVORKOVA, V. A., PAVLOVA, T. V. & ZHANG, X. 2007. Simulation and projection of Arctic freshwater budget components by the IPCC AR4 global climate models. *Journal of Hydrometeorology*, 8, 571-589.

KHVOROSTYANOV, D. V., KRINNER, G., CIAIS, P., HEIMANN, M. & ZIMOV, S. A. 2008. Vulnerability of permafrost carbon to global warming. Part I: model description and role of heat generated by organic matter decomposition. *Tellus Series B-Chemical and Physical Meteorology*, 60, 250-264.

KIRKINEN, J., MATRIKAINEN, A., HOLTINEN, H., SAVOLAINEN, I., AUVINEN, O. & SYRI, S. 2005. Impacts on the Energy Sector and Adaptation of the Electricity Network under a Changing Climate in Finland. FINADAPT, working paper 10. *Finnish Environment Institute Mimeographs*. Helsinki, Finland: Finnish Environment Institute.

LAWRENCE, D., SLATER, A. & SWENSON, S. 2011. Simulation of Present-day and Future Permafrost and Seasonally Frozen Ground Conditions in CCSM4. *Submitted to Journal of Climate*.

LAWRENCE, D. M., SLATER, A. G., TOMAS, R. A., HOLLAND, M. M. & DESER, C. 2008. Accelerated Arctic land warming and permafrost degradation during rapid sea ice loss. *Geophysical Research Letters*, 35, -.

LEHNER, B., CZISCH, G. & VASSOLO, S. 2005. The impact of global change on the hydropower potential of Europe: a model-based analysis. *Energy Policy*, 33, 839-855.

LOBELL, D. B., BANZIGER, M., MAGOROKOSHO, C. & VIVEK, B. 2011. Nonlinear heat effects on African maize as evidenced by historical yield trials. *Nature Clim. Change*, 1, 42-45.

LUCK, J., SPACKMAN, M., FREEMAN, A., TRE_BICKI, P., GRIFFITHS, W., FINLAY, K. & CHAKRABORTY, S. 2011. Climate change and diseases of food crops. *Plant Pathology*, 60, 113-121.

NATIONAL INTELLIGENCE COUNCIL, N. I. C. Year. Russia: The Impact of Climate Change to 2030 - Geopolitical Implications. *In*, 16 September 2009 2009. 1-39.

NICHOLLS, R. J. and LOWE, J. A. (2004). "Benefits of mitigation of climate change for coastal areas." *Global Environmental Change* **14**(3): 229-244.

NICHOLLS, R. J., MARINOVA, N., LOWE, J. A., BROWN, S., VELLINGA, P., DE GUSMÃO, G., HINKEL, J. and TOL, R. S. J. (2011). "Sea-level rise and its possible impacts given a 'beyond 4°C world' in the twenty-first century." *Philosophical Transactions of the Royal Society A* **369**: 1-21.

NELSON, G. C., ROSEGRANT, M. W., PALAZZO, A., GRAY, I., INGERSOLL, C., ROBERTSON, R., TOKGOZ, S., ZHU, T., SULSER, T. & RINGLER, C. 2010. Food Security, Farming and Climate Change to 2050. *Research Monograph, International Food Policy Research Institute*. Washington, DC.

NOHARA, D., KITO, A., HOSAKA, M. & OKI, T. 2006. Impact of climate change on river discharge projected by multimodel ensemble. *Journal of Hydrometeorology*, **7**, 1076-1089.

NOTZ, D. 2009. The future of ice sheets and sea ice: Between reversible retreat and unstoppable loss. *Proceedings of the National Academy of Sciences of the United States of America*, **106**, 20590-20595.

O'CONNOR, F. M., BOUCHER, O., GEDNEY, N., JONES, C. D., FOLBERTH, G. A., COPPELL, R., FRIEDLINGSTEIN, P., COLLINS, W. J., CHAPPELLAZ, J., RIDLEY, J. & JOHNSON, C. E. 2010. Possible Role of Wetlands, Permafrost, and Methane Hydrates in the Methane Cycle under Future Climate Change: A Review. *Reviews of Geophysics*, **48**, -.

PARDAENS, A. K., LOWE, J., S, B., NICHOLLS, R. & DE GUSMÃO, D. 2011. Sea-level rise and impacts projections under a future scenario with large greenhouse gas emission reductions. *Geophysical Research Letters*, **38**, L12604.

PARRY, M. L., ROSENZWEIG, C., IGLESIAS, A., LIVERMORE, M. & FISCHER, G. 2004. Effects of climate change on global food production under SRES emissions and socio-economic scenarios. *Global Environmental Change-Human and Policy Dimensions*, **14**, 53-67.

RAHMSTORF, S. 2010. A new view on sea level rise. *Nature Reports Climate Change*, **4**, 44-45.

RAMANKUTTY, N., EVAN, A. T., MONFREDA, C. & FOLEY, J. A. 2008. Farming the planet: 1. Geographic distribution of global agricultural lands in the year 2000. *Global Biogeochemical Cycles*, 22, GB1003.

RAMANKUTTY, N., FOLEY, J. A., NORMAN, J. & MCSWEENEY, K. 2002. The global distribution of cultivable lands: current patterns and sensitivity to possible climate change. *Global Ecology and Biogeography*, 11, 377-392.

ROCKSTROM, J., FALKENMARK, M., KARLBERG, L., HOFF, H., ROST, S. & GERTEN, D. 2009. Future water availability for global food production: The potential of green water for increasing resilience to global change. *Water Resources Research*, 45.

ROSHYDROMET 2008. Assessment Report on Climate Change and its Consequences.

SCHUUR, E. A. G., BOCKHEIM, J., CANADELL, J. G., EUSKIRCHEN, E., FIELD, C. B., GORYACHKIN, S. V., HAGEMANN, S., KUHR, P., LAFLEUR, P. M., LEE, H., MAZHITOVA, G., NELSON, F. E., RINKE, A., ROMANOVSKY, V. E., SHIKLOMANOV, N., TARNOCAI, C., VENEVSKY, S., VOGEL, J. G. & ZIMOV, S. A. 2008. Vulnerability of permafrost carbon to climate change: Implications for the global carbon cycle. *Bioscience*, 58, 701-714.

SEMENOV, V. A. 2011. Climate-related changes in hazardous and adverse hydrological events in the Russian rivers. *Russian Meteorology and Hydrology*, 36, 124-129.

SHAKHOVA, N., SEMILETOV, I. & PANTELEEV, G. 2005. The distribution of methane on the Siberian Arctic shelves: Implications for the marine methane cycle. *Geophysical Research Letters*, 32, -.

SHIKLOMANOV, A. I. & LAMMERS, R. B. 2009. Record Russian river discharge in 2007 and the limits of analysis. *Environmental Research Letters*, 4.

SHIKLOMANOV, A. I., LAMMERS, R. B., RAWLINS, M. A., SMITH, L. C. & PAVELSKY, T. M. 2007. Temporal and spatial variations in maximum river discharge from a new Russian data set. *J. Geophys. Res.*, 112, G04S53.

SHIKLOMANOV, I. A., BABKIN, V. I. & BALONISHNIKOV, Z. A. 2011. Water resources, their use, and water availability in Russia: Current estimates and forecasts. *Water Resources*, 38, 139-148.

SILLMANN, J. & ROECKNER, E. 2008. Indices for extreme events in projections of anthropogenic climate change. *Climatic Change*, 86, 83-104.

SMAKHTIN, V., REVENGA, C. & DOLL, P. 2004. A pilot global assessment of environmental water requirements and scarcity. *Water International*, 29, 307-317.

TAN, A., ADAM, J. C. & LETTENMAIER, D. P. 2011. Change in spring snowmelt timing in Eurasian Arctic rivers. *Journal of Geophysical Research-Atmospheres*, 116.

TATSUMI, K., YAMASHIKI, Y., VALMIR DA SILVA, R., TAKARA, K., MATSUOKA, Y., TAKAHASHI, K., MARUYAMA, K. & KAWAHARA, N. 2011. Estimation of potential changes in cereals production under climate change scenarios. *Hydrological Processes*, Special Issue: Japan Society of Hydrology and water resources, 25 (17), 2715-2725.

UNFCCC 2009. Report of the centralized in-depth review of the fourth national communication of the Russian Federation. *Document code: FCCC/IDR.4/RUS. United Nations Office at Geneva, Switzerland.* .

VAN VUUREN, D., DEN ELZEN, M., LUCAS, P., EICKHOUT, B., STRENGERS, B., VAN RUIJVEN, B., WONINK, S. & VAN HOUDT, R. 2007. Stabilizing greenhouse gas concentrations at low levels: an assessment of reduction strategies and costs. *Climatic Change*, 81, 119-159.

VAN VUUREN, D. P., ISAAC, M., KUNDZEWICZ, Z. W., ARNELL, N., BARKER, T., CRIQUI, P., BERKHOUT, F., HILDERINK, H., HINKEL, J., HOF, A., KITOUS, A., KRAM, T., MECHLER, R. & SCRIECIU, S. 2011. The use of scenarios as the basis for combined assessment of climate change mitigation and adaptation. *Global Environmental Change*, 21, 575-591.

VOLODIN, E. M. 2008. Methane cycle in the INM RAS climate model. *Izvestiya Atmospheric and Oceanic Physics*, 44, 153-159.

VOROSMARTY, C. J., MCINTYRE, P. B., GESSNER, M. O., DUDGEON, D., PRUSEVICH, A., GREEN, P., GLIDDEN, S., BUNN, S. E., SULLIVAN, C. A., LIERMANN, C. R. & DAVIES, P. M. 2010. Global threats to human water security and river biodiversity. *Nature*, 467, 555-561.

WANG, M. Y. & OVERLAND, J. E. 2009. A sea ice free summer Arctic within 30 years? *Geophysical Research Letters*, 36, -.

WARREN, R., ARNELL, N., BERRY, P., BROWN, S., DICKS, L., GOSLING, S., HANKIN, R., HOPE, C., LOWE, J., MATSUMOTO, K., MASUI, T., NICHOLLS, R., O'HANLEY, J., OSBORN, T., SCRIECRU, S. (2010) The Economics and Climate Change Impacts of Various Greenhouse Gas Emissions Pathways: A comparison between baseline and policy emissions scenarios, AVOID Report, AV/WS1/D3/R01.

http://www.metoffice.gov.uk/avoid/files/resources-researchers/AVOID_WS1_D3_01_20100122.pdf

WASHINGTON, W. M., KNUTTI, R., MEEHL, G. A., TENG, H. Y., TEBALDI, C., LAWRENCE, D., BUJA, L. & STRAND, W. G. 2009. How much climate change can be avoided by mitigation? *Geophysical Research Letters*, 36, -.

WESTPHAL, M. 2008. Summary of the Climate Science in the Europe and Central Asia Region: Historical Trends and Future Projections. *Background paper prepared for World Bank report*. . Washington D.C., USA.

WOOD, E.F., ROUNDY, J.K., TROY, T.J., van BEEK, L.P.H., BIERKENS, M.F.P., BLYTH, E., de ROO, A., DOLL, P., EK, M., FAMIGLIETTI, J., GOCHIS, D., van de GIESEN, N., HOUSER, P., JAFFE, P.R., KOLLET, S., LEHNER, B., LETTENMAIER, D.P., PETERS-LIDARD, C., SIVAPALAN, M., SHEFFIELD, J., WADE, A. & WHITEHEAD, P. 2011. Hyperresolution global land surface modelling: Meeting a grand challenge for monitoring Earth's terrestrial water. *Water Resources Research*, 47, W05301.

WORLD BANK 2009. Adapting to Climate Change in Europe and Central Asia.

WOS. 2011. *Web of Science* [Online]. Available:

http://thomsonreuters.com/products_services/science/science_products/a-z/web_of_science [Accessed August 2011].

WU, W., TANG, H., YANG, P., YOU, L., ZHOU, Q., CHEN, Z. & SHIBASAKI, R. 2011. Scenario-based assessment of future food security. *Journal of Geographical Sciences*, 21, 3-17.

ZHANG, J. L., STEELE, M. & SCHWEIGER, A. 2010. Arctic sea ice response to atmospheric forcings with varying levels of anthropogenic warming and climate variability. *Geophysical Research Letters*, 37, -.

ZHUANG, Q., MELACK, J. M., ZIMOV, S., WALTER, K. M., BUTENHOFF, C. L. & KHALIL, M. A. K. 2009. Global Methane Emissions From Wetlands, Rice Paddies, and Lakes. *Eos Trans. AGU*, 90.

Acknowledgements

Funding for this work was provided by the UK Government Department of Energy and Climate Change, along with information on the policy relevance of the results.

The research was led by the UK Met Office in collaboration with experts from the University of Nottingham, Walker Institute at the University of Reading, Centre for Ecology and Hydrology, University of Leeds, Tyndall Centre – University of East Anglia, and Tyndall Centre – University of Southampton.

Some of the results described in this report are from work done in the AVOID programme by the UK Met Office, Walker Institute at the University of Reading, Tyndall Centre – University of East Anglia, and Tyndall Centre – University of Southampton.

The AVOID results are built on a wider body of research conducted by experts in climate and impact models at these institutions, and in supporting techniques such as statistical downscaling and pattern scaling.

The help provided by experts in each country is gratefully acknowledged – for the climate information they suggested and the reviews they provided, which enhanced the content and scientific integrity of the reports.

The work of the independent expert reviewers at the Centre for Ecology and Hydrology, University of Oxford, and Fiona's Red Kite Climate Consultancy is gratefully acknowledged.

Finally, thanks go to the designers, copy editors and project managers who worked on the reports.

Met Office
FitzRoy Road, Exeter
Devon, EX1 3PB
United Kingdom

Tel: 0870 900 0100
Fax: 0870 900 5050
enquiries@metoffice.gov.uk
www.metoffice.gov.uk

Produced by the Met Office.
© Crown copyright 2011 11/0209p
Met Office and the Met Office logo
are registered trademarks